SPECTROSCOPIC STUDIES OF

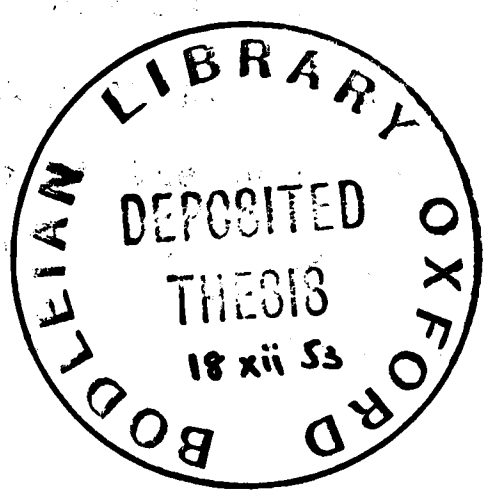
SIMPLE MOLECULES

Abstract of
A Thesis presented for the degree of D.Phil.
in the University of Oxford

by

H. C. Rowlinson
Exeter College

July 1953



A B S T R A C T

In the introduction to this thesis it is explained that there are two spectroscopic methods of obtaining information about the highly excited electronic energy levels of molecules. The first is by examining directly the transitions to these levels from the ground state of the molecule, the second by discovering transitions between the high levels themselves. In the molecule CO, given as an example, only one transition involving the ground state lies at wave-lengths greater than 2000 Å, and much information has been obtained at shorter wave-lengths. However, for CO the second method has proved more fruitful, for many transitions of this molecule may be observed in the visible and near u-v regions of the spectrum. In this property CO is unusual, partly because it is a stable gaseous species of which a plentiful supply may be provided for a discharge tube, and partly because of the peculiar stability of its upper states and its high dissociation energy. On the other hand the majority of diatomic molecules do not

possess so many emission systems above 2000 Å and for these it was desired to find a general method for examining them at shorter wave-lengths. It is known that oxygen in the air absorbs light in this region, and so a vacuum spectrograph was designed and built around a 1 m. glass grating ruled 30,000 lines/inch. In order that the identification of the observed spectra should be as simple as possible, it was desired to obtain absorption spectra rather than emission ones. Previous work in this direction has been confined largely to gaseous or volatile substances, but for a general method a long absorption tube surrounded by a furnace is necessary, so that involatile solids may be heated. Now the most feasible source of continuous radiation from 2000 - 400 Å is the Lyman source, a powerful condensed spark through a silica capillary. This is almost a point source and so the intensity falls off very rapidly as it is moved away from the slit; thus the introduction of a long absorption tube requires a very bright source and a very fast spectrograph. The intensity in this work has been increased by the use of an aluminized mirror collecting light from the source and focussing it on the slit. In this manner the absorption spectrum of five diatomic molecules has been examined between 1300 - 2000 Å, and some measure of the generality of the method

is that in every case at least two new energy levels have been observed.

In Part I of the thesis, after details of the design and operation of the spectrograph have been given, the observed spectra are recorded for the monoxides of silicon, germanium and tin, and also for stannous sulphide. The new molecular energy levels are, in cm^{-1}:-

	State	ν_e	ω_e	$x_e\omega_e$
SiO	?	79650		
	$H\left(^1\Sigma^+\right)$?	76427	1155	15
	G	[72011]	829	5
	$F\left(^1\Sigma^+\right)$?	$68562\cdot_5$	$1114\cdot_6$	$7\cdot_2$
	$E\left(^3\Sigma^+\right)$?	$52863\cdot_2$	675	$4\cdot1_5$
GeO				
	F	$67474\cdot4$	$809\cdot0$	$5\cdot66$
	E	$49637\cdot3$	$504\cdot3$	$4\cdot8$
SnO				
	F	58809·6	724	21
	?	57491 (ν_0)	462	-
	other fragmentary systems			
SnS				
	F	56886 (ν_0)	repulsive	
	?	55928 (ν_0)	dissociates before v' = 1	
	other fragmentary systems.			

For SiO the states observed are compared with those known for CO, in addition it is suggested that the highest level, together with the H and F levels form a Rydberg series leading to 10·5 e.v. as the ionization potential of SiO.

In a discussion of the dissociation energies of these molecules by comparison of the spectroscopic and thermo-chemical evidence, the following best values for D_0'' were obtained (in k.cal./mol.):-

SiO	GeO	SnO	SnS
~ 180	154 ± 5	122 ± 2	110 ± 1

In Part II of the thesis the observed emission spectrum of aluminium monofluoride is described. The source used was a heated hollow cathode discharge tube where the cathode contained a mixture of aluminium and aluminium trifluoride. Later the absorption spectrum of this molecule was examined in the vacuum ultra-violet and six systems observed, together with a group of unanalysed bands at very short wave-lengths. The new states of AlF discovered are as follows:-

State	ν_e	ω_e	$x_e\omega_e$	$z_e\omega_e$	Observed Transitions
$d(^3\Sigma)$?	72350	~940			d → a
$c(^3\Sigma)$?	69640	~940			c → a
H ?	67312	958	7·0		H ← X
G $^1\Sigma^+$	66325	948	8·0	0·02	G ← X and G → A
$F(^1\Pi)$?	65785	955	5·0	0·01	F ← X , F → A
$E(^1\Pi)$?	63739(ν_0)				E ← X , E → A
$b^3\Sigma$	61331·3	933·5	$4·9_0$		b → a
$D^1\Delta$	61225	902	6·5		D → A
$C^1\Sigma^+$	57687	938·4	5·18		C ← X , C → A
$B^1\Sigma^+$	54241·5	862	7·0	0·012	B ← X
$a^3\Pi_2$	33659·5				
$a^3\Pi_1$	33612	830·9	$4·5_5$		a → X ?
$a^3\Pi_0$	33574·5				

The A and X states referred to are the $A^1\Pi$ and $X^1\Sigma^+$ discovered previously. The a → X transition is very weak, and this makes the absolute levels of the triplet states rather doubtful. Plausible dissociation products are assigned to these states on the basis of a dissociation energy of AlF of 147 k.cal./mol. This value is supported by a calculation of the latent heat of sublimation of aluminium from vapour pressure data.

SPECTROSCOPIC STUDIES OF SIMPLE MOLECULES

A Thesis presented for the degree of D.Phil.
in the University of Oxford

by

H. C. Rowlinson
Exeter College

July 1953

CONTENTS

Page

PART I

The Construction and Use of a New Vacuum Spectrograph

Introduction 1
Design of the Spectrograph 8
The optical arrangement 9
The mechanical arrangement 10
The end plate 11
The slit mounting 12
The plate holder and its carriage 15
The grating mounting 16
The pumping line 20
Assembly and Adjustment of the Spectrograph . . 22
The problem of scattered light 26
The Photographic Plates 28
The Lyman Source 33
The Absorption Spectrum of SiO 37
The Absorption Spectrum of GeO 54
The Absorption Spectrum of SnO and SnS . . . 63
The Dissociation Energies of SiO, GeO, SnO and SnS 72
Rydberg Series of Tin 89

PART II

The Band Spectrum of Aluminium Monofluoride

Introduction 99
The Emission Spectrum 101
The Absorption Spectrum 117
Discussion 126
References 138

PART I

The Construction and Use of a New Vacuum Spectrograph

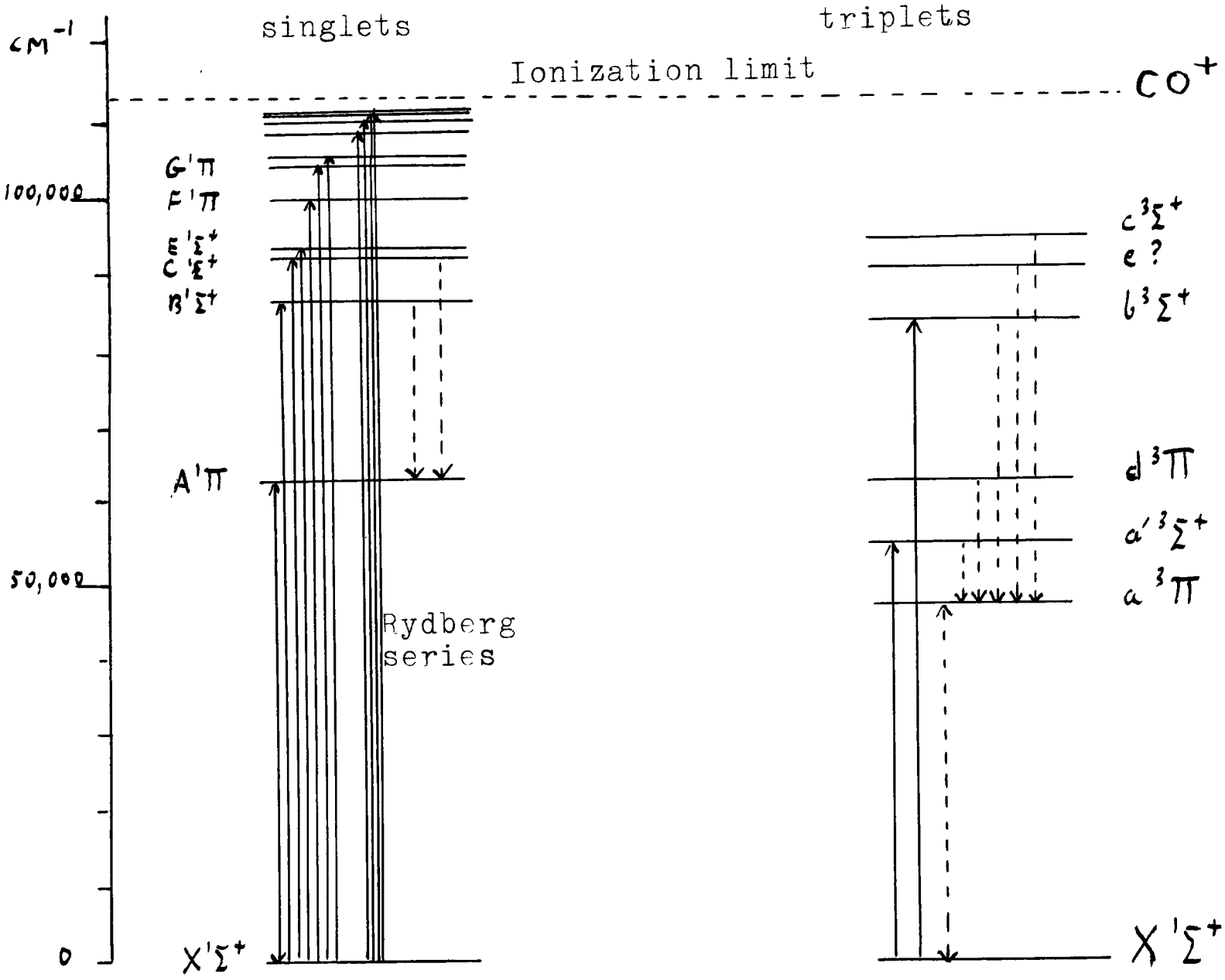
PART I

The Construction and Use of a New Vacuum Spectrograph

Introduction

Of the several hundred diatomic molecules whose spectra have been observed, only twenty have been investigated in the spectral region below 1900 Å. This is unfortunate in that many new electronic energy levels will lie in this region, particularly for lighter molecules, and also that molecular ionization potentials which are of the same order as atomic ones, mostly lie above 6 e.v. This means that the ground state Rydberg transitions will converge to limits in the vacuum ultra-violet.

On an energy scale the gap between zero energy and that possessed by light of 2000 Å is equal to the gap between 2000 Å and 1000 Å, and for those molecules which have been studied most electronic levels lie in the higher energy region. For example CO has only one resonance transition above 2000 Å, the Cameron bands, and an energy diagram for this molecule is below.



A transition thus ——— lies in the Schumann region
similarly - - - - - lies above 2000 Å.

Our knowledge of the higher energy levels in CO does not come mainly from vacuum ultra-violet studies but from transitions between excited states giving rise to spectra in the visible and infra-red. It is only because CO has a high dissociation energy and is stable in many discharges

that these transitions are known at all. There is no technique available for observing the emission spectrum of highly excited states of less stable molecules, particularly of those which are very involatile, and these must be studied in absorption. It was for this purpose that this work was carried out, in the hope that moderately stable states would be discovered giving only short extrapolations to their dissociation limits. By the correlation of such limits with the various atomic products it will be possible to determine the correct dissociation energy from the ground state of the molecule, and by application of the non-crossing rule to ascertain the most probable atomic dissociation products of the intermediate states. Although with the possible exception of silicon monoxide no new molecular Rydberg series have been observed, five such atomic series have been found for metallic tin.

However this spectral region is not accessible with ordinary spectroscopic or photographic techniques due to the absorption of radiation by the atmospheric oxygen and by gelatin. The Schumann-Runge system of O_2 begins at about 1950 Å at room temperature and converges to a limit at 1759 Å; beyond lies a strong region of continuous absorption stretching to 1330 Å with a maximum at about

1450 Å. At this point the absorption is comparable with metallic absorption of visible frequencies, for the intensity of radiation is reduced to half by a path length of ·0014 cm. of oxygen at S.T.P. Thus for a path length of 3 m. the partial pressure of oxygen must be less than 4×10^{-3} mm. of Hg for half the radiation to reach the plate. Such a pressure is readily obtainable with modern vacuum pumps providing the bore of the pumping line is kept large. Further, the transparency of possible solids for use as prisms decreases with wave-length; a good sample of quartz will transmit to 1450 Å but its coefficient falls rapidly below 1850 Å, fluorite transmits to 1300 Å and lithium fluoride enables the region to be extended a little further. However, all these possess the disadvantage that their transparency at short wave-lengths decreases after they have been irradiated for some time. Thus a concave reflexion grating spectrograph is the usual type, and such instruments can be divided into two limiting kinds in which the incident light strikes the grating either along (or nearly along) its normal, or at 80° or more to it, the so-called grazing incidence.

A concave grating at normal incidence was first used by Lyman in 1906, making possible the determination of wave-lengths by geometric means. The use of a grating

at grazing incidence, first developed for the study of X-rays, was extended to ultra-violet spectra by Hoag and developed very considerably by Siegbahn, Edlen and others at Upsala. The advantage of the normal incidence arrangement is, in our experience, primarily that of speed, but also it gives more linear dispersion and is less critical to focus. The advantages of grazing incidence are that it is possible to obtain the very shortest wave-lengths (below 200 Å) only from this type, and that it gives a larger dispersion from a given grating. However, in our experiments this last advantage is nullified by a tendency of the line image to astigmatic defects which results in as good resolution being obtained with normal as with grazing incidence despite the higher dispersion of the latter. Further minor points are that it is easier to illuminate completely a given grating from a small source at grazing incidence, also with this arrangement the surface of the grating subtends a smaller solid angle at any point on the plate thus tending to reduce scattered light. As will be explained later a much shorter slit can be used with normal incidence.

However, these differences are largely the result of experiment and were not available when in an earlier work[1] a grazing incidence spectrograph was built around a concave

grating by Wood of approximately 1 m. radius and ruled 30,000 lines per inch on speculum metal. In this instrument a great deal of trouble was experienced from scattered light, and the construction of baffles and the use of matt black paint only reduced the scatter a small amount. The next step was to "aluminize" the grating,[2] a thin film of aluminium being applied by evaporation from a heated tungsten filament at very low pressure. The reflectivity of aluminium for light of these short wave-lengths is much higher than that of speculum metal and the improvement in speed of the spectrograph was most noticeable. Plates taken of various emission sources, for example an h/f oscillator, a hollow cathode, and a 4000 V. A.C. discharge tube were quite satisfactory; however it was desired to study spectra in absorption as the common impurities in emission spectra, CO, N_2, NO, have strong systems in this region and the interpretation of any spectrum was going to be complicated. To this end a Lyman source (see p.33) was developed to emit continuous radiation from 2000 Å to 1100 Å, but the extreme brilliance of this source in the visible and near ultra-violet caused the intensity of the scattered light reaching the plate to be comparable with that of the diffracted light. This scatter was definitely from the surface of grating itself, it had perhaps been

badly stored at an earlier stage in its career and the ruled portion was visibly etched. It was therefore decided to get a new grating for this instrument, ruled by Siegbahn on Pyrex glass it has a radius of curvature of 1 m., a ruled area of 30 x 10 mm. and 1152 lines per mm.; this grating arrived in January 1952. Meanwhile it was thought that the speculum grating might give better results at nearly normal incidence, and a rough test with the various components held in clamps on the dark-room bench indicated that this was so; for example the Schumann-Runge system of oxygen was photographed in absorption against the continuum from a commercial hydrogen lamp, an impossibility with the grazing incidence instrument due to the low intensity of the source. Thus it was decided to construct a normal incidence spectrograph round this speculum grating; however on completion the Siegbahn grating, now aluminized, was found to give much better results and it is this that is now in use.

Design of the Spectrograph

There was available a length of seamless brass tubing of 6" internal diameter, and it seemed that this would make an admirable vacuum jacket. Two mechanical arrangements are thus possible; the grating can be mounted at one end, the plate holder at the other and the slit placed in a side-arm, or the slit and plate holder arranged close together on one end-plate. The second design was chosen on the grounds of simplicity and rigidity. Now our special plates are 5" × 2" and it would be difficult to fit a plate of this size (in its holder) and a tube for the slit into a distance of six inches. However, the provision of a small bulge or "blister" on the side of the cylindrical vacuum can gave sufficient room for light from the slit to reach every portion of the grating. This can be seen in fig. I (plan of spectrograph). Furthermore the grating was mounted on a Dural girder connected directly to the same end-plate as the slit and plate holder in order to avoid upsetting the optics by expansion and contraction of the vacuum joints. Thus the spectrograph can be divided into four main parts; the End-plate holding the slit-tube and the plate-holder in its box, the Grating holder and its mounting, the Vacuum can, and the Pumping line.

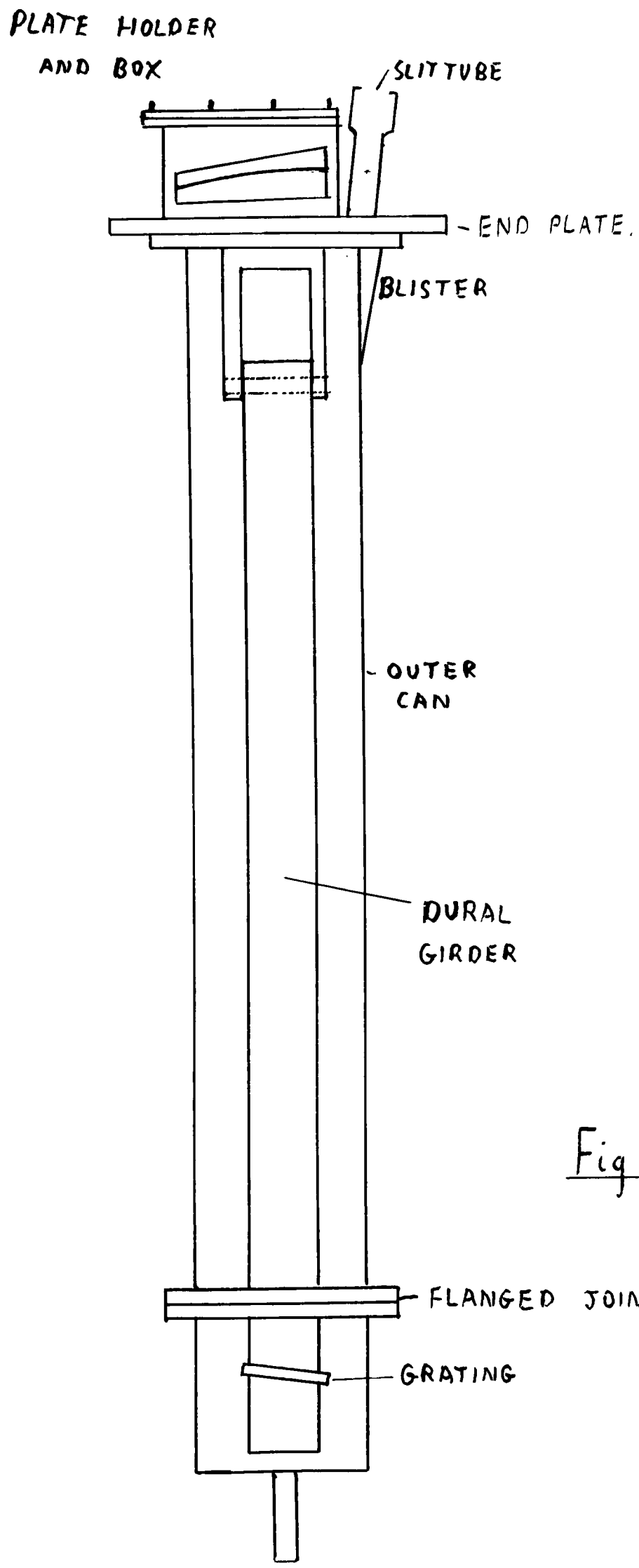

PLATE HOLDER
AND BOX
SLIT TUBE
END PLATE.
BLISTER
OUTER
CAN
DURAL
GIRDER
FLANGED JOINT
GRATING

Fig I

The Optical Arrangement

This is shown diagrammatically in fig. II. The slit, grating pole and plate surface all lie on the Rowland Circle of radius equal to half that of the grating curvature. This is the necessary condition for the optics of all concave grating spectrographs, to a first approximation. It was decided that the instrument was to be used primarily in the region 2000 Å to 1000 Å and that this should be recorded on one plate.

Now the dispersion $\frac{d\lambda}{dx} = \frac{ndcos\beta}{r}$

where x is distance along the plate in mm.

n is the spectral order,

d is the separation of successive rulings,

r is the grating curvature radius,

and β is the angle of diffraction of light of wavelength λ.

Also $\lambda = nd(\sin\alpha + \sin\beta)$ where α is the angle of incidence, and these equations give a dispersion of 8·46 Å/mm. at 1500 Å assuming normal incidence. This gives a range of about 1050 Å on a 5" plate. Thus in order that the 1000 Å mark should lie at the short-wave end of the plate, the angle subtended by the slit and the direct image (≡ 0 Å) at the centre of the Rowland circle was defined at $10^{o}0'$. This gives an angle of incidence of $2^{o}30'$ and revised

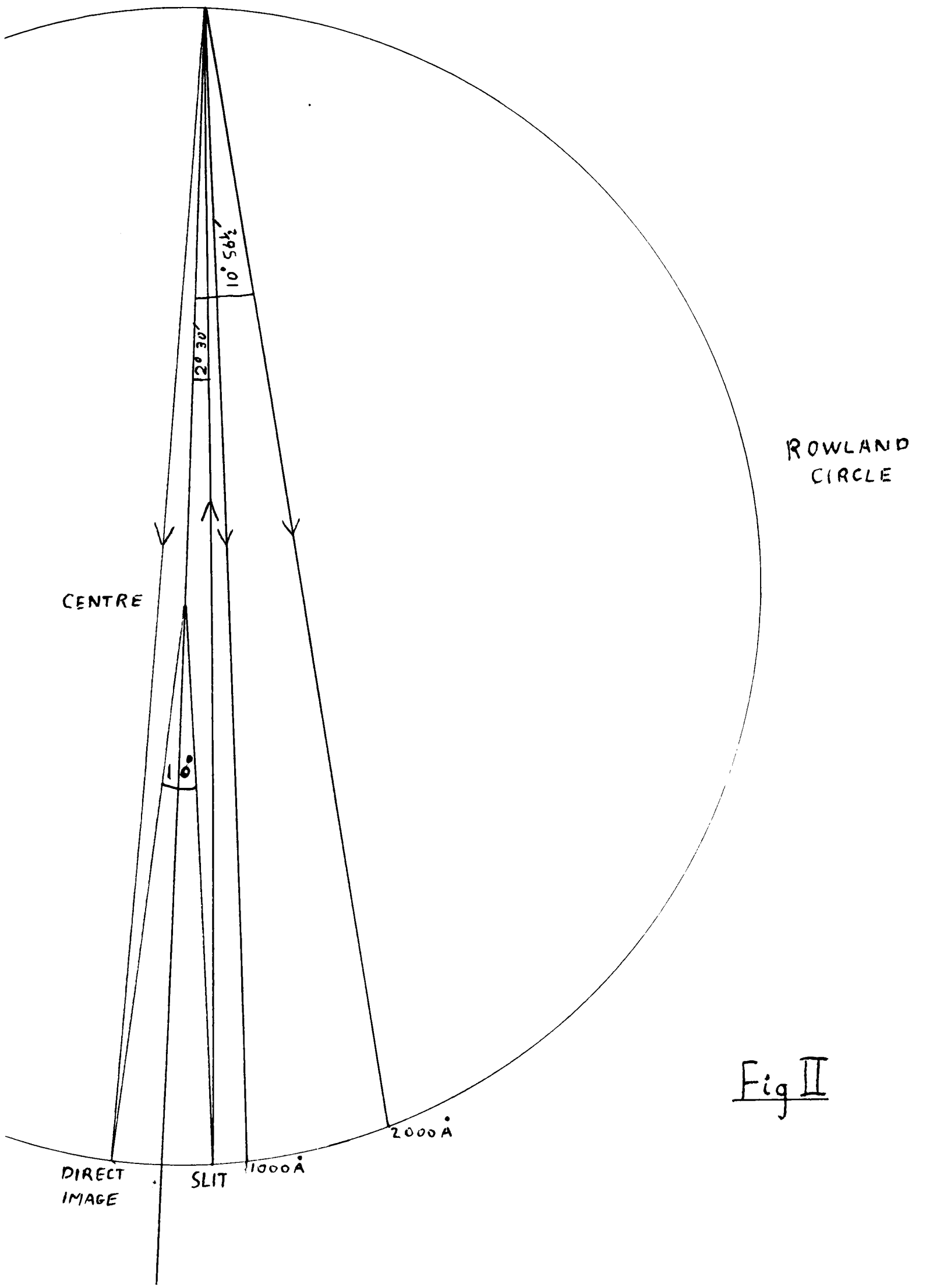

GRATING
POLE
10° 49½'
2° 30'
1°
ROWLAND
CIRCLE
CENTRE
2000 Å
1000 Å
DIRECT
IMAGE
SLIT

Fig II

values of the dispersion are thus:- 1000 Å - 8·56 Å/mm., 2000 Å - 8·44 Å/mm. at angles of diffraction respectively $4^{o}11\frac{1}{2}'$ and $10^{o}56\frac{1}{2}'$.

The Mechanical Arrangement.

Plan and Elevation of the spectrograph are given in figures I and III. The outer can is 35" long plus the 6" cap, this arrangement being dictated by the maximum length of object capable of being faced in our lathe, but it has the advantage that the grating may be adjusted or removed without moving the main can which supports the Dural girder. The flanges shown are of $\frac{3}{8}$" brass and carry grooves to contained the $\frac{1}{8}$" diam. gasket. This gasket is of sulphur-free rubber and is cut from a length, the ends merely being cut flat with a scalpel and pressed together. The shape of the groove is said by the makers of the gasket to be critical, for in this case the metal faces are intended to come together under vacuum and the gasket must then be sufficiently compressed. This system has the advantage of avoiding distortion of the metal faces, which may be bolted together, and these gaskets are used throughout the instrument.

The end-plate is 11" square and of $\frac{3}{8}$" brass, and to it are silver-soldered the plate holder box and slit-tube.

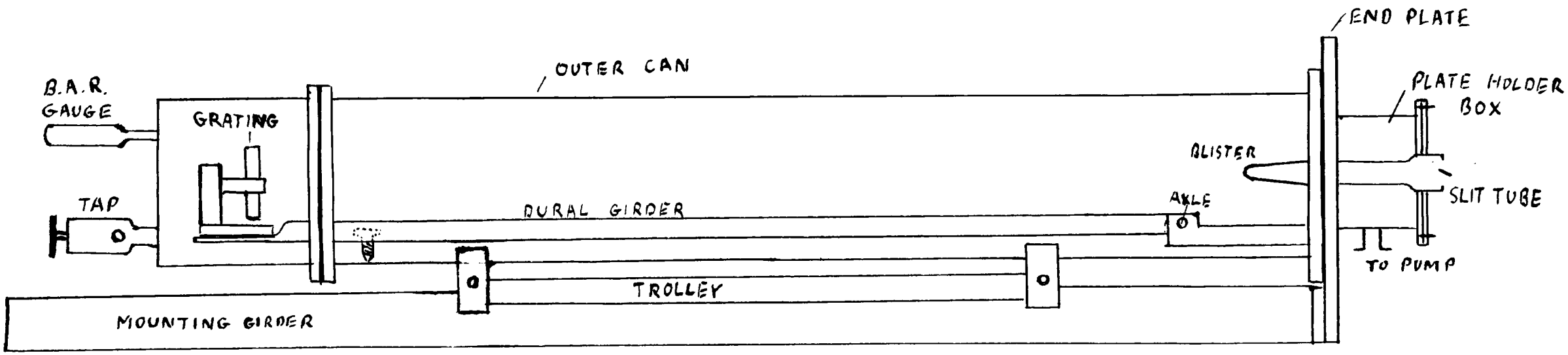

B.A.R.
GAUGE
GRATING
TAP
OUTER CAN
DURAL GIRDER
TROLLEY
MOUNTING GIRDER
END PLATE
PLATE HOLDER
BOX
BLISTER
AXLE
SLIT TUBE
TO PUMP

Fig III

To the end cap are attached a B.A.R. thermocouple pressure gauge and a needle valve to admit air. This is to improve on the earlier instrument where the air was let back through the pumping line, arousing a suspicion that a small amount of oil was getting back as well.

The spectrograph is mounted on a 4" × 2" channel section iron girder upon which the can is supported by a wheeled trolley so that it may be rolled back with ease. To one end of the girder is welded an 8" cross member to which the brass end-plate is bolted.

The End Plate

Plan and Elevation of this are shown in figures IV and V. There are cut away portions to allow light from the slit to reach the grating and light from the grating to reach the plate. The plate holder box is extended beyond the hole in the end-plate to allow more room for inserting the plate. In fig. IV can be seen the "blister" on the outer can and also slit tube with a tapered socket at its outer end. The vacuum seal between the plate holder box lid and its flange is by the $\frac{1}{8}$" gasket and ten bolts, and to the bottom of this box the pumping line is attached. Also shown here are the $\frac{1}{4}$" square rail and post on which the plate holder slides and to which it is finally fastened,

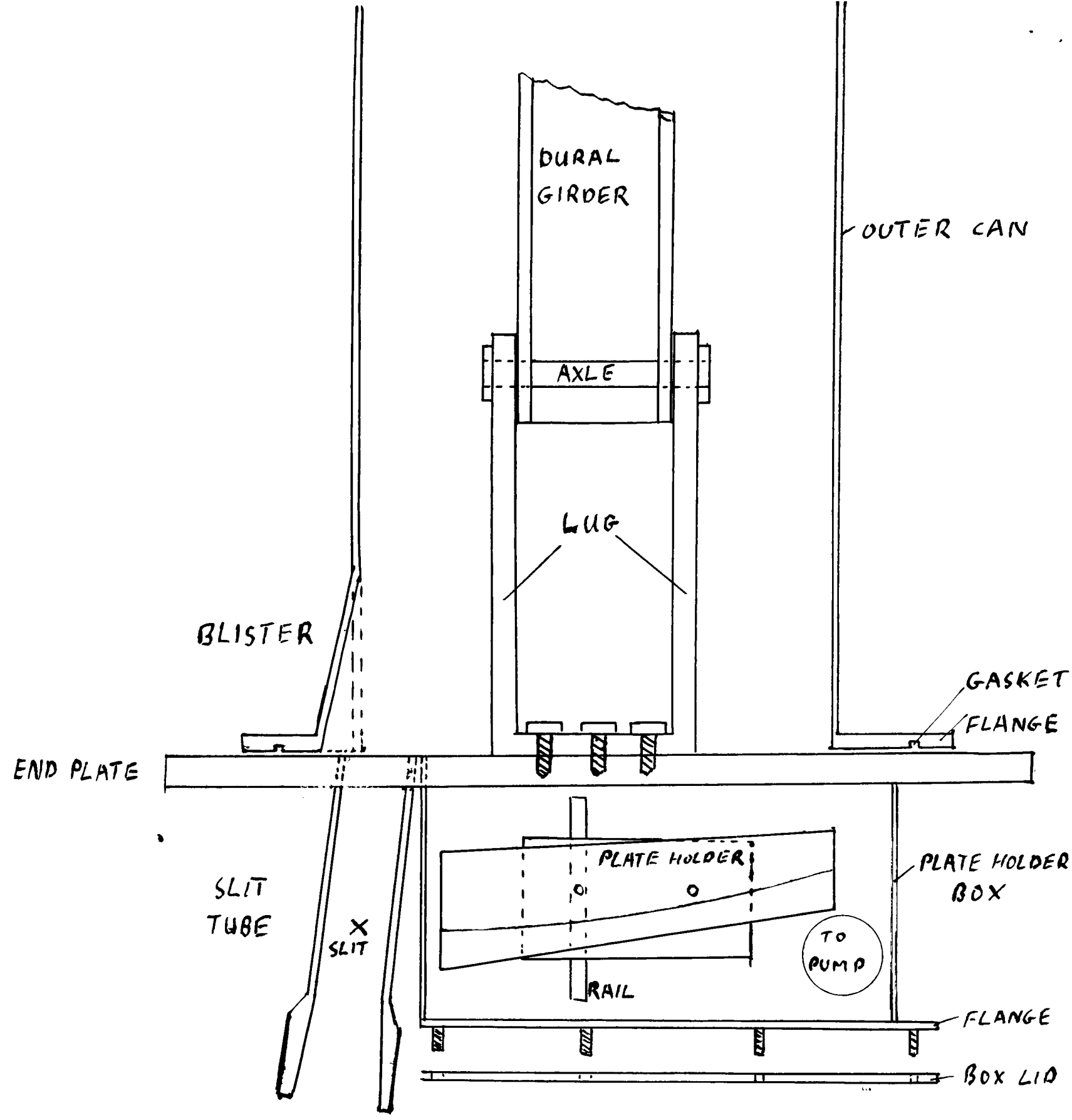

DURAL
GIRDER
OUTER CAN
AXLE
LUG
BLISTER
GASKET
FLANGE
END PLATE
PLATE HOLDER
PLATE HOLDER
BOX
SLIT
TUBE
SLIT
TO
PUMP
RAIL
FLANGE
BOX LID

Fig IV

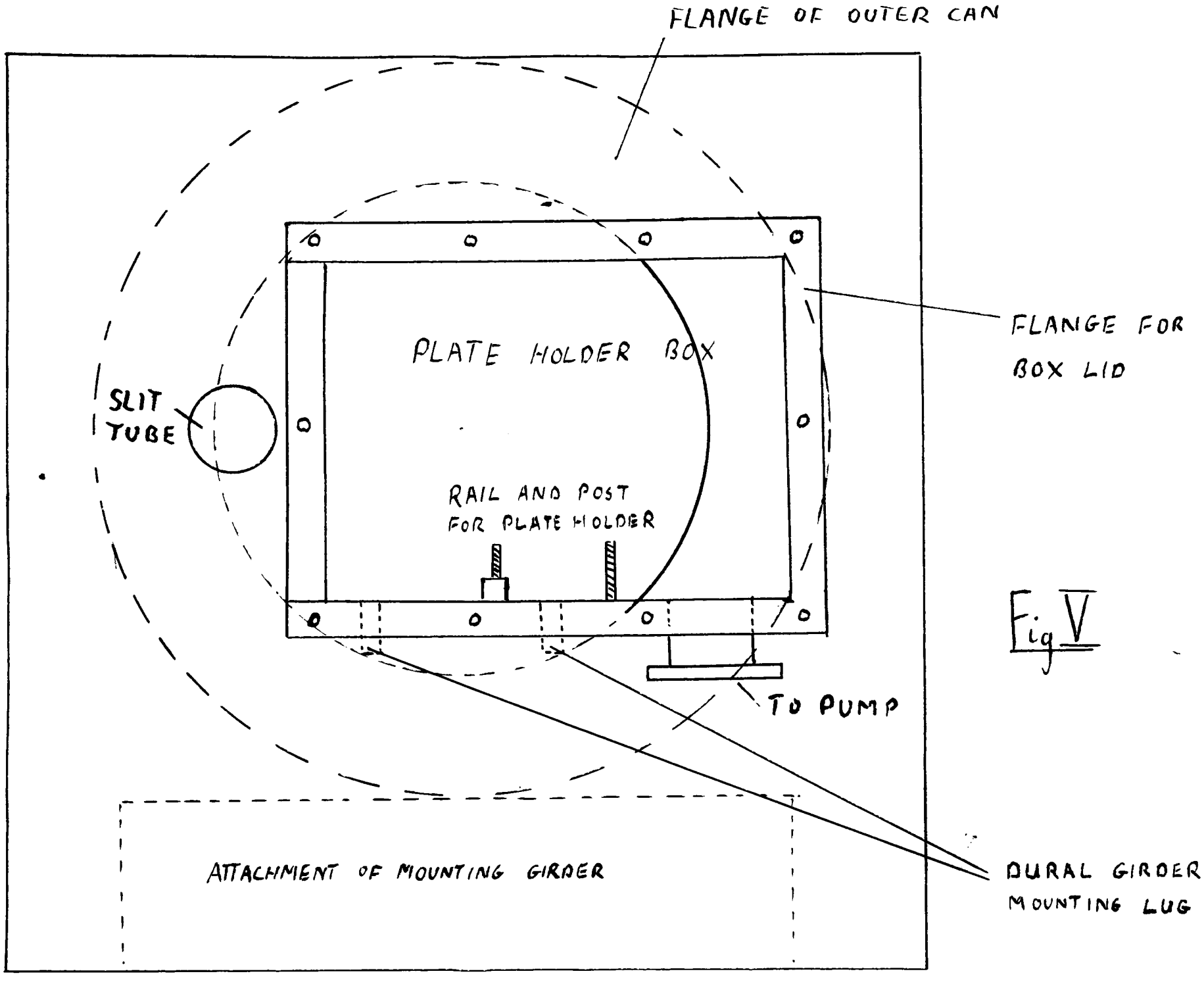

FLANGE OF OUTER CAN
FLANGE FOR BOX LID
PLATE HOLDER BOX
SLIT TUBE
RAIL AND POST FOR PLATE HOLDER
TO PUMP
ATTACHMENT OF MOUNTING GIRDER
DURAL GIRDER MOUNTING LUG

Fig V

as can be seen also in fig. VII.

To the other side of the end-plate is bolted the lug for mounting the Dural girder on which the grating is carried, but omitted from these diagrams are eight $\frac{3}{8}$" brass bolts for fastening the flange on the outer can to the end-plate.

The Slit Mounting

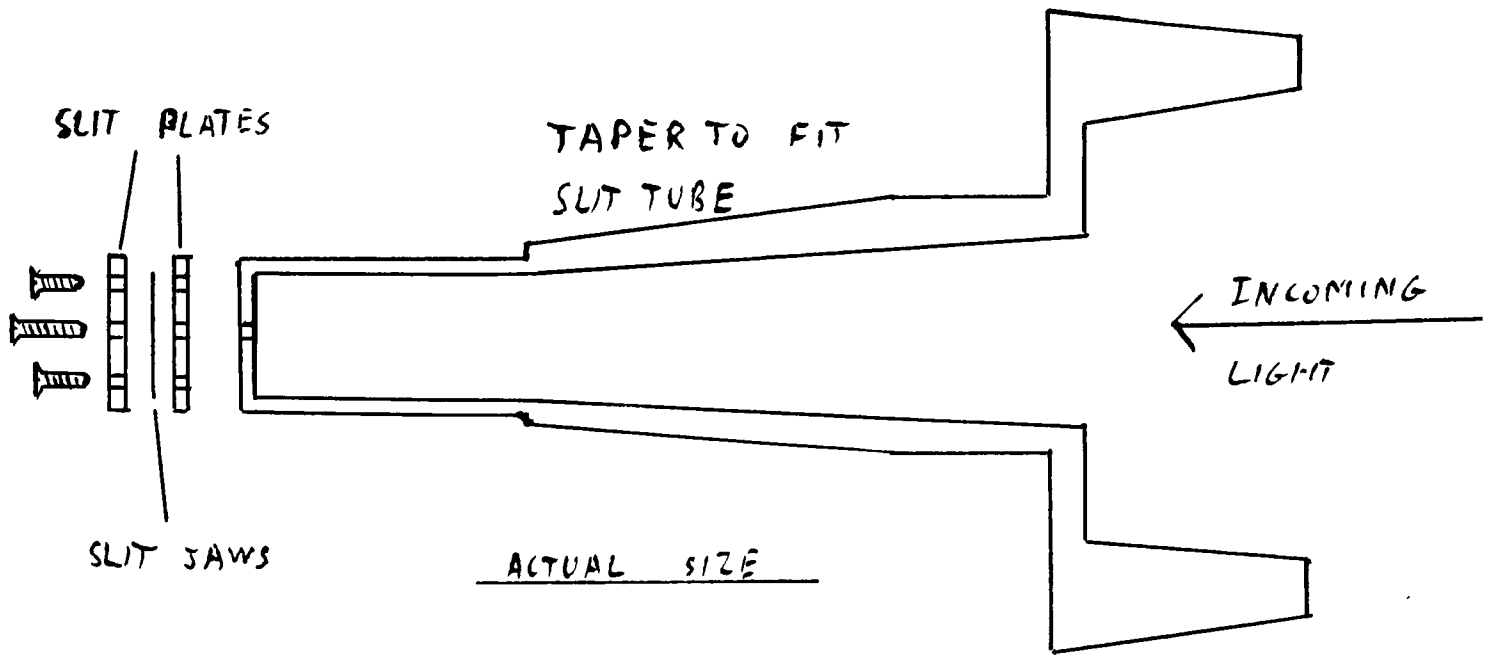
This is shown in fig. VI in cross section, the whole being turned from a brass block. The internal socket and external cone at the end remote from the slit are to fit parts of the grazing incidence instrument already existing; the internal one to take the mounting for an LiF window, the outer one to take a brass bellows for the collimation of light sources. It is noticeable that the portions which were attached to the older instrument are of much larger diameter than is necessary for the new, this is due to the dependence of optimum slit length on angle of incidence.

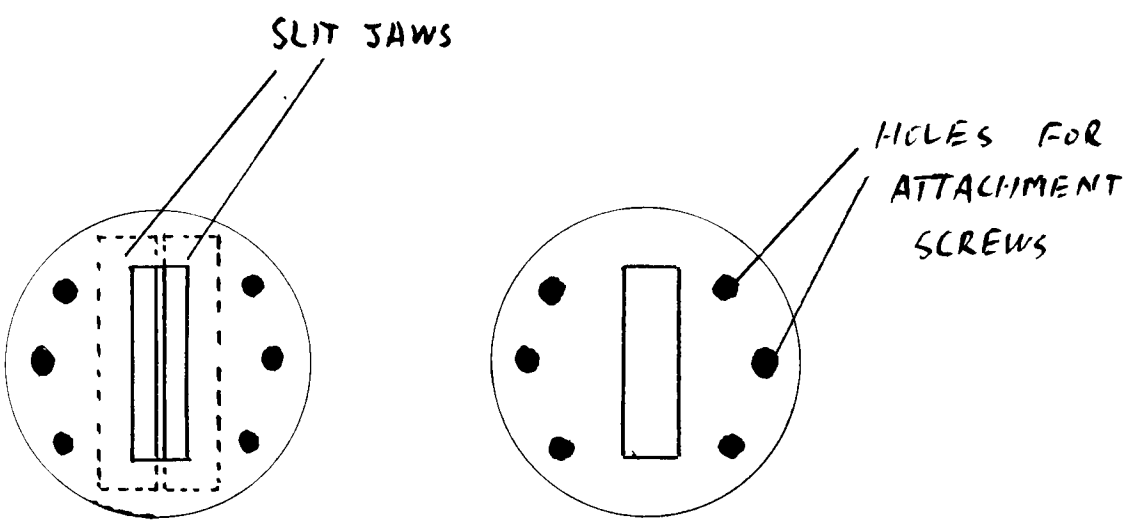
For any grating a point on the slit will be imaged in the focal plane as a line of length

$$z = k l = l\left[\sin^2\beta + \frac{\sin^2\alpha\cos\beta}{\cos\alpha}\right]$$

where α and β are angles of incidence and diffraction, and

SLIT MOUNTING





SLIT PLATES

TWICE ACTUAL SIZE

Fig VI

l is the length of the grating rulings. To obtain maximum brightness at the centre of the image the minimum slit length is $l\left[\frac{\sin^2\beta\cos\alpha}{\cos\beta} + \sin^2\alpha\right]$, and this increases rapidly towards grazing incidence. In fact for the older instrument and the speculum grating the slit length was 3·7 cm., whereas this normal incidence spectrograph requires a length of ·2 mm. at 1000 Å at 1·2 mm. at 2000 Å. For the glass grating the minimum required length is one-third of these values, so the actual slit length of 10 mm. gives an image of full intensity over almost this length.

It can be seen that no provision has been made for moving the slit at right angles to the Rowland circle, i.e. towards the grating. It is necessary only to provide the grating and the plate holder with such a movement and all three can be brought to the Rowland circle. However, the slit must be capable of rotation in its own plane in order to bring it parallel to the grating rulings and this is achieved by rotating the whole mounting in the cone and socket joint between it and the slit-tube. The movement is controlled by a side-arm and screw soldered to the mounting.

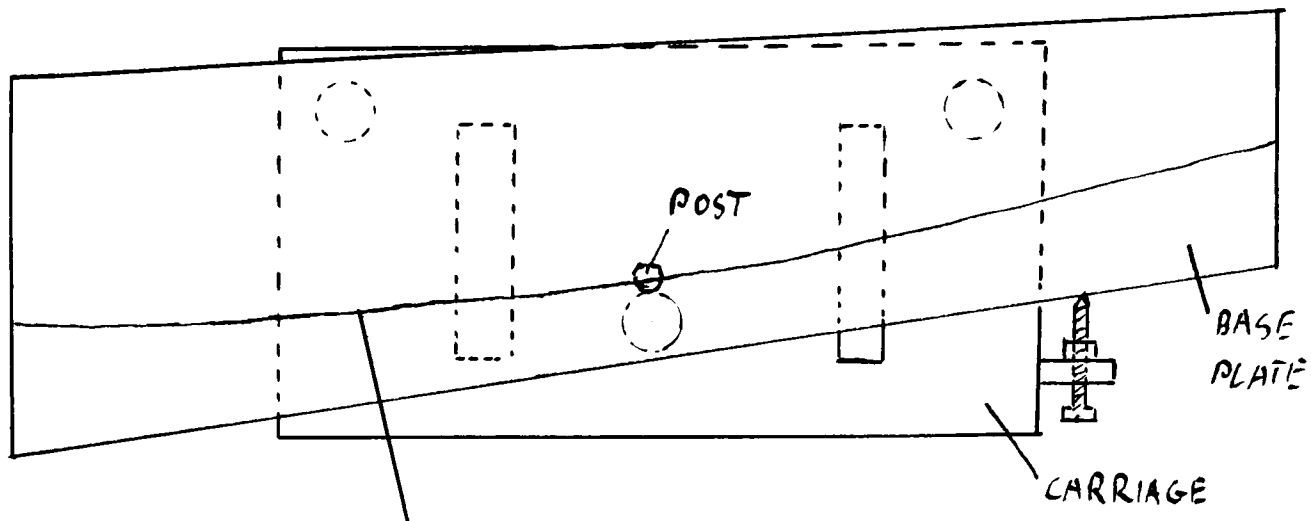
The slit jaws are made from razor blades, the best kind being the single edged as the double edged are barrel

shaped. Each new blade is lapped gently on a smooth carborundum stone and tested for straightness against an engineer's precision-made straight edge. A small amount of lapping appears to improve most blades, but continuing the process causes the edge to get worse and worse and it is desirable to stop at the optimum point. The best portions of two blades are then broken off and mounted under a high-power microscope between the slit plates; strips of copper foil are placed between the plates where the jaws are not, in order to prevent buckling of the plates which puts the two slit jaws out of the same plane. It is possible in this manner to construct slits as narrow as ·01 mm., although the one used in this work was about ·022 mm. wide. On the grounds of simplicity and space it was not possible to include a continuously controllable slit, however the great disadvantage of the present arrangement is that the jaws tend to rust and need replacement about once a year. A weakness in the design is the small cross-sectional area of the cone and socket joint between the slit mounting and the slit tube; unless only very lightly greased this joint continues to contract for some time after evacuation, causing the slit-grating distance to shorten and this point must be watched particularly when focussing in air.

The Plate Holder and its Carriage

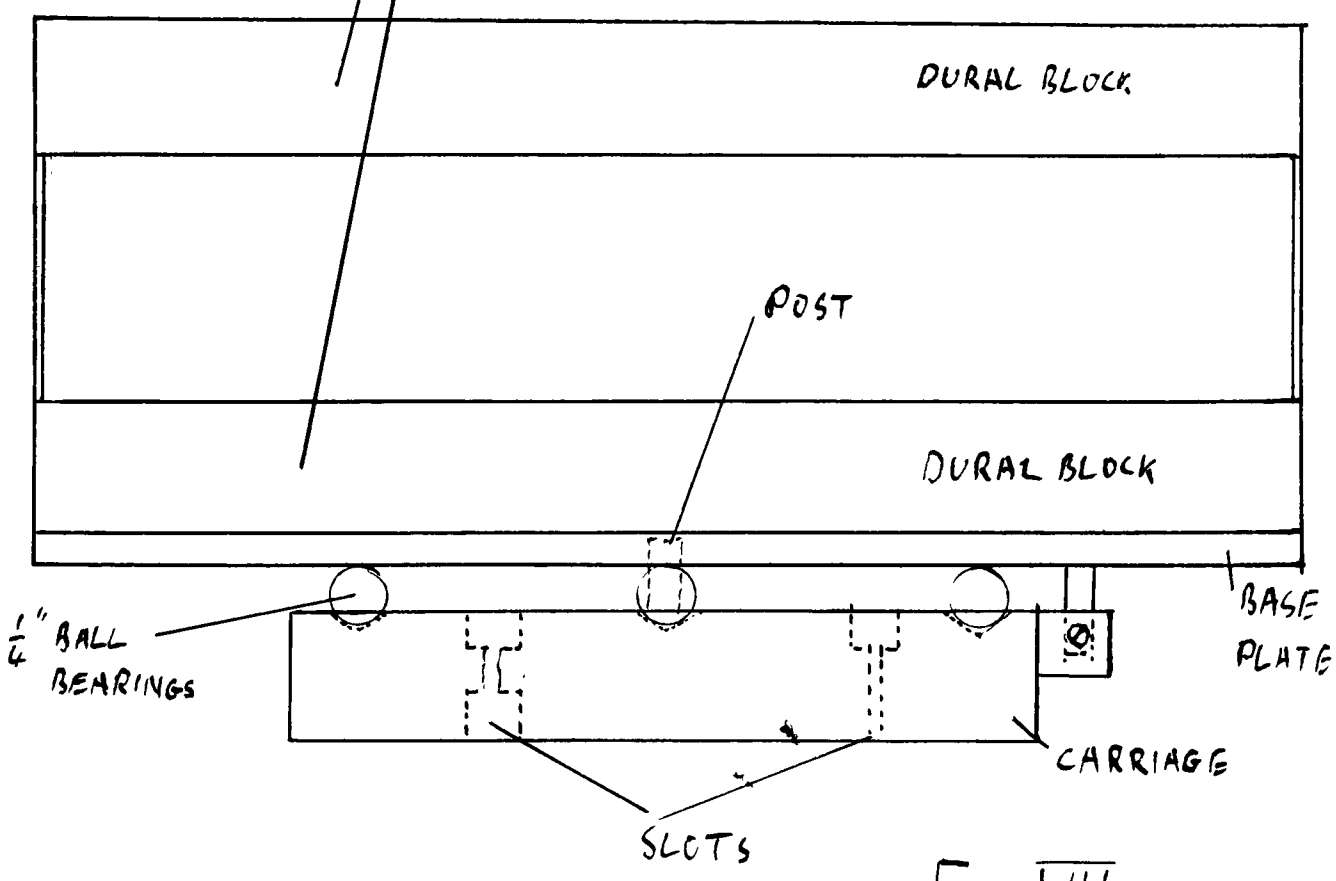
These are shown in fig. VII. The two Dural blocks [5" × 1" × ½"] have a curved 50 cm. radius cut on their rear faces, and against these faces the plate is held by a spring plate which is not shown. These two blocks are held apart by two plates [2·1" × 1" × 1/16" and 2·1" × ½" × 1/16"] at their ends, and through this gap of 5" × 1·1" the light passes from the grating to the plate.

It is necessary that the plate should be able to move in two directions, first along the axis of the instrument and secondly to rotate about a vertical line through its centre. Both of these are necessary in order to bring the whole length of the plate onto the Rowland circle. To obtain the second motion the Dural blocks are screwed to an ⅛" brass base plate [5" × 1½" × 1"] which rests on three ¼" ball bearings; upon these it may revolve about an ⅛" post set under the centre point of the plate. This motion is controlled by the screw and lug shown and may be locked in its final position by two screws holding the base-plate to the carriage. This carriage is of Dural [3" × 1½" × ½"] and has on its upper face the three ¼" ball bearings in their conical holes and the ⅛" post for the rotation of the plate holder. Its under side has a



PLAN

CURVED SURFACE OF 50cms. RADIUS AGAINST WHICH PLATE IS HELD.



ELEVATION

Fig VII

square groove cut away to fit the rail on the floor of the plate holder box, and two grooves cut right through the carriage enable it to be bolted firmly to this box when its final position is found (see also fig. V).

The Grating Mounting

It has been said that the grating was to be fastened to the same end-plate as the slit and plate holder in order to avoid length changes on evacuation. To do this it is necessary to have a beam down the centre of the can fastened to the end-plate at one end and carrying the grating at the other. Such a beam 40" long would be difficult to mount rigidly in so small a space, and so it was decided to make the beam flex in a controlled manner rather than risk gradual twisting or bending which would spoil the focus and alignment. A channel section Dural girder 36" long by $2\frac{1}{4}$" × 1" externally and $1\frac{7}{8}$" × $\frac{3}{4}$" internally was kindly provided by the British Aluminium Co. Ltd. of Banbury. This is mounted in a U-shaped lug bolted to the end-plate, the joint between girder and lug being by a horizontal axle as shown in figures I, III and IV.

At the end of the girder remote from the slit the arrangement is as shown in fig. VIII. The walls are cut away to allow the grating mounting to revolve; there is a

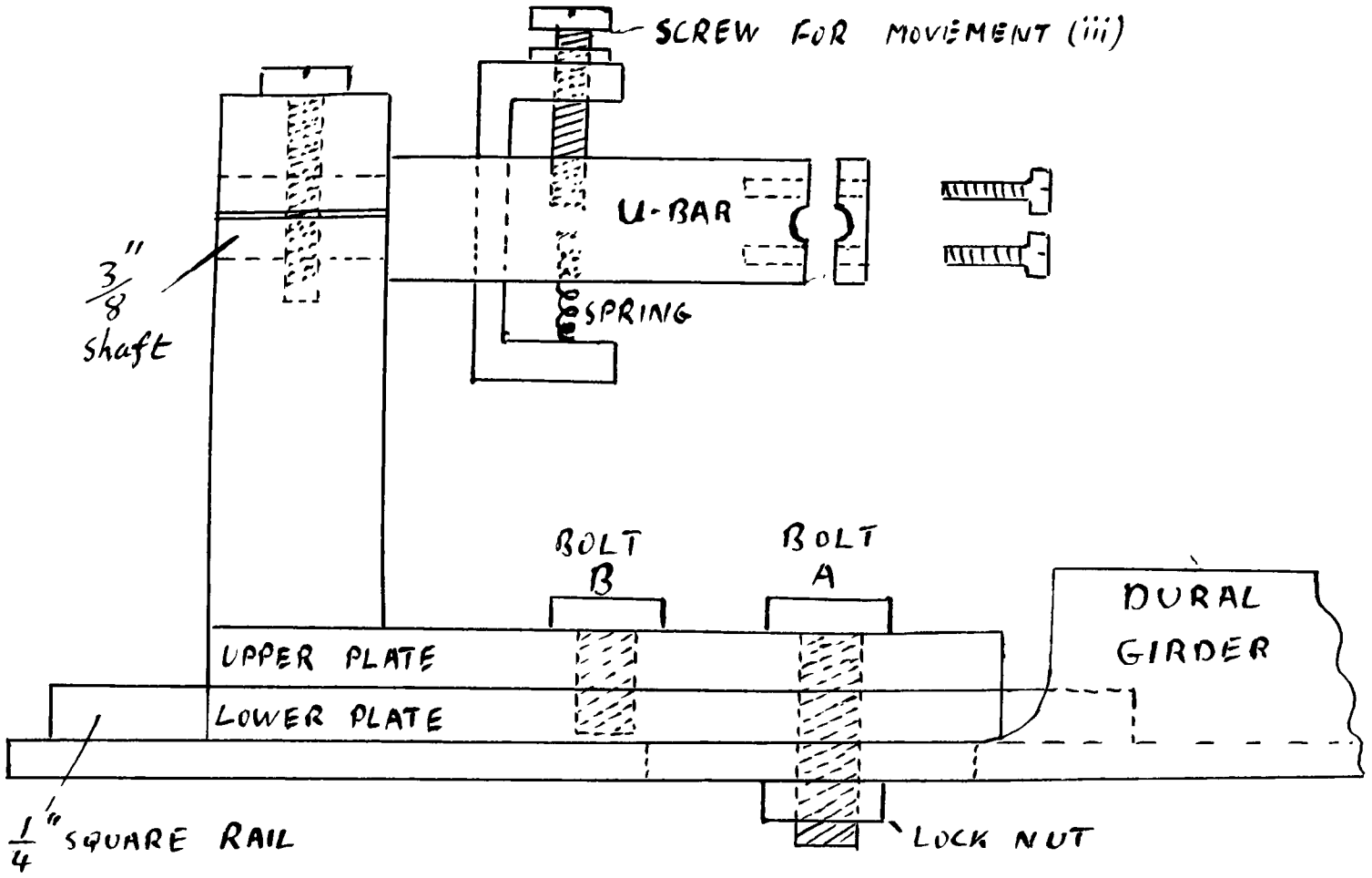
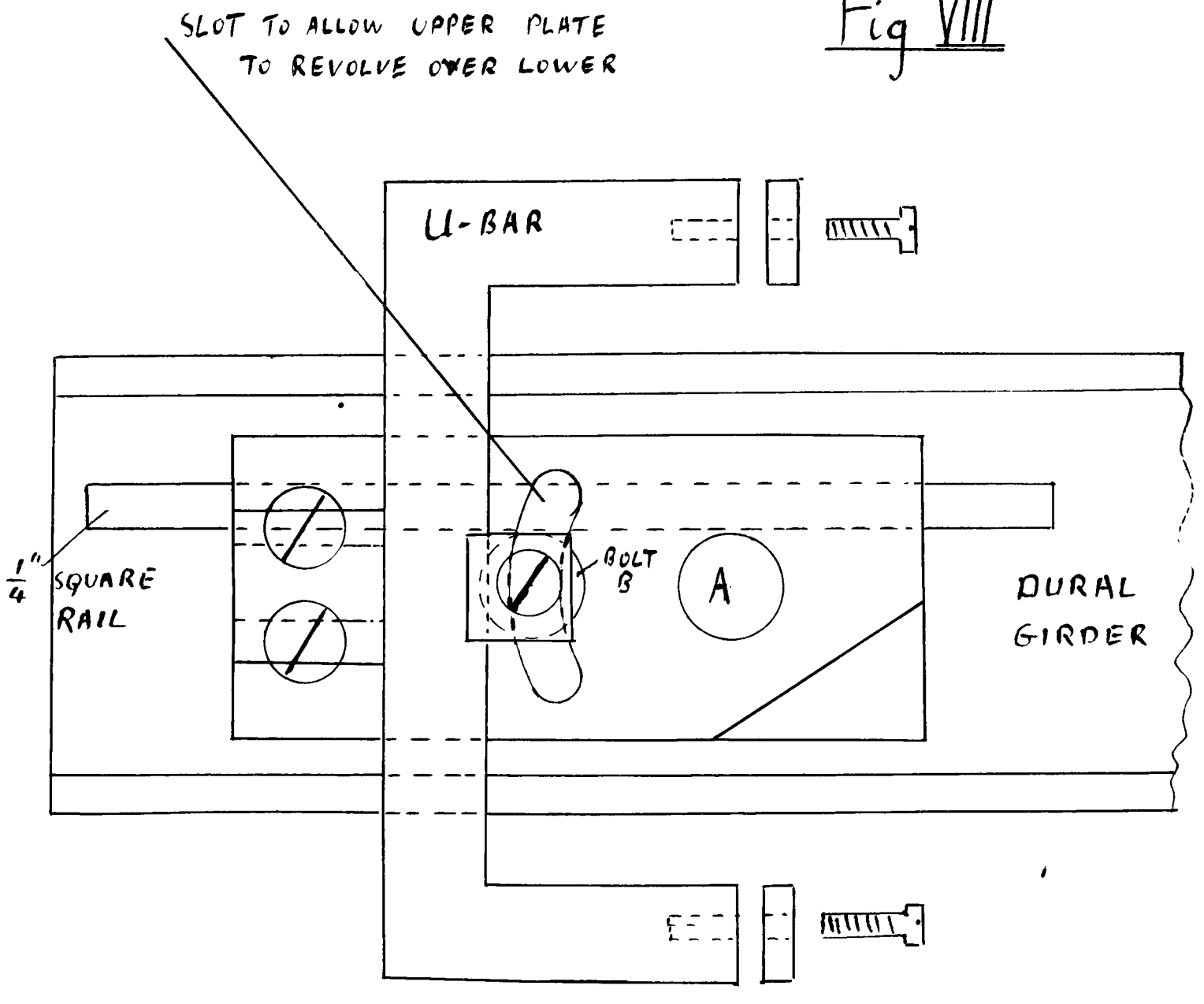
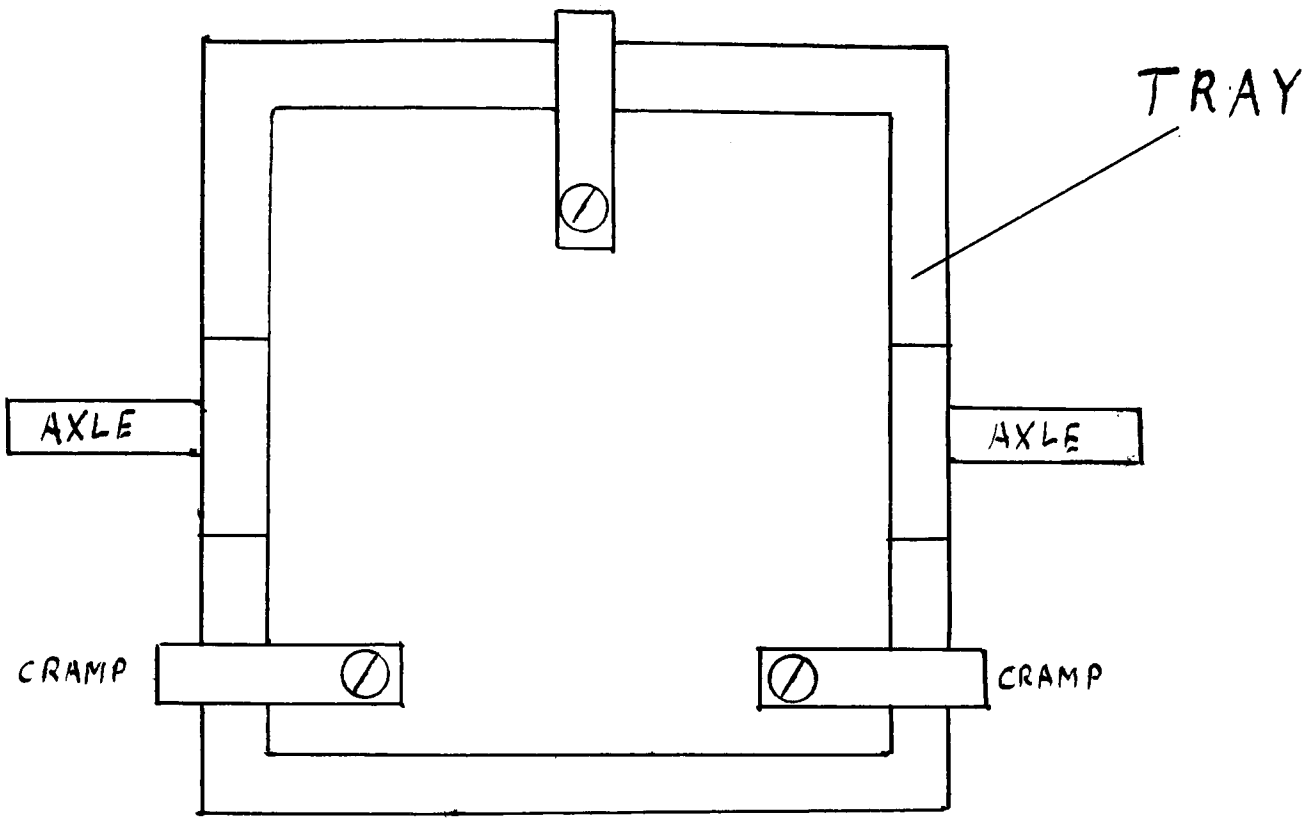
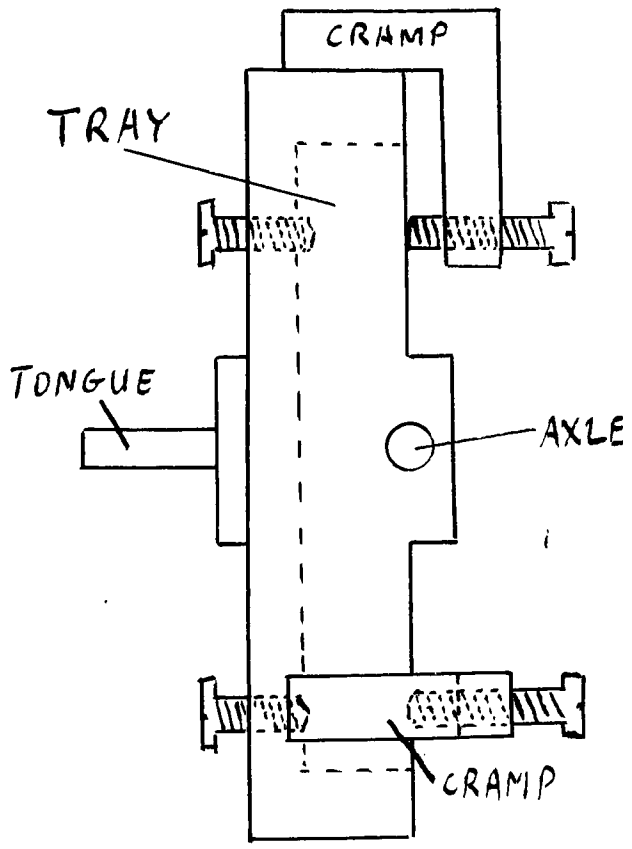

SCREW FOR MOVEMENT (iii)
U-BAR
SPRING
3/8" shaft
BOLT B
BOLT A
DURAL GIRDER
UPPER PLATE
LOWER PLATE
1/4" SQUARE RAIL
LOCK NUT

Fig VIII


SLOT TO ALLOW UPPER PLATE TO REVOLVE OVER LOWER
U-BAR
1/4" SQUARE RAIL
BOLT B
A
DURAL GIRDER

GRATING MOUNTING





ALUMINIUM BLOCK FOR GLASS GRATING

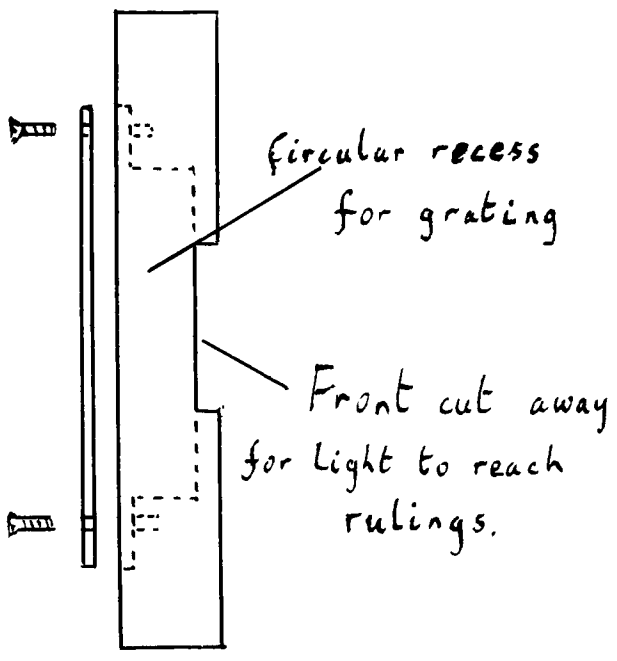


Fig IX

¼" square rail for the mounting to slide upon and a slot for this mounting to be bolted to the girder when the optics are finally arranged. In addition there is a knurled screw for raising and lowering the girder and grating as a whole.

Now the movements necessary for the grating are five, assuming that it is correctly mounted in its holder.

(i) Movement vertically to ensure that the grating pole, slit centre and plate are all in the same horizontal plane.

(ii) Movement approximately along its own axis to enable the grating pole to be brought to the Rowland circle.

(iii) Rotation about a horizontal chord at right angles to the rulings. This is necessary in order that the equatorial plane of the grating may pass through the slit centre, as both coma and curvature of the spectral lines increase on the square of the distance from this plane.

(iv) Rotation about the grating normal, both through small angles and through 180^{o}. The first is necessary to bring the rulings vertical after which the slit may be made parallel to them; the second is needed for three reasons,

(a) The selection of that side of the grating that gives most diffracted light.

(b) The mounting of the grating correctly in its holder.

(c) The operation known as "rolling" the grating.

(v) Rotation about a vertical axis through the grating pole. This is needed, together with movement (ii) to select the wave-length range required and in addition is needed for the operation of "rolling" the grating.

This "rolling" of the grating is needed on some instruments due to error of run in the rulings of the grating. This causes the focal curve to depart from the Rowland circle and to become an ellipse with its major axis inclined to the normal. Thus over one half of the circle the focal curve lies inside, and on the other outside. This can be corrected by "rolling" the grating round the Rowland circle so that a point not the pole becomes the point of contact, an operation requiring movements (ii) and (v). The best position is found by focussing on one portion of the spectrum only and rotating the grating through 180^{o} of movement (iv) to examine the two halves of the focal curve until they coincide. However, this operation is usually required for instruments having a large plate holder which can only be made circular, for this mounting of the grating in aberration can give excellent focus over 90^{o} of the Rowland circle. As the present instrument is a single position one the operation was not found necessary as the plate holder can be moved to fit the focal curve rather than the Rowland circle.

The grating mounting is shown in fig. IX. The speculum grating is ruled on a block 6·25 cm. square and 0·75 cm. thick and the glass grating, which is circular of 1·75 cm. radius and 0·6 cm. thick, was mounted in an aluminium block of the same size as the speculum grating in order that the two may be interchangeable. In either case the whole is fitted into a tray just large enough to hold it; from the back of the tray project three screws, against which the grating is held by three cramps. From the sides of the tray project two axles whose axis should lie through the grating pole, and it is about these axles that rotation about the horizontal chord of the grating is obtained (movement iii). As shown in figures VIII and IX the axles are clamped to the ends of a U-bar and movement (iii) is controlled by a screw against which the tongue projecting from the back of the tray is held by a small spring. From the back of the U-bar projects a $\frac{3}{8}$" shaft whose axis lies along the grating normal, and this shaft is clamped to the vertical post of the grating mounting. The small adjustment of movement (iv) is obtained by rotation about this shaft, the 180° movement by unclamping the whole tray and reversing it.

The vertical post is fastened to the upper of two $\frac{1}{4}$" Dural plates which rotates over the lower plate about the

bolt A, being fastened by the bolt B. The bolt A is vertically under the grating pole and rotation about it provides movement (v); the two plates sliding together on a square rail on the Dural girder provide movement (ii), this being locked by a nut on bolt A through a slot in the girder. The vertical movement (i) is caused by raising the whole girder by means of a knurled screw acting on the bottom of the vacuum can.

The Pumping Line

The grazing incidence spectrograph was evacuated by means of a short 1¾" internal diameter pipe to a Metrovac O 3B oil diffusion pump backed by a Speedivac single-stage rotary pump. It was desirable to use the same pumps to evacuate the new spectrograph also, and this entailed the use of taps of large bore to shut off either instrument. It is essential to keep the bore of the pumping line on the low pressure side of the diffusion pump as large as possible, otherwise the pumping rate is rapidly reduced. To this end a tap was designed of the flap-valve type where the flap was moved on and off its seating by means of a screw sealed to the atmosphere by a Hydroflex metal bellows. The design is shown in fig. X, and due to the size of the bellows the maximum permitted lift is ½".

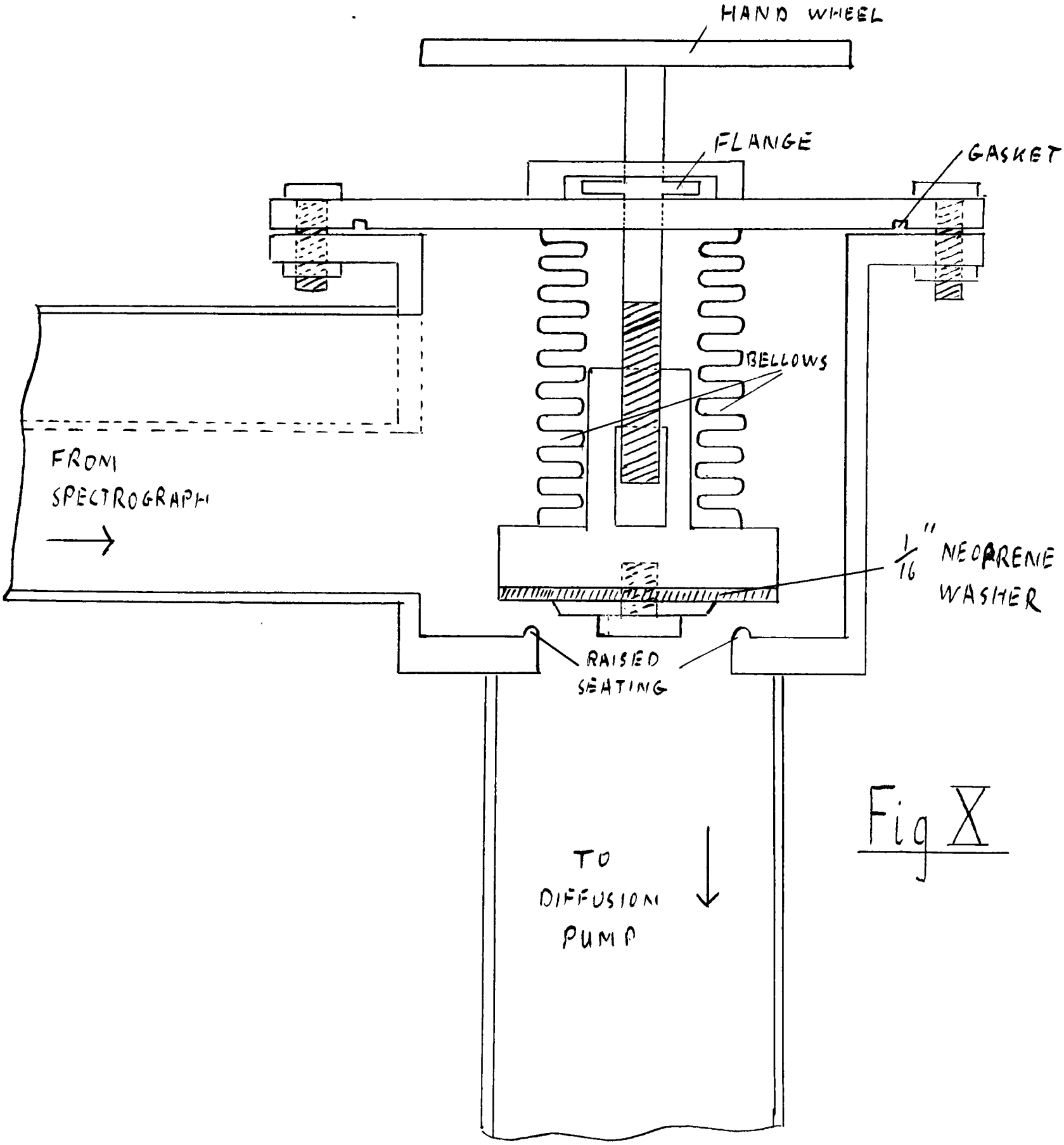
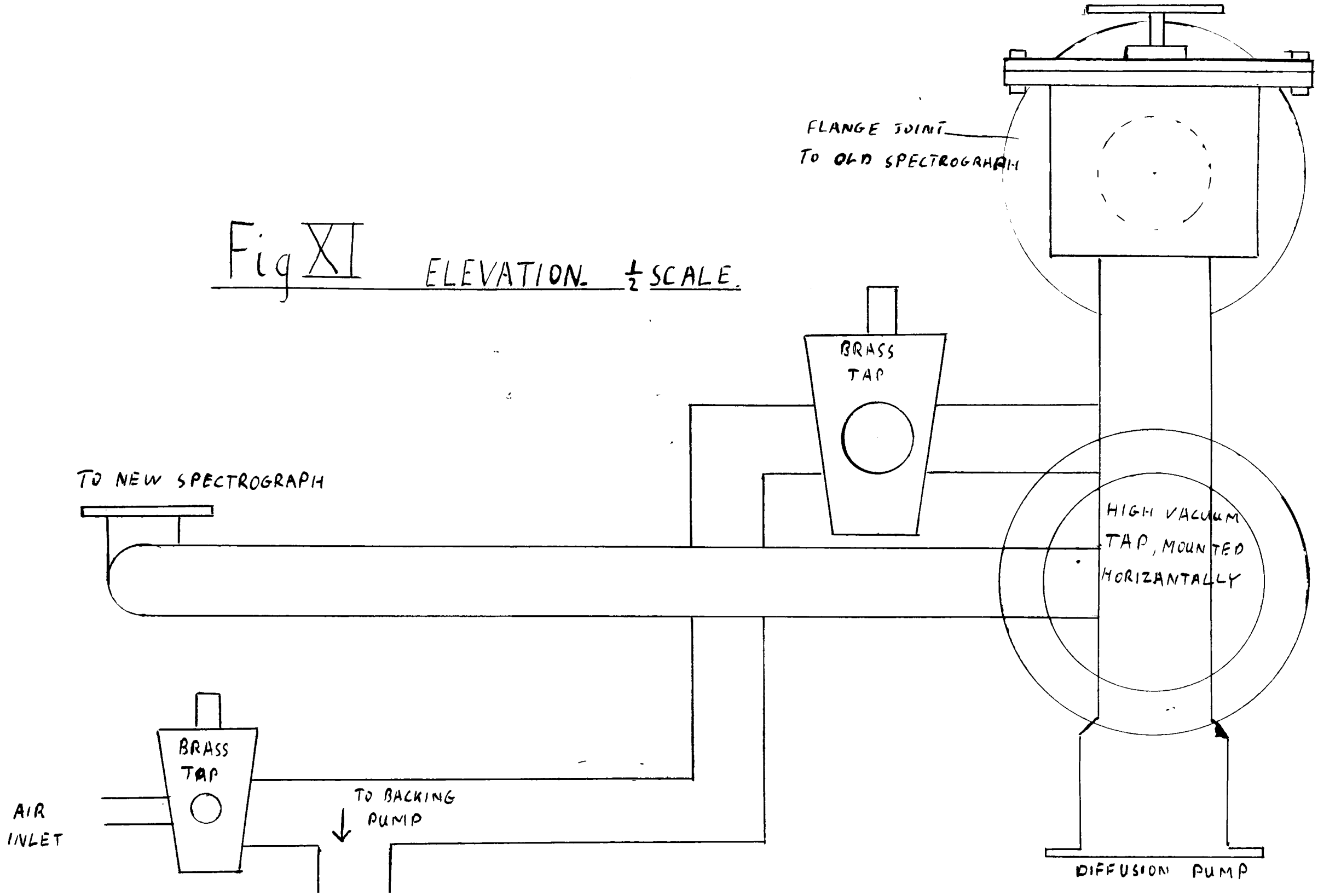

HAND WHEEL
FLANGE
GASKET
BELLOWS
FROM SPECTROGRAPH
1/16" NEOPRENE WASHER
RAISED SEATING
TO DIFFUSION PUMP

Fig X

However, this leaves the area through which the gas is pumped at almost 2 sq. in., equivalent to a tube of diameter over 1½". The seal is by a $\frac{1}{16}$" Neoprene washer onto a raised circular projection on the tap base. The gasket is attached to the moving portion of the tap and the necessary freedom to allow it to seat properly is given by undercutting for $\frac{1}{20}$" below the threaded portion. The movement of the tap is limited by the end of the operating screw coming up against the upper side of the flap.

The arrangement of the pumping line is shown in fig. XI. The oil diffusion pump is retained in the same position as before, but the backing line and the air inlet tap had to be lowered by 6" to avoid the new high vacuum line. The two brass taps shown are of similar design to ordinary glass taps and are most unsatisfactory. The flange and bore of the old high vacuum line remain the same, but the bore of the new line is 1" as the volume to be evacuated is only one-sixth of that of the earlier instrument.

Fig XI ELEVATION. ½ SCALE.



Assembly and Adjustment of the Spectrograph

The assembly of the spectrograph follows obviously from the details given of its design. The grating was placed in its holder so that its normal bisected at right angles the line of the axles on its tray. The method of doing this has been adequately described by Downie[1] p.44. The nuts on the axle fastening the Dural girder to its mounting lug were tightened until the girder could just be moved vertically but no horizontal play was possible at the end where the grating is mounted. The $\frac{1}{8}$" vacuum gaskets were cut sharply at right angles to their axes, and made somewhat longer than the grooves they had to fit, so that a little compression was necessary to push them in. This apparently helps to make the joint air-tight, and no trouble has been experienced with these gaskets except physical decomposition causing them to become brittle and need replacing every six months or when dismantled, whichever is the longer.

As much as possible of the focussing of the spectrograph was done in air, and for this purpose the slit was illuminated by a tungsten band-lamp. A fairly wide slit of 0·06 mm. was employed and the correct collimation of the lamp observed before focussing the lamp on the slit with a quartz lens . First of all the height of

the grating was adjusted in order that the axis of the instrument may be horizontal (movement (i)), and then movement (iii) was considered. For this purpose the grating was revolved until the reflected light giving the direct image fell on the slit plates, and careful adjustment of the screw pressing on the tongue on the back of the grating tray caused this image to fall alongside the slit on the same horizontal level.

The next adjustment was to bring the grating onto the Rowland circle and to select the wave-length range, movements (ii) and (v). The best way of doing this with reasonable accuracy is by fixing the position of the direct image. From fig. II it can be seen that the distance between the slit and the direct image is $2 \times 50 \times \sin 5^{\circ}$, and this is 87·16 mm. Similarly the distance of the direct image from the normal to the optic axis which passes through the slit is $87{\cdot}16 \times \sin 5^{\circ} = 7{\cdot}60$ mm. These distances may be measured to perhaps ·2 mm. with calipers and a pin fixed at the point desired. The grating was rotated until the tip of the pin was illuminated by the reflected light and then moved along the Dural girder until the direct image was focussed at the pin. This was rather a tedious procedure as each horizontal movement of the grating had to be accompanied by an equivalent

rotation, but by use of a high-powered microscope focussed on the pin, the position of the direct image could be fixed with great sensitivity. It was next desired to adjust the slit tilt until the slit was parallel to the grating rulings. This instrument is much less sensitive to slit tilt than the grazing incidence one due to the greatly reduced length of image given by any point on the slit. Any error in this adjustment results in the lines on the plate going out of the vertical before any large increase in width is observed. However, a sodium lamp was focussed on the slit instead of the band-lamp and the sodium doublet in the yellow could be observed on the Rowland circle about 70 cm. from the end-plate. With some trouble a high-powered microscope could be focussed on these lines and the slit tilt adjusted until they were extremely sharp.

It was thought that the position of the plate holder could most easily be adjusted photographically, and for this purpose it was brought roughly to the Rowland circle by means of a ruler. The sodium lamp was replaced by a copper arc and a plate taken of the copper lines between 2000 Å and 1850 Å. These came on the correct portion of plate indicating that the long-wave limit of the instrument was about 2060 Å, and were sufficiently in focus for adjustments

over a longer wave-length range to be made. For this purpose a discharge tube source was put before the slit, separated by the lithium fluoride window. The tube was of silica of 2·5 cm. bore and had two internal electrodes with a constriction in between. The discharge was excited by a 4000 V. 2 K.W. transformer and when running in air at approximately 5 mm. pressure gave plenty of bands due to N_2, NO and CO in the region between 2060 Å and 1350 Å. These were photographed on Ilford Q2 plates and the plate holder carriage moved along its rail until the centre of the plate was in best focus. The time taken to evacuate the spectrograph between exposures was approximately ten minutes, quite small compared to the time taken to process a plate, dry it and consider its focus relative to those of previous plates.

When the centre of the plate was in the correct position the plate holder carriage was fastened down by the bolts provided and the plate holder itself rotated on its post and ball bearings until the best focus along the whole length of the plate was obtained. This in turn was screwed to the carriage and these adjustments have not subsequently been touched, in fact the resolution of the instrument is considerably better than that obtainable on Ilford Q2 plates, as can be seen from the plate reproduced

later on the Rydberg series of tin (see p.89). When the slit is removed for adjustment it is desirable to check the slit tilt after replacement by a copper arc photograph; this is not necessary after mere cleaning. It is of interest that the copper arc plates have two weak features at about 1600 Å of self-reversed lines, and this can only be the copper resonance lines at 3248 Å and 3274 Å appearing as a half order due to some irregularity in the ruling of alternate lines on the glass grating.

The Problem of Scattered Light.

At the stage in the focussing described above when copper arc plates were first taken it was found that the light scattered inside the spectrograph completely blackened the plate. The majority of this was the light reflected from the grating towards the direct image and then scattered from the side of the vacuum can. The whole of the inside of the spectrograph was painted with matt black paint, but this reduced the scatter very little. The next step was to place a baffle in front of the grating so that light fell only on the ruled portion, and to mount two baffles in such a position that all the light travelling towards the direct image hit their faces remote from the plate. All these baffles were attached to the Dural girder so that the

vacuum can may be withdrawn without disturbing them. These measures cut the scattered light to quite small amounts, however for absorption work it is desirable to have no background, and a further baffle was constructed to prevent light from hitting the surface of the baffle in front of the grating. It has been a principle that any stray light reaching the plate must have been scattered from a blackened surface more than once. This last baffle is circular of about 5½" diameter and is mounted on the Dural girder 36 cm. from the end-plate. In it are cut two rectangular holes, one of 1·4 x 0·6 cm. allows light from the slit to reach the grating and the other of 10 x 2 cm. allows light from the grating to reach the plate. From between these two a further vertical baffle runs to the end-plate between the slit tube and the plate holder box, and this last one is made in two pieces to allow the girder to flex at its axle. Thus the light from the slit enters an oblong box and only that light which is travelling towards the ruled portion of the grating is allowed to leave through the smaller rectangular hole. By these means the scattered light reaching the plate has been cut down to negligible proportions on all except the longest exposures on low-contrast plates.

The Photographic Plates

During the course of the work on the grazing incidence instrument Ilford plates were used of three different emulsions, Q1, Q2 and Q3. These are Schumann plates in that they contain sufficiently little gelatin to be sensitive down to at least 900 Å, but they are sold ready for use and require no special treatment other than rather more careful handling than is necessary with ordinary emulsions. They were all coated on special thin plate glass, 5" × 2", in order that they should follow the curve of the plate holder, and after exposure those that were not to be preserved were returned for recoating. It was found that Q1 plates were too slow for our purpose, and Q3 were extremely blotchy and had too large a grain-size; thus the Q2 emulsion had come to be used as our standard plate.

However, in the summer of 1952 it was discovered that the Kodak Research Laboratory were producing an experimental far U-V plate and they very kindly provided some samples. Preliminary tests showed that these were greatly superior to the Q2 plates; they were only slightly faster but gave so much greater contrast and smaller grain-size that absorption bands and particularly lines that were quite invisible on Q plates were readily measured on the Kodak

ones. In the section on the spectrum of GeO prints are given of the same bands photographed on the two plates. However, the better plates had their disadvantages, amongst which is the method of use which will be detailed below and is extremely laborious. Also at first Kodaks could only coat thick glass with this emulsion which meant that the plate was only properly in focus at one point, but such is the depth of focus of the instrument that these plates can in fact be used over two or three hundred Ångströms without difficulty. The greatest disadvantage of the Kodak plates was their lack of reproducibility. Frequently plates were fogged or had faults in the emulsion causing large streaks or complete holes to appear in the spectrum, and they are all very sensitive to changes in conditions of development.

The method of preparation of the Kodak plates is secret, but the idea is to coat the plates with a suspension of silver bromide in a very thin solution of gelatin. The plates are then laid flat and on hardening of the gelatin the majority of the silver bromide is concentrated in a layer near the surface of the glass. In order to use the plates in the Schumann region the gelatin is washed away with warm water and the nearly pure bromide left behind. Thus during and after

processing the plates are extremely delicate to handle and even when dry are scratched by the slightest contact. The method of sensitization of the plates is as follows:

(i) The plate must be held during processing and it was originally suggested by the manufacturers that the plate should be attached to another by adhesive tape. This is probably a bad idea as is explained below.

(ii) The plate is immersed for two minutes in a fog-clearing bath consisting of 2 gm. potassium ferri-cyanide and 1 gm. potassium bromide in 100 c.c. of water, and then washed for two minutes in running water.

(iii) The gelatin is washed off in water between 41° and 43°C. For this purpose a two-litre beaker filled to the brim is used, and the plate is immersed at right angles to the plane of the safe-light in order to minimize the risk of fogging. After 30 seconds immersion the plate is raised slowly so that the meniscus scours the gelatin from the surface. This movement should take 5-7 seconds and be repeated twelve times. Finally the plate is withdrawn from the water much more slowly, taking perhaps 30 seconds, and the surface tension draws off most of the adherent water leaving no drops.

(iv) The plate is placed in the dry-box which is carefully wrapped in black cloth and there it is allowed to dry on filter paper for fifteen minutes. A slow current of air may be passed through the box.

The developer used is Kodak D 76 d, a buffered borax semi-fine grain developer to which is added a special anti-fogger solution provided by Kodak. At 21°C caution is required to use this developer, the plate must be carefully watched until the maximum contrast is obtained without excessive fog. This takes some four to eight minutes and the temperature must not be allowed to fall below 21°C as this reduces the speed of the plate without reducing the fog.

The initial samples of these plates were found to be insensitive below 1800 Å. This was thought to be due either to absorbed water or to ageing of the fog-clearing bath. Later it was discovered that the major factor was absorption of light by some grease from the adhesive tape which softened in the warm water and coated the plate. In this spectral region many greases have very high extinction coefficients and for this reason it is desirable that the fingers should not touch the surface of the water. Both these difficulties were overcome by the use of a little wire holder.

Recent samples of this emulsion have suffered very badly from fogging, as many as two out of three of the plates were useless on development. It seems likely that this was due to the developer; previously this was

used in the usual manner as a stock solution and this method was quite satisfactory with several batches of plates. In future, however, it will be desirable to develop each plate in a separate sample from a fresh unopened bottle.

In spite of the disadvantages of this Kodak plate all the spectra measured in this work were recorded on them. It now seems likely that Q1 emulsions may again be of use as their slowness is compensated by the increased speed of this spectrograph. They do not give quite as high contrast as the Kodak plates but they produce a much cleaner image and are perfectly reproducible.

The Lyman Source

There are three known sources of continuous radiation at wave-lengths shorter than 2000 Å. The hydrogen continuum from a heavy-current discharge tube extends to 1650 Å, the Hopfield He continuum can be produced with good intensity from 900 Å to 600 Å, but it is only the Lyman discharge tube which covers the whole range. This consists of a heavy-current condensed spark through a capillary of quartz or alumina; the origin of the continuous emission is not certain but it seems likely that it is particles from the walls raised to a very high temperature, for the continuum is independent of the gas in the tube. Lyman sources have been described by many workers[3,4,5], but a fairly simple tube designed in an earlier work[2] has proved satisfactory for this, with one notable improvement. This tube is illustrated in fig.XII, and the improvement is in the design of the outer electrode. The two disadvantages of all Lyman sources are that the capillaries rapidly become bored out and that the powder produced covers the slit of the spectrograph. The first is overcome by making the central tube demountable through the B19 cone and socket and the second by the redesigned outer electrode. Previously this was cylindrical and powder was scattered copiously throughout the apparatus, however the provision of the

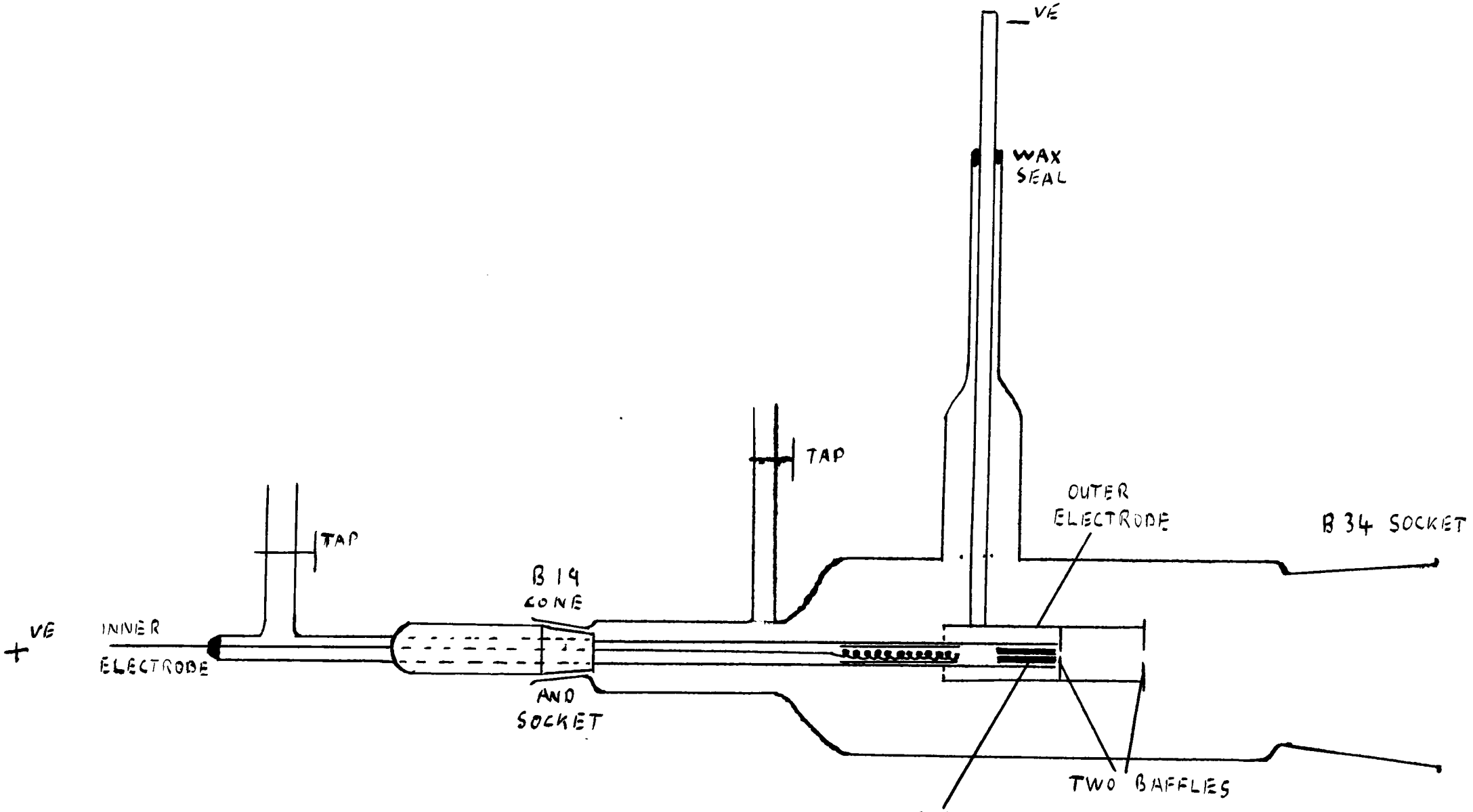

VE
WAX SEAL
TAP
OUTER ELECTRODE
B 34 SOCKET
TAP
B 19 CONE
+VE
INNER ELECTRODE
AND SOCKET
TWO BAFFLIES
SILICA CAPILLARY
HELD IN PLACE BY ASBESTOS WOOL

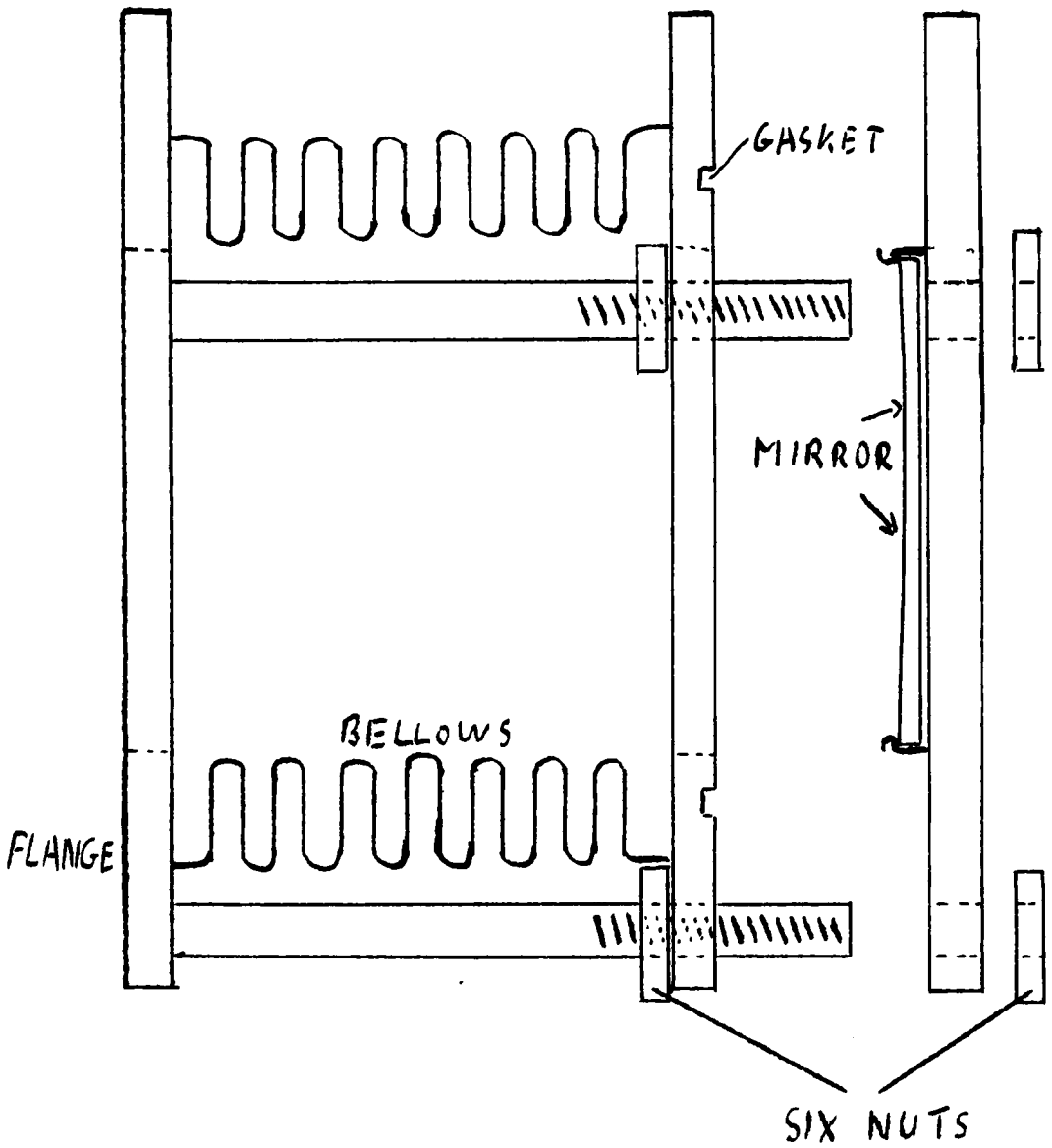
FIG XII

double baffle has greatly reduced this trouble. It is interesting that after the baffle was put in place the lines of silicon in the discharge appeared in absorption rather than emission, except for highly excited Si III and Si IV.

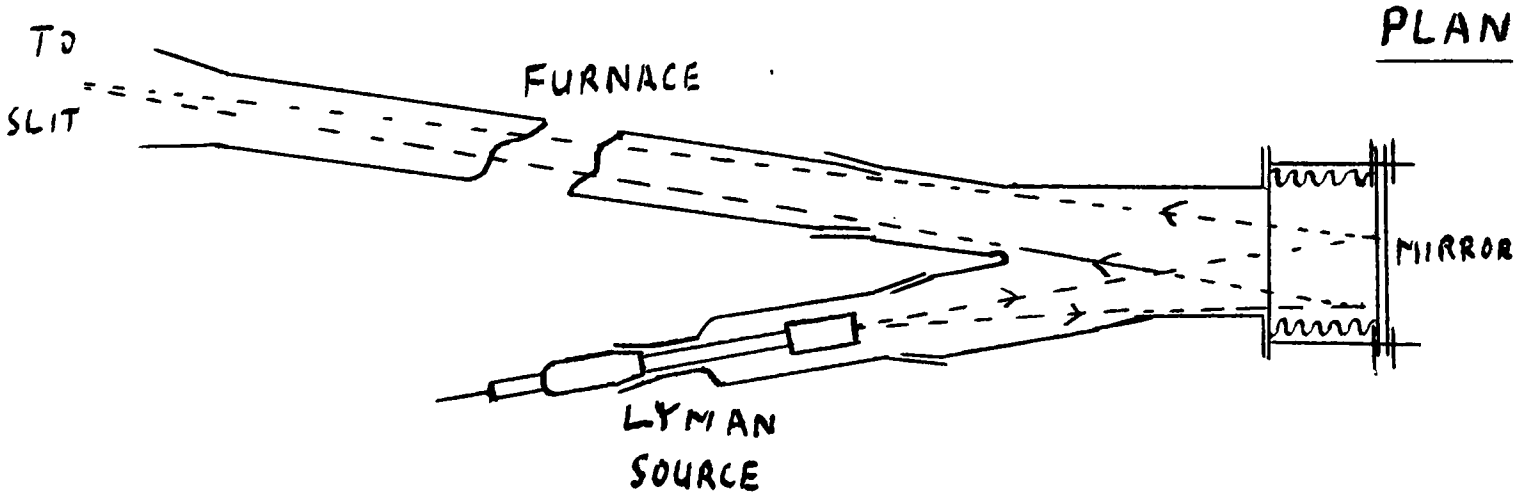
The electrical arrangements were unchanged; a 6 μF condenser bank is charged to 8000 V. by a voltage-doubling circuit from a 4000 V. transformer. A Variac in the primary enables the output voltage to be increased slowly although some care is necessary to prevent surges with two transformers in series. The power is switched through the tube by a mechanical switch operated by a timing circuit variable from $\frac{1}{4}$ sec. to $3\frac{1}{2}$ sec. Despite heavy sparking this switch rarely needs adjustment and is preferable to the more usual series spark gap because it allows the capillary to be warmed up carefully before the full discharge is put through it. A further projected improvement in the source is the provision of special non-inductive condensers which should increase the momentary current through the capillary.

Previous absorption studies in this region have almost entirely been limited to gases or readily volatile substances. In these cases the spectrograph can be filled with the substance or a narrow absorption cell provided, and here

the Lyman source may be brought close to the slit. However, it was now desired to study substances which need a high temperature before they have any appreciable vapour pressure; this requires an absorption tube between the source and the slit, and as this distance is increased so must the brightness of the source if exposure times are not to become unduly long. In conventional spectroscopy this difficulty is overcome by use of a lens to focus the light on the slit, however at these wave-lengths lithium fluoride is the only possible lens material and this is prohibitively expensive apart from the difficulty of mounting it in a vacuum system. This problem was overcome by the use of a mirror; two dioptre biconcave spectacle lens blanks were surface aluminized and mounted to collect light from the source and focus it onto the slit. Each surface lasted about six exposures, but the aluminium was readily removed with caustic soda and a new mirror evaporated on. The arrangement of the optic path and the mounting for the mirror are shown in fig. XIII. It can be seen that movement of the bellows controlled by six nuts allows plenty of freedom for the mirror and as the distance from the slit to the mirror is about 150 cm. the adjustment of the nuts is extremely critical. This adjustment is performed in the following manner:- with the vacuum can



ELEVATION



PLAN

FIG XIII

on the spectrograph rolled back, an electric light bulb is mounted behind the circular light baffle mentioned previously. In this there is a 1·4 × 0·6 cm. hole through which light must pass from slit to grating, now it passes the other way from bulb to slit. With the capillary tube of the source removed, one can see through the holes in the outer electrode to the mirror, and on these holes the image of the slit is now focussed by manipulation of the mirror. This is the rough adjustment, the final one is achieved by evacuating the source and absorption tube and, with the discharge at very low power, moving the mirror until the maximum amount of light falls on the 1·4 × 0·6 cm. hole in the baffle. This light must now reach the grating. To evacuate the source it is necessary to place a small glass window and gasket over the hole in the end-plate through which the slit-tube passes.

Garton (loc. cit.) uses entirely rubber ring seals in his source on the grounds that any grease tends to wipe out the continuum below 2000 Å. No trouble has been traced to this source, and the maker's specifications give these waxes and greases very low vapour pressures at room temperature.

The Absorption Spectrum of Silicon Monoxide

Of the group of twenty molecules formed from Group IVb and Group VIb elements, all except CTe have been shown[6] to give rise to at least one ultra-violet band system generally appearing readily in emission. Many of these have also been observed in absorption; it is convenient to call them A - X systems. The existence of weaker E - X systems lying to shorter wave-lengths has been shown for many of these molecules, in particular for SiS, SiSe and SiTe.[7] The values of ν_e for the A and E states are given in cm^{-1}: (The A state is also called D.)

	SiTe	SiSe	SiS	SiO
A	28664	32449	35029	42835
E	33991	38506	41923	

It is likely from these figures that the E state of SiO will lie at about 51000 cm^{-1} or 1960 Å, and an examination of the absorption spectrum was undertaken.

Experimental. When a mixture of silicon and silica is heated to 1500°C in a King furnace there is sufficient SiO present for absorption spectra to be observed.[8] However, vapour pressure measurements[9] indicated that equilibrium pressures of between 2 and 10 mm. of SiO are reached between 1300 and 1460°C, and these temperatures can be obtained in a "Globar" furnace. Using an alumina absorption tube containing the mixture in boats, exposures of 20 to 30

minutes were taken with the Lyman source running in hydrogen at a pressure of slightly less than 1 mm. The lithium fluoride window was not used in these experiments and the furnace tube was attached directly to the collimating bellows in front of the slit. The procedure adopted was to evacuate the whole spectrograph, tube and source to a pressure of a micron; heat up the furnace which caused the pressure to rise slightly, and then turn off the diffusion pump. A slow stream of hydrogen was allowed to enter the source until the pressure rose to $\frac{1}{2}$ mm. and at this pressure the hydrogen was streamed through the apparatus by the rotary pump, the main tap being very nearly closed to slow down the rate of flow.

Results. In this manner exposures were taken on thick glass Kodak plates at temperatures between 1300°C and 1460°C. Three certain new systems were discovered, the E ← X system of red degraded bands forming a long progression between 1970 Å and 1715 Å, an F ← X system of five red degraded sequences between 1530 Å and 1400 Å and two progressions at still shorter wave-lengths. Plate I shows the last two of these systems, of which the F ← X is extremely strong; as is shown, the three central sequences appear in our Lyman continuum even when the furnace is cold and this must be due to absorption

λ(Å) ⟶

FURNACE TEMPERATURE

1460°C

1300°C

ROOM TEMPERATURE

79605 cm⁻¹

3,1? 2,1
2,0 1,0 0,0 1,0

H⟵X SYSTEM OF SiO

PROGRESSIONS DUE TO SiO

4,0 3,0 2,0 1,0 0,0
4,1 3,1 2,1 1,1

F⟵X SYSTEM OF SiO

4,6

4,2 3,1 2,0
5,4 4,3 3,2 2,1 1,0
3,3 2,2 1,1 0,0
4,5 3,4 2,3 ,2 0,2
2,4
1533·6 Å
1526·8

1371·4 Å
1393·7
1402·7

Si IV CO CO CO CO Si II CO

PLATE I.

by a concentration of SiO gas formed momentarily from the silica capillary. Similarly many silicon lines appear in absorption and it is these that are largely used as our wave-length standards, taken from Kiess[10] and calculated from Moore.[11] Unfortunately no plate of the E← X system was taken that is suitable for reproduction, the measurements were taken from a thin strip at the edge of the continuum of the 1460°C plate. This plate was over-exposed at the long wave-length end in order to observe the continuum below 1400 Å and it was only along the edge of the spectrum that the bands appear, perfectly suitable for measurement but not for reproduction. A further plate of 10 minutes' exposure will be taken when new "Globars" are available, as these burned out after operating at this high temperature.

Table I contains the wave-lengths, frequencies, vibrational analysis, intensities and observed minus calculated (O - C) values for the band-heads of the E← X system. The best equation to represent the observed heads is:

$$\nu_h = 52863{\cdot}2 + 675\,(v' + \tfrac{1}{2}) - 4{\cdot}15\,(v' + \tfrac{1}{2})^2 - 1242{\cdot}03\,(v'' + \tfrac{1}{2}) + 6{\cdot}047\,(v'' + \tfrac{1}{2})^2$$

The absorbing molecule is identified as SiO by the ground state differences which are taken from Herzberg.[12]

Table I

Band heads of the E ← X system of SiO

Wave-length λ_{vac} in Å	Frequency ν_{vac} in cm^{-1}	Intensity	Vibrational analysis v' v"	O - C in cm^{-1}
1994·66	50133·9	1	0 , 2	+0·4
1968·53	50799·3	1	1 , 2	-2·1
47·29	51353·4	1	0 , 1	+1·3
43·19	51461·8	1	2 , 2	+2·7
22·32	52020·5	3	1 , 1	+1·7
1898·40	52675·9	4	2 , 1	-1·6
75·26	53325·9	3	3 , 1	-8·0
55·20	53902·5	overlapped	2 , 0	-4·4
32·93	54557·5	5	3 , 0	+0·5
11·64	55198·6	7	4 , 0	-0·2
1791·05	55833·2	7	5 , 0	+1·2
71·29	56456·0	9	6 , 0	-1·5
52·10	57074·4	10	7 , 0	0·0
33·63	57682·4	6	8 , 0	-0·6
15·72	58284·6	6	9 , 0	+1·7

The intensities throughout this work are estimated visually on a scale of ten separately for each system.

It can be seen from the Deslandres scheme in table II that the position of the 0,0 band cannot be fixed with certainty as there may be other weak bands at longer wavelengths and the system extended to the bottom right of the diagram. This is of no importance for the purpose of calculating dissociation energies, but is unfortunate if one tries to estimate the position of emission systems corresponding to transitions between excited levels.

In table III are given similar quantities for the F← X system, but no Deslandres scheme is appended, for it is apparent from Plate I that the system falls into obvious sequences. Such is the strength of this system that the 2,1, 1,1 and 2,2 bands could be measured only on the plate taken with the furnace cold, because of overlapping by earlier members of the sequences. The majority of the other heads were measured on the plate at 1300°C; at the highest temperature the absorption is strong enough to be almost continuous in many places.

The best equation to represent the observed F← X heads is:-

$$\nu_h = 68562{\cdot}5 + 1114{\cdot}6\ (v' + \tfrac{1}{2}) - 7{\cdot}2\ (v' + \tfrac{1}{2})^2$$
$$- 1242{\cdot}03\ (v'' + \tfrac{1}{2}) + 6{\cdot}047\ (v'' + \tfrac{1}{2})^2.$$

Table II

Deslandres scheme for band heads of E← X system of SiO

v'					
9	58284·6				
	602·2				
8	57682·4				
	608·0				
7	57074·4				
	618·4				
6	56456·0				
	622·8				
5	55833·2				
	634·6				
4	55198·6				
	641·1				
3	54557·5	1231·6	53325·9		
	655·0		650·0		
2	53902·5	1227·6	52675·9	1214·1	51461·8
			655·4		662·5
1	-		52020·5	1221·2	50799·3
			667·1		665·4
0	-		51353·4	1219·5	50133·9
v'/ v"	0		1		2 v"

Table III

Band heads of the F ← X system of SiO

Wave-length λ_{vac} in Å	Frequency ν_{vac} in cm^{-1}	Intensity	Vibrational analysis v' v"	O - C in cm^{-1}
1524·10	54612	0	4 , 6	-2
21·57	722	2	3, 5	-5
18·91	837	3	2 , 4	-1
1497·45	66780	2	4 , 5	-4
94·63	906	4	3 , 4	-3
91·89	67029	6	2 , 3	-2
89·25	148	6	1 , 2	-3
86·58	269	6	0 , 1	0
68·32	68105	4	3 , 3	+2
65·14	253	6	2 , 2	+3
62·37	382	9	1 , 1	0
59·91	497	10	0 , 0	-1
48·98	69014	3	5 , 4	+5
45·85	163	4	4 , 3	+4
42·77	311	4	3 , 2	+3
39·72	458	8	2 , 1	+3
36·84	597	8	1 , 0	-1
21·14	70366	6	4 , 2	+1
17·78	533	4	3 , 1	+7
14·67	688	4	2 , 0	+3

In table IV are the two progressions shown in plate I to shorter wave-lengths of the F←X system, and in table V is a list of unallocated heads, some of which may fall into systems as discussed below.

Discussion. The discussion of the bearing of these new systems on the determination of the dissociation energy of SiO will be postponed until we have considered similar systems of GeO, and SnO. However, two points of interest remain. By comparison with CO it would be expected that molecules in these highly excited states of SiO would undergo transitions to other such states emitting bands in the visible and near u-v regions. A number of sources which emit the D↔X system strongly are known, but so far no such bands have been identified. These sources include arcs of silicon or silicon and graphite, discharges through small-bore silica tubes or in $SiCl_4$ plus oxygen, and flames containing $SiCl_4$. The only reported bands due to an oxide of silicon are those by Cameron,[13] and Pankhurst.[14] The former gave five double-headed bands between 4393 and 4648 Å and a single band at 4214 Å, all red degraded. The latter extended the system to about 3673 Å, but from his published reprint it can be seen that the heads are very diffuse and the structure complicated. More work on the system was done by Woods[15] at much larger dispersion and she analysed

Table IV

Deslandres scheme of progressions due to SiO

v' \ v"	0		1
4	75222	1225	73997
	790		778
3	74432	1213	73219
	792		808
2	73640	1229	72411
	810		808
1	72830	1227	71603
	819		
0	72011		

The band at 74432 is badly overlapped by a Si III emission line.

Table V

Other red-degraded bands probably due to SiO

λ_{vac} in Å	ν_{vac} in cm^{-1}		Intensity
1575·58	63469		1
62·74	63990		1
50·65	64489		1
38·89	64982		0
1434·71	69701		3
03·94	71228		8
1392·23	71827		2
86·93	72102		3
67·51	73126		3
1338·72	74698		?
38·24	74725		?
30·37	75167	H	4
09·20	76383	H	5
1292·16	77390	H	2
90·19	77508	H	2
72·28	78599	H	2
76·00	78370		2
56·20	79605		1

a 0,0 band of a $^2\Sigma \longrightarrow {}^2\Sigma$ system of SiO^+ at 3840 Å and also found the 4270 Å group of Pankhurst. All three workers suggested that the unanalysed bands are due to SiO_2, but Woods reported that there are weak background bands from 3650-4270 Å and a single band at 6530 Å. Now the frequency of the 0,0 band of an F → E transition for SiO would be 15,914 cm^{-1}, while 6530 Å is equivalent to 15,310 cm^{-1}, and it is possible that this is the 0,1 band of such a transition. From the presence of the long v" = 0 progression in the E ← X system it would be expected that the v' = 0 bands would be the strongest in an F → E transition. Similarly the 0,0 band of an F → D system would lie at 25,858 cm^{-1} ≡ 3866 Å, and some of the bands reported in the papers above may well be due to this transition in SiO. Not all, for both the F - D and F - E systems would probably be violet-degraded; however, some of Pankhurst's bands are degraded this way. It is greatly desirable to measure such bands under good dispersion partly in order to determine the electronic configuration of the E and F states by rotational analysis, and partly to fix the level of the zero of the E state. Some experiments have recently been conducted in this laboratory to try to develop a good source of these bands, using a discharge into a hollow cathode containing a mixture of

Si and SiO_2. These have not yet been successful.

A further point of interest in these new observations is the possibility of a Rydberg series in SiO and the correlation of the energy levels of this molecule with those of CO. We would expect the ionization potential of SiO to lie below that of CO, which is 14·00 e.v., as the potential of Si is only 8·15 e.v. compared with 11·26 e.v. of carbon. In searching for a Rydberg series we may pick out a fragment of another system from amongst the bands in Table V. This level may be called H, leaving the symbol G for the state which gives rise to the two progressions in table IV. It can be seen that the H ← X system closely resembles the F ← X, the ω_e values being respectively 1155 and 1115 cm^{-1}, and thus they both appear as short close sequences.

v' \ v"	0		1
2	78599	1209	77390
	1091		
1	77508		overlapped by C,O
	1125		
0	76383	1216	75167

H ← X system of SiO.

Furthermore the last band capable of measurement on our plate, again resembles the 0,0 band of $F \leftarrow X$ and $H \leftarrow X$; its frequency is 79605 cm^{-1} and we may arrange these three in a Rydberg series for 0,0 heads obeying this equation;

$$\nu = 84790 - \frac{R}{(m+0{\cdot}6)^2}$$

where m = 2,3,4, and O-C values are -40, +40 and 0.

This gives a reasonable value of 10·5 e.v. for the ionization potential of SiO.

The measurements at these short wave-lengths are not very accurate due to the use of thick glass plates which do not fit the focal curve, and also because the correction curve stopped at 1302 Å. The disappearance of the continuum at short wave-lengths is partly due to the drop in reflectivity of the aluminium mirror and grating and partly to absorption of light by traces of water vapour. This last has been overcome by the use of argon instead of hydrogen, and more particularly by placing trays of P_2O_5 covered with wire gauze inside the spectrograph and leaving it evacuated overnight. Thus when "Globars" again become available for the furnace it will be of great interest to examine the spectrum of SiO at wave-lengths down to 1100 Å and to see if this Rydberg series is real.

We may now consider the connection between the observed levels of SiO and CO. The relationship between the spectrum of the latter and its electronic configuration was considered by Mulliken;[18] the method of arriving at this configuration for the ground state of the molecule is explained in Mulliken's paper and in ref. 12, chap. VI, and we may write:-

$$CO \ldots KK(z\sigma)^2(y\sigma)^2(w\pi)^4(x\sigma)^2 \ldots {}^1\Sigma^+$$

The KK shells are completed, the greek symbol is the quantum number λ ($\lambda = |m_l|$) and the z, y, x etc. represent decreasing strength of binding and replace the nomenclature $(\sigma\,2s)^2(\pi 2p)^4$ etc. on the grounds that the principal and azimuthal quantum numbers only have meaning for molecules close to united atoms such as hydrides.

In a similar manner we may give the ground state of SiO this configuration,

$$SiO \ldots KKL(z\sigma)^2(y\sigma)^2(w\pi)^4(x\sigma)^2 \ldots {}^1\Sigma^+$$

and the first two excited states these:-

$$\ldots (y\sigma)^2(w\pi)^4(x\sigma)(v\pi) \ldots {}^3\Pi \text{ and } {}^1\Pi.$$

$$\ldots (y\sigma)^2(w\pi)^3(x\sigma)^2(v\pi) \ldots {}^1\Sigma^-(2),\ {}^2\Delta,\ {}^3\Sigma^+,\ {}^3\Sigma^-,\ {}^1\Delta.$$

For CO both the ${}^3\Pi$ and ${}^1\Pi$ levels are known in their transitions to the ground state, however the ${}^3\Pi - X{}^1\Sigma^+$ (Cameron) bands are forbidden and in absorption require a

path length of about 1 metre atmosphere to be observable. This may be compared with the $^1\Pi \leftarrow X^1\Sigma^+$ (4th positive) which appear on our plates from the minute traces of CO produced in the source. Thus the known $A^1\Pi$ state of SiO (also called $D^1\Pi$) may be definitely correlated with the $^1\Pi$ state of CO, and we would not expect the $^3\Pi \leftarrow X^1\Sigma^+$ transition of SiO in absorption through the path lengths available.

Now the molecule CO^+ has three known states, $X^2\Sigma^+$, $A^2\Pi$ and $B^2\Sigma$ obtained from CO by the removal of an $(x\sigma)$, a $(w\pi)$ or a $(y\sigma)$ electron respectively. A Rydberg series of CO is known leading to each of these states (Tanaka et alia[19,20]) but it is only that leading to the ground state of CO^+ that is of interest now. This obeys the equation[19]

$$\nu = 113029 - \frac{R}{(m + 0{\cdot}12)^2} \qquad m = 4,5,6 \ldots 12$$

and as both the 0,0 and 1,0 bands of each member were observed an average $\triangle G_{\frac{1}{2}}$ value of 2175 cm^{-1} was found. The first member of this series is said by Moffitt[17] to be the $B^1\Sigma^+$ state of CO having this configuration (in Mulliken's notation[18])

$$CO.B^1\Sigma^+ \ldots KK(z\sigma)^2(y\sigma)^2(w\pi)^4(x\sigma)(u\sigma)$$

where a non-bonding $x\sigma$ electron has been excited to the $u\sigma$ Rydberg orbital. Now T_o for this $B^1\Sigma^+$ state of CO is

86918 cm^{-1} and the value of ν obtained by putting m = 2 in the Rydberg equation above is 88613 cm^{-1}. This confirms that this Rydberg series is a series of $^1\Sigma^+$ states obtained by excitation of the ($u\sigma$) electron, and it is reasonable to assume that the F state in SiO corresponds to the $B^1\Sigma^+$ in CO. This and the other relationship will be considered in table VII by means of comparing the fraction of the ionization potential represented by the height of each level above the ground state, i.e. $\frac{T_o}{I}$ and the ratio of the vibrational frequency of each state to that of the ground state, e.g. $\frac{\omega_A}{\omega_X}$.

Table VI

States of SiO, excluding those of Uhler[23]

State	ν_e	ω_e	$x_e\omega_e$
?	79650		
H($^1\Sigma^+$)?	76427	1155	15
G	[72011]	829	5
F($^1\Sigma^+$)?	$68562\cdot_5$	$1114\cdot_6$	$7\cdot_2$
E($^3\Sigma^+$)?	$52863\cdot_2$	675	$4\cdot1_5$
$D^1\Pi$	42835·3	848·5	5·84
$X^1\Sigma^+$	0	1242·03	6·047

Finally we may consider the connection between the E and G levels of SiO and corresponding states in CO. The most noticeable point about the E ← X and G ← X systems is the smallness of ω_e' which immediately recalls the $a'\,^3\Sigma^+$ state of CO. This too is observed in absorption with moderate strength[22] as a v" = 0 progression, and is believed[18] to be one of the states due to the excitation of a ($w\pi$) electron to the $v\pi$ state. It is possible that the correct term type for the E states of all this group may be fixed by a rotational analysis of the E ↔ X system of SiS; in the meantime it may tentatively be designated $^3\Sigma^+$. There is no obvious analogue of the G state of SiO amongst those of CO, but it is not to be expected that there would be much similarity among these highly excited states, except for Rydberg series.

Table VII is a comparison of the states of CO and SiO. Many of the SiO states have been found by Uhler[23] by considering the perturbations in the $A^1\Pi$ level. Such levels have the sign ⩽ before their T_0 values. It does not seem to have been noticed before that the F and $G^1\Pi$ levels of CO may be two members of a Rydberg series

$$\nu = 113029 - \frac{R}{(m + 0{\cdot}88)^2} \qquad m = 2,3$$

similar to that of Worley[21] for N_2. This is believed

to be the series

$$CO \ldots KK(z\sigma)^2(y\sigma)^2(w\pi)^4(x\sigma)\ np\pi\ \ {}^1\Pi\ .$$

If this is so the calculated ω_e for $G\,{}^1\Pi$ is much too small.

Table VII

CO				SiO			
State	T_o	ω/ω_x	$T_o/_I$	State	T_o	ω/ω_x	$T_o/_I$
$e\,{}^3\Sigma^-$	$\leqslant 64800$	$\geqslant 0.49$	$\leqslant 0.57$	$e\,{}^3\Sigma^-$	$\leqslant 43070$	$\geqslant 0.55$	$\leqslant 0.51$
$d\,{}^3\Pi_i$	61785	0.52	0.55				
$a'\,{}^3\Sigma^+$	55380	0.56	0.49	$E({}^3\Sigma^+)$?	52583	0.54	0.62
$a\,{}^3\Pi_r$	48474	0.80	0.43				
				?	79605	-	0.94
				$H({}^1\Sigma^+)$?	76427	0.93	0.90
				G	[72011]	0.67	0.85
$G\,{}^1\Pi$	105266	0.50?	0.93				
$F\,{}^1\Pi$	99730	0.97	0.88				
$E\,{}^1\Sigma^+$	92923	0.98	0.82				
$C\,{}^1\Sigma^+$	91926	0.98	0.81				
$B\,{}^1\Sigma^+$	86918	0.96	0.77	$F({}^1\Sigma^+)$?	68563	0.90	0.81
				${}^1\Pi$ or ${}^1\Delta$	$\leqslant 44700$	-	$\leqslant 0.53$
$I\,{}^1\Sigma^-$	$\leqslant 66380$	$\geqslant 0.48$	$\leqslant 0.59$	$I\,{}^1\Sigma^-$	$\leqslant 44300$	$\geqslant 0.55$	$\leqslant 0.51$
$F'\,{}^1\Pi$	$\leqslant 66230$	-	$\leqslant 0.59$	${}^1\Pi$ or ${}^1\Delta$	$\leqslant 42800$	$\geqslant 0.55$	$\leqslant 0.50$
$A\,{}^1\Pi$	64747	0.70	0.57	$A\,{}^1\Pi$	42640	0.69	0.50
$X\,{}^1\Sigma^+$	0	1.00		$X\,{}^1\Sigma$	0	1.00	

The Absorption Spectrum of Germanium Monoxide

The ultra-violet absorption spectra of the molecules GeO, GeS, GeSe and GeTe have been studied[16] and for each molecule two absorption systems were found, with the exception of GeO. The values of T_e for these states are listed below:-

State	GeO	GeS	GeSe	GeTe
E		38884·8	35462·6	(31470)
A or D	37766·9	32889·5	30845·7	27750·8
X	0	0	0	0

The strongest bands of the E states in each case lay in long v" = 0 progressions and it seemed likely that such bands of GeO would lie just in the vacuum ultra-violet. Their interest lies in the fact that the E states of GeS and GeSe could be followed almost to their dissociation limits, and it was hoped that this could be done for GeO also.

Experimental. A sample of GeO was prepared by the method of Dennis and Hulse.[24] The stable dioxide is dissolved in KOH, neutralized and acidified with HCl until the solution is 5N, when the $GeCl_4$ is reduced for four hours at 90°C by hypophosphorous acid. The divalent hydroxide is precipitated slowly by ammonia in an inert atmosphere of nitrogen; this process taking an hour,

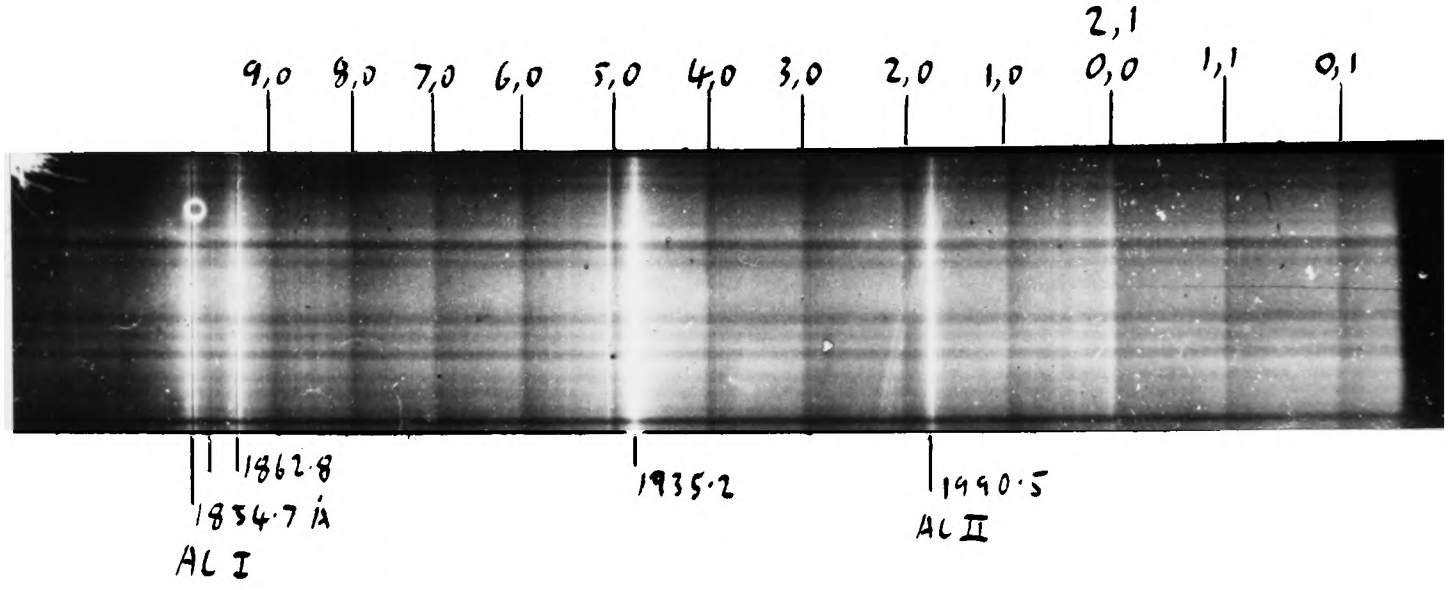
during which the solution is held at 95°C. The hydroxide immediately decomposes into the dark brown monoxide which appears as a flocculent precipitate, and it is washed by decantation, filtered and dried at 500°C, all in the inert atmosphere. When dry the GeO is quite stable and almost black.

Six grams of this solid were placed in boats inside an alumina tube outside which a wire furnace was wound to give the maximum possible heated length. The tube was then included in the light path as shown in fig. XIII, and with a temperature of 750°C an exposure of 25 minutes was taken on a Q2 plate. This showed no signs of an E← X system, however between 1520 and 1430 Å there was a system of red-degraded bands consisting of six separate sequences. This we will call the F← X system. Further shorter exposures of 10 minutes using the Kodak plates with their higher resolution enabled twelve red-degraded bands between 2065 and 1869 Å to be photographed. This plate is reproduced in Plate II(a) and it can be seen that the alumina capillary used in the source gave very few lines suitable for use as wave-length standards, particularly at the long-wave end of the plate. For this purpose a copper arc in air was added after the exposure as seen in Plate II(b). Furthermore the strong self-reversed aluminium

doublet at 1854-62 Å blocks out the progression just where it might be expected to converge. To overcome this a later plate was taken with a silica capillary and is shown in Plate II(c). Silica also has a strong group of lines around 1850 Å which overlaps one member of the progression, however the next but one member (12,0) was measured from this plate.

The measurements of the band-heads of the E ← X system are given in table VIII, under the headings wave-length in vacuo, frequency, intensity, vibrational analysis and observed minus calculated (O - C) values. A Deslandres scheme for this system is drawn out in table IX, and again it can be seen that the value of v' cannot be ascertained. In this case a further complication is the near equality $\omega_e'' \simeq \omega_e'$ at low v' values which means, for example, that the 0,0 and 2,1 bands overlap. In an attempt to get more information on this part of the system, plates were taken on a Hilger small quartz instrument using the same absorption tube and a hydrogen lamp as continuum. The bands measured thus were very weak, however the 0,2 and 0,3 were obtained this way but there was evidence of more bands to longer wave-lengths which could only mean that the v' numbering used here is too low.

(a)



(b)

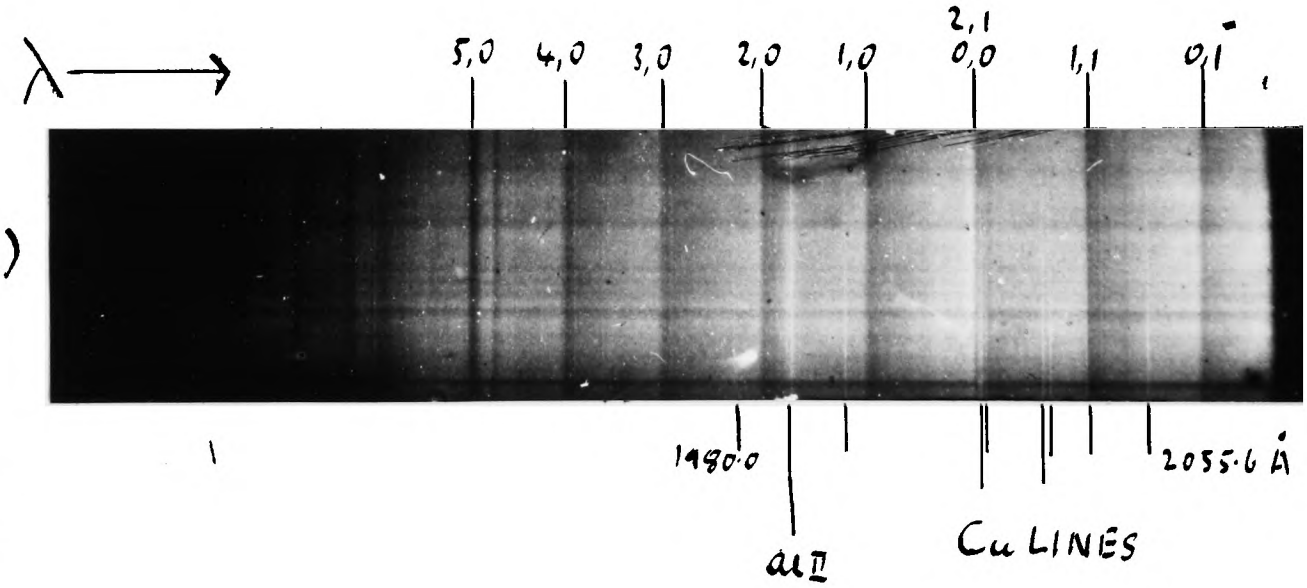


PLATE II

E ⟵ X SYSTEM OF GeO

(c)

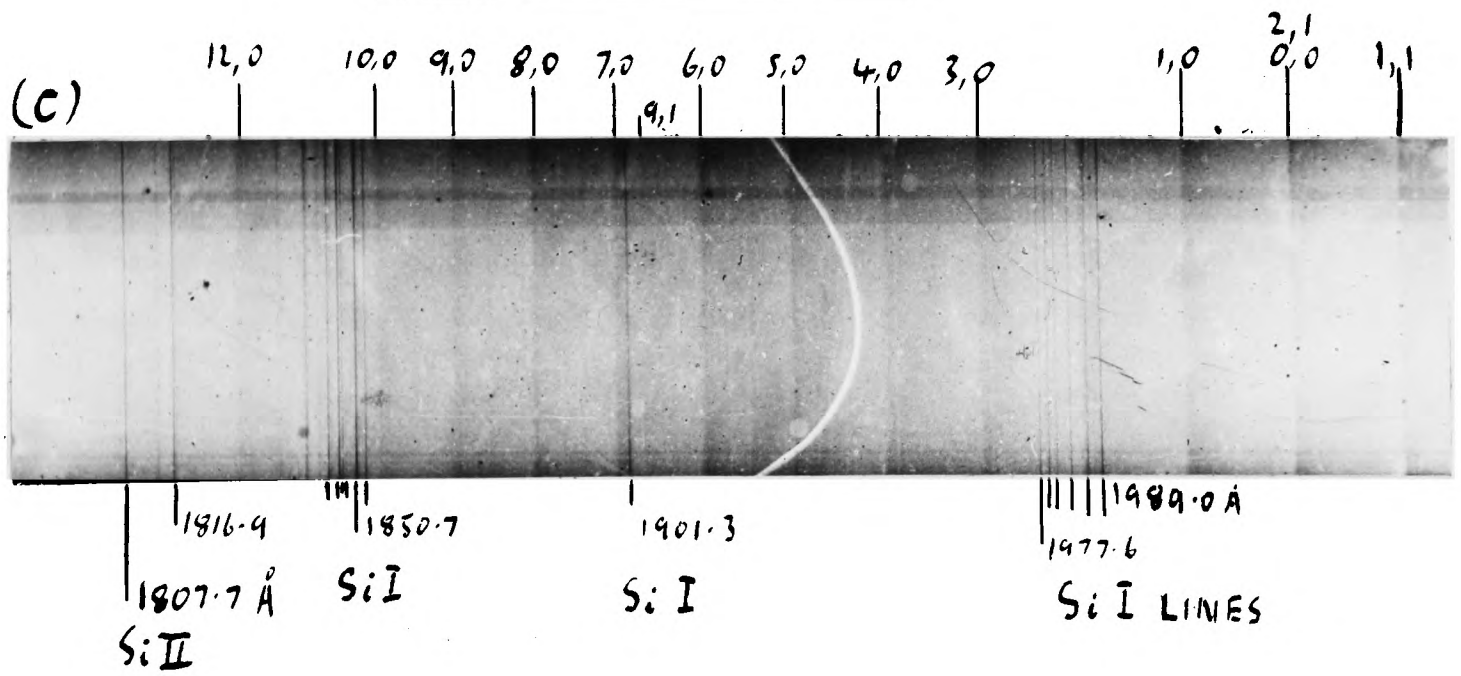


Table VIII

Band heads of the E ← X system of GeO

Wave-length λ_{vac} in Å	Frequency ν_{vac} in cm^{-1}	Intensity	Vibrational analysis v' v"	O - C in cm^{-1}
2151·0	46491	3	0 , 3	0
2107·4	47452	4	0 , 2	+1
2065·2	48421	8	0 , 1	+1
44·5	48912	9	1 , 1	-2
24·4	49397	10	(2 , 1 (0 , 0	+6 0
04·5	49888	9	1 , 0	-3
1984·9	50380	9	2 , 0	+4
66·6	50850	9	3 , 0	-2
48·7	51318	9	4 , 0	0
31·5	51773	9	5 , 0	-1
14·9	52222	9	6 , 0	+1
04·0	52521	0	9 , 1	-5
1899·0	52659	9	7 , 0	+1
83·6	53090	9	8 , 0	+5
69·1	53502	8	9 , 0	-1
54·9	53911	4	10 , 0	-1
28·5	54690	0	12 , 0	-9

The estimate of intensities is only visual and qualitative.

Table IX

Deslandres scheme of E ← X system of GeO

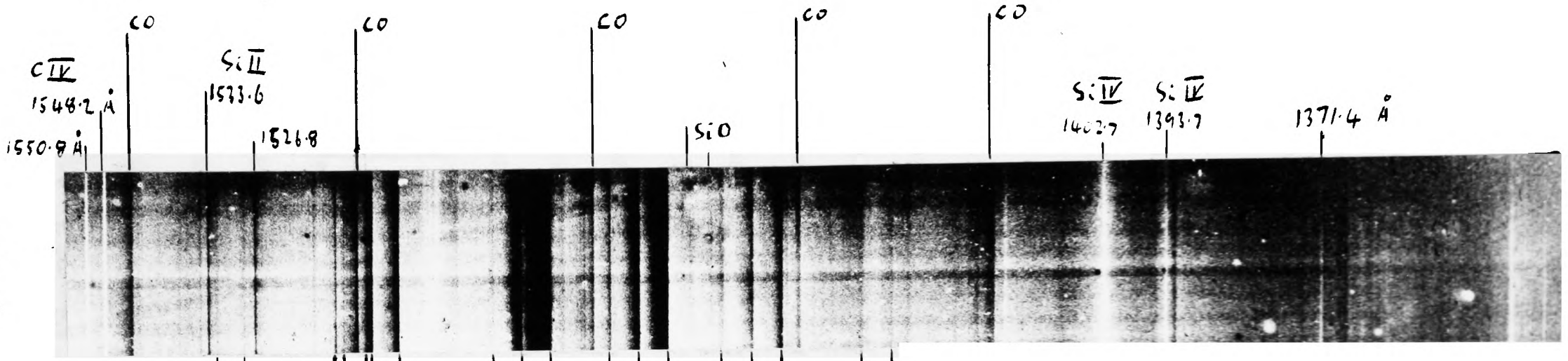
v' \ v"	0		1		2		3
12	54690						
	382						
11	[54308] calc.						
	397						
10	53911						
	409						
9	53502	981	52521				
	412						
8	53090						
	431						
7	52659						
	437						
6	52222						
	449						
5	51773						
	455						
4	51318						
	468						
3	50850						
	470						
2	50380	983	49397				
	492		485				
1	49888	976	48912				
	491		491				
0	49397	976	48421	969	47452	961	46491

The best equation to represent the observed band-heads for the E ← X system is:-

$$\nu = 49637{\cdot}3 + 504{\cdot}3\ (v' + \tfrac{1}{2}) - 4{\cdot}8\ (v' + \tfrac{1}{2})^2 - 985{\cdot}5\ (v'' + \tfrac{1}{2}) + 4{\cdot}3\ (v'' + \tfrac{1}{2})^2 .$$

It can be seen from the prints in Plate II that the heads are slightly diffuse due to the isotope effect in Germanium which has three isotopes of approximately equal abundance. Also the equation above assumes that the potential energy curve is that of a harmonic oscillator and the beginning of the departure from this curve is seen in the 12,0 band. This is of interest in the discussion of the dissociation energy of GeO.

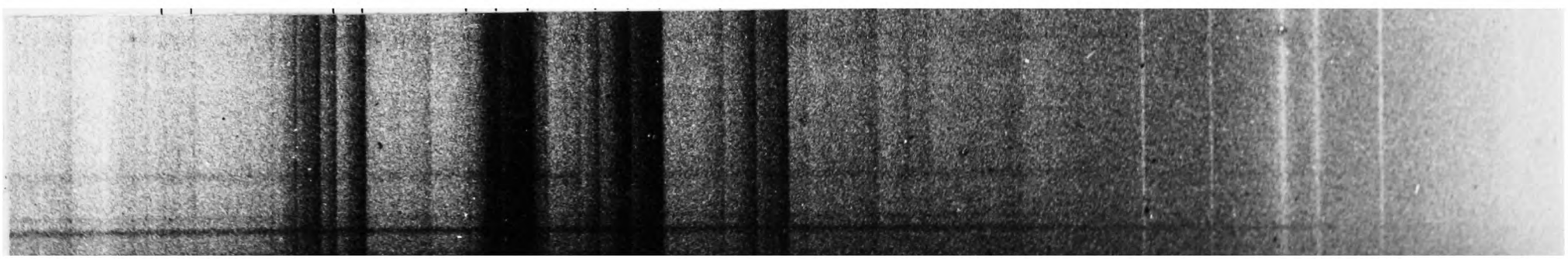
The F ← X system of this molecule was photographed first on an Ilford Q2 plate and later on a Kodak experimental plate. The two are reproduced in Plate III, the Kodak plate being the upper one , and the improvement of resolution with the latter is amply demonstrated. The system is rather more strongly developed on the Q2 plate as it was taken with a freshly prepared sample of GeO, and the six obvious red-degraded sequences are readily distinguished. The presence of many silicon lines on the plates taken with silica capillaries is of great use as wave-length standards, but on the Q2 plates only strong broad lines are resolved.



KODAK PLATE

F ← X SYSTEM OF GeO.

λ ←



Q2 PLATE

PLATE III

The equation for the observed band-heads of the F ← X system is:-

$$\nu = 67474{\cdot}4 + 809{\cdot}0\ (v' + \tfrac{1}{2}) - 5{\cdot}66\ (v' + \tfrac{1}{2})^2$$
$$- 985{\cdot}5\ (v'' + \tfrac{1}{2}) + 4{\cdot}30\ (v'' + \tfrac{1}{2})^2$$

and a list of wave-lengths, frequencies etc. is given in table X. The only two unallocated bands are at 1515·1 and 1511·9 Å and are resolved from a CO band on the Kodak plate; their intensities are comparable with those of the first two bands of the 0,1 sequence. The genuine 2,3 head lies between these two, at 1513·9 Å and is extremely weak and overlapped by the rotational structure of the CO band. These two unallocated bands may be part of another system or possibly broad absorption lines, in which case their origin is obscure.

A discussion of the bearing of these new systems on the determination of the dissociation energy of GeO will be postponed until we have considered a similar system of SnO. It is apparent that the spectrum of GeO resembles that of SnO and PbO rather than that of SiO and CO; in the first place the A level of GeO, known from the A↔X transition, was shown by Sen Gupta[25] to be $A\,^1\Sigma^+$ like the heavier members of the group, rather than $A\,^1\Pi$ like SiO and CO. Sen Gupta's analysis is probably correct, it is unlikely that he would neglect the Q branches, but he

Table X

Band heads of the F ← X system of GeO

Wave-length λ_{vac} in Å	Frequency ν_{vac} in cm^{-1}	Intensity	Vibrational analysis v' v"	O - C in cm^{-1}
1532·0	65275	0	1 , 3	-3
28·2	65437	0	0 , 2	-4
09·7	66237	4	1 , 2	-1
05·8	66408	5	0 , 1	-1
1492·0	67024	0	2 , 2	-1
87·9	67207	8	1 , 1	0
83·9	67390	10	0 , 0	+5
$74·9_5$	67799	2	3 , 2	-1
70·8	67991	6	2 , 1	-2
66·6	68185	8	1 , 0	+1
58·5	68565	1	4 , 2	+2
54·2	68766	3	3 , 1	-2
49·9	68770	5	2 , 0	0
38·1	69534	0	4 , 1	+2
33·9	69742	0	3 , 0	+1

appears to have observed fewer lines due to other isotopes than would be expected. Also in these experiments no higher states similar to SiO and CO have been discovered, particularly to short wave-lengths of the F ← X system. Thus we may draw up a list of the known states of GeO.

State	ν_e	ω_e	$x_e\omega_e$
F	67474·4	809·0	5·66
E	49637·3	504·3	4·8
$A\,^1\Sigma^+$	37766·9	651·3	4·24
$X\,^1\Sigma^+$	0	985·5	4·30

The Absorption Spectrum of Stannous Oxide and Sulphide

In order to complete the examination of the spectra of this group of molecules, it was decided to record the spectrum of SnO in absorption below 2000 Å. The E↔X transition of SnO has been examined both in absorption and emission[26,27]; it lies in the normally accessible ultra-violet with its ν_e at 36295 cm^{-1} and consists principally of a long v" = 0 progression similar to the E← X systems found for SiO and GeO. However, by analogy with these molecules an F← X system should lie in the vacuum ultra-violet, and this indeed was found to be so.

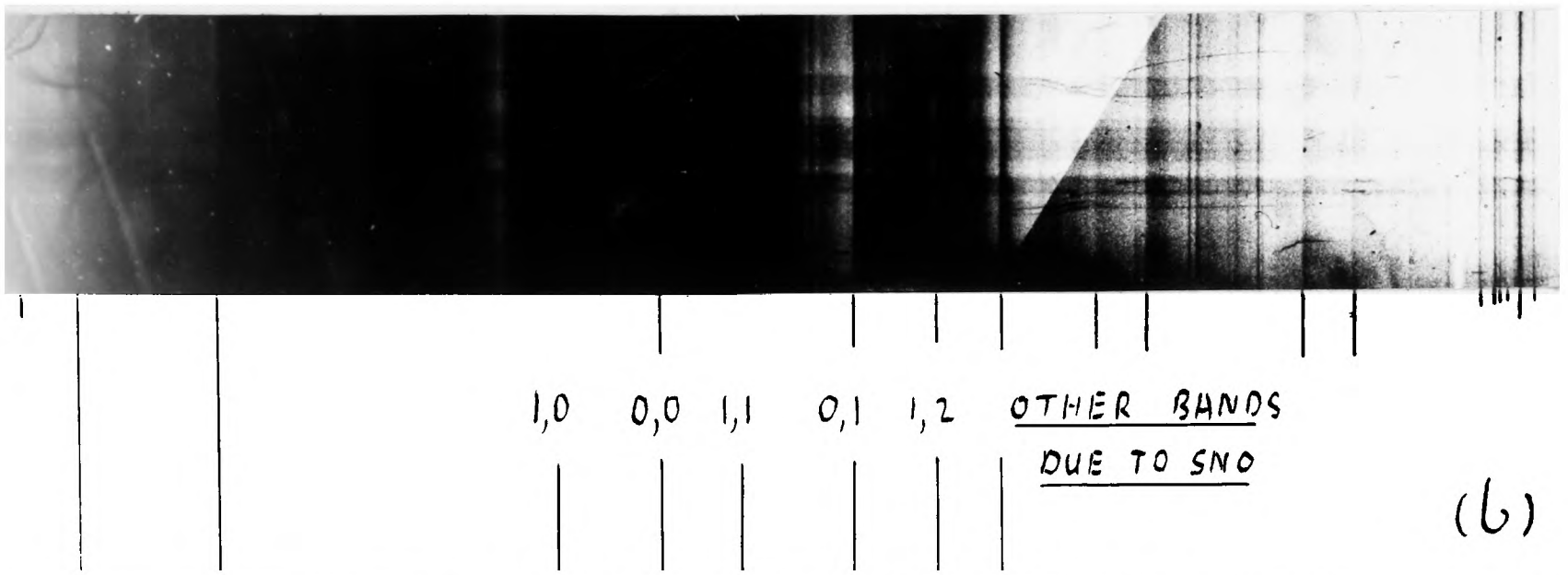
Experimental. A mixture of tin and stannous oxide was placed in boats in an alumina tube heated by a "Globar" furnace. Trouble was experienced from powder scattering from the furnace at above 900°C; this tended to block the slit, and in bad cases to cover the aluminium mirror. It was to overcome this that the tin was added to the oxide, in the hope that when the metal had melted the whole mass would form a "slag" and stay in the boats. This was not very successful as the tin only formed itself into globules and the powder scattered as before; however, by avoiding rapid heating the slit remained clear enough for many plates to be taken. It was unfortunate that the recording of these spectra coincided with the worst batch of Kodak

plates and many of these were found on development to be completely fogged. The remainder tended to be blotchy and of low contrast with one or two fortunate exceptions. In plate IV(a) is an enlargement of an early plate taken with the furnace at 1200°C. This strength of the absorption was never obtained again, as is seen by comparison with plate IV(b) taken at 1150°C; however, in the latter, continuous absorption has not blotted out the short wave-length end of the spectrum. At still higher temperatures the bands of SnO became fainter and were replaced by tin lines, and by 1440°C the density of the tin vapour was sufficient to record five interesting Rydberg series of this element. An attempt to suppress tin and increase SnO by using stannic instead of stannous oxide was unsuccessful. Nevertheless an F←X system is clearly present on Plate IV(b) together with other fragmentary systems.

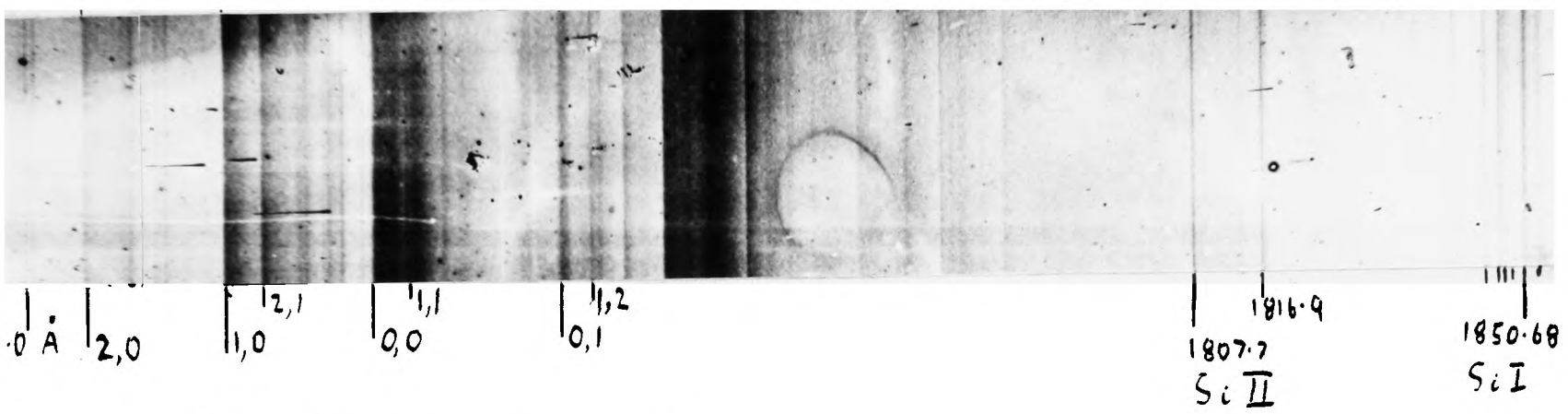
Results. The Rydberg series of tin are not related to the present discussion and will be considered later; the wave-lengths, frequencies etc. of the F←X system are given in table XI together with a Deslandres scheme of the bands. In table XII are the other bands believed to be part of fragmentary systems of SnO.

λ ⟶

(a)



(b)



F ← X SYSTEM OF SnO

PLATE IV

(C)

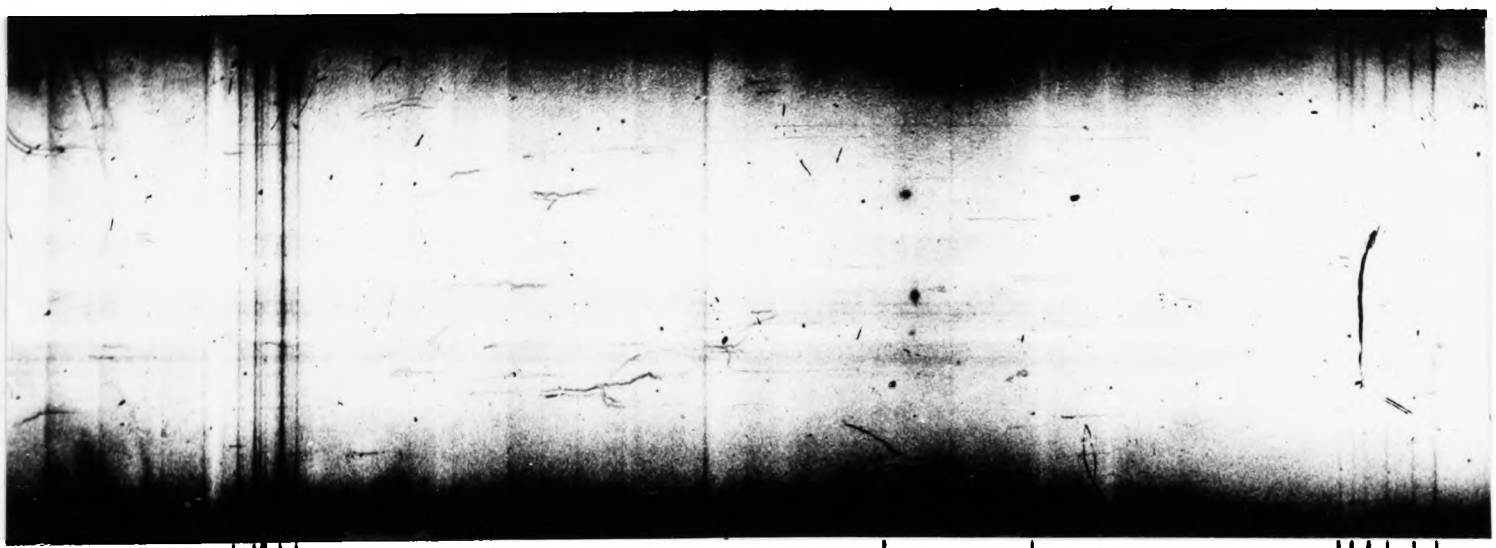


Table XI

The F←X system of SnO; red-degraded Band-heads

Wave-length λ_{vac} in Å	Frequency ν_{vac} in cm^{-1}	Intensity	Vibrational analysis v' v"	O - C in cm^{-1}
1729·8	57810	2	1 , 2	-1
1726·1	57935	4	0 , 1	-2
1710·8	58453	1	2 , 2	+2
1705·9	58620	8	1 , 1	+1
1702·0	58754	10	0 , 0	+2
1687·5	59259	5	2 , 1	0
1682·5	59434	6	1 , 0	0
1664·6	60073	2	2, 0	-1

Deslandres Scheme of F←X system of SnO

v' \ v"	0		1		2
2	60073	814	59259	806	58453
	639		639		643
1	59434	814	58620	810	57810
	680		685		
0	58754	819	57935		

Table XII

Other red-degraded bands due to SnO

Wavelength λ_{vac} in Å	Frequency ν_{vac} in cm^{-1}	Intensity	Wavelength λ_{vac} in Å	Frequency ν_{vac} in cm^{-1}	Intensity
1877·7	53256	0	1759·9	56821	0
1829·0	54675	0	1758·4	56870	1
1822·4	54872	1	1755·3	56921	2
1808·6	55291	line ?	1750·0	57142	6
1802·0	55493	2	1745·1	57302	6 d
1800·5	55539	0	1739·4	57491	10
$1795·8_5$	55684	0	1734·1	57667	3
1783·2	56079	3	1725·4	57958	4
$1780·1_5$	56175	1	1540·3	64925	2
1777·6	56257	2	1533·2	65224	2
1776·0	56307	2	1499·9	66670	0
1775·0	56338	3	1494·5	66914	0
1770·2	56491	3 d	1484·7	67354	2
$1764·3_5$	56678	3	1462·9	68358	1 d

The best equation to represent the F←X band heads is:-

$$\nu = 58809{\cdot}6 + 724\,(v' + \tfrac{1}{2}) - 21\,(v' + \tfrac{1}{2})^2 - 822{\cdot}4\,(v'' + \tfrac{1}{2}) + 3{\cdot}73\,(v'' + \tfrac{1}{2})^2.$$

The strongest remaining feature of the spectrum is the red-degraded band at 1739·4 Å and this may be the 0,0 band of a system with an upper state of which $\Delta G_{\frac{1}{2}}$ is 462 cm^{-1}. A Deslandres table of the band due to such a system is:-

1	57958	816	57142	804	56338
	459		464		-
0	57491	813	56678		
v' \ v''	0		1		2

This accounts for the peculiar appearance of the 0,1 band of the F←X system as it is now overlapped by the 1,0 band of the system above. In table XII several other pairs of bands may be found with a frequency difference of about 815 cm^{-1} which is the first vibrational difference of the ground state of SnO.

Further weak bands probably due to SnO occur at much shorter wave-lengths and are also given in table XII. In addition there is some slight evidence for continuous absorption around 1499-1484 Å. However, of much greater importance is the appearance of a continuum between 1937·5 and 1926·2 Å on the plate taken at 1200°C. This is shown

in plate IV(c), which is a reproduction of the longer wave portion of IV(a); this continuum may be of importance in the discussion of the dissociation energy of SnO.

Stannous sulphide.

It can be seen from the large $x_e\omega_e$ value that the vibrational levels of the F state of SnO are converging very rapidly, and it was thought to be of interest to study the spectrum of SnS in a similar manner. Three systems of this molecule are known[28] together with some unassigned bands which may be collected into progressions but whose analysis is uncertain. The E←X system has been studied in absorption[8] by heating a mixture of tin and tin sulphide in a King furnace to 1350°C; however, with the longer path length available in a "Globar" furnace temperatures of 1250 and 1150°C were employed here. The addition of the tin was intended to suppress bands due to S_2 and in this it was almost successful, but more trouble was experienced with powder scattering from the furnace and also from distillation of sulphur onto the slit. Nevertheless two plates were taken and are reproduced in Plate V, one at 1250°C on a Kodak plate and the other at 1150°C on a Q1 plate which is very slow but of rather finer grain. On the higher temperature plate many weak bands between 1930 and 1860 Å are present, and there are

$\longleftarrow \lambda$

Si I 1901·34 Å

1850·68 Å

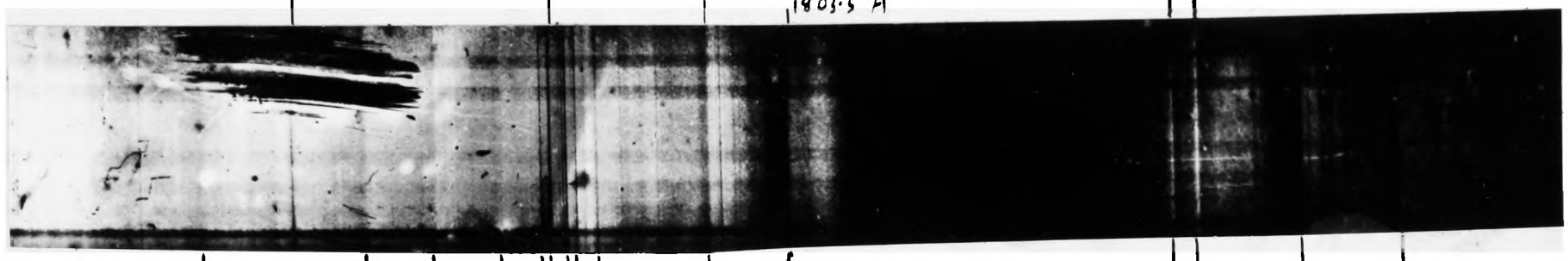
1819·2 Å

1803·5 Å

1727·3 Å

1722·5 Å

KODAK PLATE 1250°C



BANDS OF SnS

LINES OF Si I

$v''=2$, 1, 0,

$v'=0$ PROGRESSION OF SnS

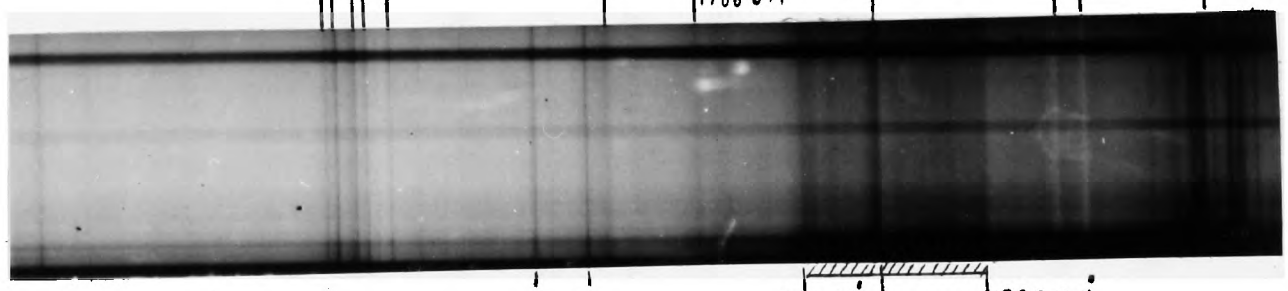
Si IV

BANDS OF SNO.

1788·0 Å

1757·9 Å

Q 1 PLATE 1150°C



Si II

1770·9 Å

1739·5 Å

CONTINUOUS ABSORPTION OF SnS

PLATE V

also two strong bands at 1819·2 and 1803·5 Å before a continuum starts. At shorter wave-lengths only bands due to SnO are seen.

On the lower temperature plate the first observed bands are at 1803·7 Å and 1788·0 Å and there is a region of continuous absorption stretching from a sharp limit at 1770·85 Å to a strong band at 1757·9 Å and then apparently to another limit at 1739·5 Å. The latter, however, is a strong SnO band, and it was thought that the long wave limit was the violet degraded S_2 band at 1770·75 Å reported by Maeder[29]. However, this is the 1,0 band of his C←X system and there is no trace on our plates of the 0,0 band at 1796·9 Å although they are reported to be of equal strength. Thus this continuum and the strong band at 1757·9 Å may be the F system of SnS which has become repulsive; the other bands observed are listed in table XIII. The three strongest bands at 1819·2, 1803·5 and 1788·0 appear to form a v' = 0 progression as the ground state constants of SnS are $\omega_e = 487·7$, $x_e\omega_e = 1·34$ (see 12). The other weaker bands perhaps form v" = 0 progressions and these possibilities are presented below.

v' = 0 progression

55928	479	55449	479	54970

v" = 0 progressions

53762				52522
376				394
53386			and	52128
377				396
53009	478	52522		51732

It will become clear in the discussion of the dissociation energies that the most important feature of this spectrum is the continuum, and that these fragmentary systems add little to our knowledge of the molecule.

Table XIII

Band believed to be due to SnS

λ_{vac} in Å	ν in cm^{-1}	Degradation	Intensity
1933·1	51732	Red	0
1918·3	52128	R	0
1904·0	52522	R	0
1892·4	52844	R	0
1886·5	53009	R	1
1875·6	53317	R	0
1873·2	53386	R	1
1860·0	53762	R	0
1819·2	54969·5	R	5
1803·5	55449	R	8
1788·0	55928	R	8
1770·9	56470	Violet	8
1757·9	56887	R	10

The Dissociation Energies of SiO, GeO, SnO and SnS

Having studied the bands of these molecules in the Schumann region, it is now possible to consider what new light they shed upon the dissociation energies of these molecules.

Introduction. There are two sorts of experimental results that are of use in determining dissociation energies, the spectroscopic and the thermochemical. The first follows from the definition of dissociation energy, which is that energy required to dissociate a molecule in the lowest vibrational level of its ground state to its constituent atoms in their ground states, at infinite distance and zero velocity. Thus if we can observe bands due to transitions from the ground state vibrational levels to those of an upper state until the former converge, such a convergence limit gives the dissociation energy D_o'' immediately, unless there is a potential maximum in the ground state. However, such convergence is rarely observed, certainly not for molecules of reasonable stability, and instead use has to be made of extrapolations.

The vibrational energy levels of a diatomic molecule can be represented by:-

$$G(v) = \omega_e(v+\tfrac{1}{2}) - x_e\omega_e(v+\tfrac{1}{2})^2 \pm y_e\omega_e(v+\tfrac{1}{2})^3 \text{ etc.}$$

In cases where many bands are observed, values of $y_e\omega_e$ and possibly further terms can be calculated and in these cases it is desirable to use a graphical extrapolation of a curve of $\Delta G(v + \frac{1}{2})$ against $(v + \frac{1}{2})$ when D''_o will be the area under the curve. If only a few levels are known the first two terms will often represent them satisfactorily and here the graph is linear, i.e.

$$D_o = \left(\omega_e^2 \Big/ 4x_e\omega_e\right) - \tfrac{1}{2}\omega_e.$$

This is known as the linear Birge-Sponer extrapolation or L.B.X. and tends to give values of D''_o some 20% higher than the true value where this is known accurately. This applies only to molecules where the binding is primarily covalent; for those with largely ionic character the L.B.X. gives value considerably too low as is shown by the Group III halides.

Similar considerations apply also to the excited states of a diatomic molecule, but in addition here it is necessary to identify the atomic products of dissociation. A great deal of information is available about atomic energy states and one of the reasons for this work is a desire to correlate upper molecular energy levels and the known atomic ones. If the extrapolations of these excited states are short, each level so correlated gives a possible upper and a

certain lower limit for the dissociation energy of the ground state. It is here that observed continuous absorption or predissociation is so useful as both these phenomena are caused by repulsive states giving a good upper limit to D_o'' if the atomic products are known. Thus the arrangement of known energy levels in a complete potential energy diagram for a molecule is usually a matter of weighing probabilities and it is not possible to give an unequivocal answer. For example, for two of the molecules most studied spectroscopically, N_2 and CO, the dissociation energy is still in doubt.

By way of contrast the thermochemical method of obtaining dissociation energies is, in principle, exact. The spectroscopic measurements are usually accurate to a wave number, and it is the interpretation that is in doubt, whereas the thermochemical measurements are themselves the source of uncertainty. The data required are vapour pressures for calculating latent heats of sublimation, specific heats for calculating entropies and changing $\triangle H$ with temperature, and heats of reaction. More work is being done on these quantities and a measure of the difficulties involved, particularly at high temperatures, is the variation in the results of different workers.

However, specific heats used here have been taken from the admirable compilation of Kelley[30] and other thermochemical data from the National Bureau of Standards,[31] unless other sources are mentioned.

Silicon monoxide. The four molecules we have considered fall into two groups. In the first (SiO and GeO) the spectroscopic value for the dissociation energy is derived from the newly discovered E states; on the other hand the E states of the other molecules (SnO and SnS) are already known and other values for D_o are obtained from extrapolation of the higher levels and continua.

A thermochemical value for the dissociation energy of SiO may be obtained from the results of several workers. Two reactions have been used,

$$H_2(g) + SiO_2 \longrightarrow H_2O(g) + SiO(g) \text{ between } 1470\text{-}1900^{\circ}K$$

and $$Si + SiO_2 \longrightarrow 2SiO(g) \text{ between } 1330\text{-}1920^{\circ}K.$$

In the first the product was analysed in two ways. Grube and Spiedel[32] decomposed the SiO gas on an iron wire and analysed for silicon, while Tombs and Welch[9] analysed the gas stream for water by thermal conductivity. The risk of extraneous water from the furnace, glass etc. was minimized by assuming that the effect was least at the

highest temperatures and back-calculating the results assuming a constant adventitious water pressure. A critical analysis of these results has been made by Baughan[33] and the table below is his.

The other reaction of solid silica and quartz giving SiO gas was studied by loss of weight of a Knudsen effusion vessel by Schäfer and Hörnle[34]. The internal consistency of their results is admirable and they agree quite well with those of Tombs and Welch[9] who measured the weight loss from a boat in a stream of argon. These results enable a value to be obtained for the heat of formation of SiO and they are set out in the following table.

Reaction	Authors	ΔH_{291}	Q_f SiO(g)
$H_2 + SiO_2 =$	Grube and Spiedel	135·4	19·1
$H_2O + SiO$	Tombs and Welch	131·0	21·5
$Si + SiO_2 = SiO$	Schäfer and Hörnle	166·3	22·0
	Tombs and Welch	168·8 172·8	20·8 18·8

Thus we may take Q_f SiO(g) at 298°K = 21·6 ± 1 k.cal./mol and using

$Si(c) = Si(g)$ $\quad \Delta H_{298} = 88$ k.cal./mol.

$O_2(g) = 2O(g)$ $\quad \Delta H_{298} = 118·3$ " "

there results $SiO(g) = Si(g) + O(g)$ $\quad \Delta H_{298} = 168·7$ k.cal./mol.

$\therefore \quad \Delta H_o = 167·5$ k.cal./mol.

This result agrees well with that of Brewer and Mastick[35] who arrive at ΔH = 165 k.cal./mol. from the reaction $SiO_2(c) = SiO(g) + \frac{1}{2}O_2$. Another measurement is that of Gel'd and Kochnev[36] who determined the rate of effusion of SiO from a small vessel containing solid SiO. There is some dispute over whether the solid was SiO or a mixture of Si + SiO_2; the former is probably true in which case ΔH = 170 k.cal./mol., otherwise this value is reduced to 160 k.cal./mol. (see ref. 35). We may thus take the best thermochemical value of D_0 to be 167·5 ± 2·5 k.cal./mol.

The spectroscopic value of the dissociation energy of SiO may be determined from the vibrational constants of the E state. This state of the heavier molecules of this group will be shown to dissociate into the same atomic products as the ground state, in this case Si ^3P and O ^3P. Which of the multiplets of the atoms is involved is in doubt, but in SiO this does not matter as the total multiplet separation is only 1·3 k.cal. Now for the E states of some of these molecules the vibrational levels can be followed almost to their convergence limit and this gives an excellent value for D_0'. Also it is found that this value of D_0' is about 45% of the value given by a L.B.X. of the first few levels. In SiO we only observe nine levels and these are represented by a two constant

expression. It seems a reasonable assumption that the true value of D_o' will be about 45% of that given by the linear extrapolation.

Values of true D_o' for E states expressed as a percentage of the L.B.X. value;

SnO	SnS	SnSe
46%	40%	40%
GeO	GeS	GeSe
45%	47%	58%

It will be realized that this percentage affects the result for D_o'' to a very small extent compared to the value of ν_e for the state involved.

In this case $\nu_e = 52863{\cdot}2\ cm^{-1}$, $\omega_e = 675\ cm^{-1}$ and $x_e\omega_e = 4{\cdot}15\ cm^{-1}$, thus $D_o' \doteq 27100\ cm^{-1}$ of which 45% is $12200\ cm^{-1}$. Added to ν_o this gives:-

$$D_o'' = 65400\ cm^{-1} = 186 \pm 1{\cdot}3\ k.cal./mol.$$

Now the highest observed band of the E←X system is at $58300\ cm^{-1}$, = 167 k.cal./mol. and it is apparent that if the analogy with the other molecules of this group is good, then the thermochemical value of ΔH_o must be too low. It is possible that in this case the E state dissociates to an excited silicon atom; either the ^1D or ^1S [at 18 k.cal. and 44 k.cal. respectively above ground state Si] are possible, because if the analogy with the heavier

molecules is rejected, the 45° relationship must be rejected too. In favour of the theory that CO and SiO are different from the heavier members of this group, is the difference in their first excited states which are $^1\Pi$ in CO and SiO and $^1\Sigma^+$ in GeO and SnO. Also many more excited levels of CO and SiO are known; on our plates no transitions of GeO above the F←X can be seen, whereas for SiO at least two more states lie immediately above the F←X. All this tends to the view that the thermochemical value of 167 k.cal./mol. for D_o of SiO is correct and that the E state of SiO is not analogous to those of the oxides, sulphides and selenides of germanium and tin. However, on the other hand in favour of the higher value there are two more points; firstly the similarity of appearance of all the E←X transitions. They all consist of long v" = 0 progressions and at low v' values the strongest bands in each case are those with v" about two or three. This gives doubt to their 0,0 bands as explained before, and shows that for each molecule the internuclear distance in the E state is larger than that in the ground state. Now it is unlikely that states formed from $M\,^3P + O\,^3P$ in the heavier molecules would so greatly resemble any state from $M\,^1D + O\,^3P$ in the lighter ones.

The second point in favour of the high value for the dissociation energy is that given by linear extrapolation of the ground state vibrational levels. It has been shown[35,8,37] that for this group of oxides the L.B.X. gives a value for D_o agreeing with the thermochemical one where this is known accurately. This will be seen to be true for GeO and SnO. For SiO the linear extrapolation gives D''_o = 180 k.cal. and in addition there is a small positive $y_e\omega_e$ term which will tend to increase this figure.

Thus in this case it seems impossible to give an unequivocal answer for the dissociation energy, but in the opinion of the author the balance of probability lies with the higher value of about 180 k.cal./mol. If this is correct then we must conclude that the latent heat of sublimation of silicon is about 105 k.cal./mol. rather than 88 k.cal./mol., for it does not seem likely that Q_f SiO is much in error as the value given above is from two methods and four authors. In fact it is reasonable to suppose that ΔH_L Si would be more than 4 k.cal./mol. greater than that of Ge, for the value for carbon is of the order of 170 k.cal./mol. and that for tin about 62 k.cal./mol.

Latent heat of sublimation of elements in k.cal./mol.

C	Si	Ge	Sn	Pb
170 (N.B.S.)	105	85 ± 4	62 ± 2	46·5 (N.B.S.)

Germanium Monoxide. In the case of this molecule the position is fortunately not so obscure. For the thermochemistry two sets of results are available, those of Bues and v. Wartenberg[38] and Jolly and Latimer[39]. The former measured the vapour pressure of GeO over solid GeO while the latter measured this vapour pressure over a mixture of Ge and GeO_2. Jolly and Latimer find that GeO is not a stable solid in the temperature range considered and reinterpreted the earlier data on this belief. Their result is:-

$$\tfrac{1}{2}Ge(s) + \tfrac{1}{2}GeO_2(s) = GeO(g) \qquad \Delta H_{298} = 53{\cdot}7 \pm 1{\cdot}0 \text{ k.cal./mol.}$$

In addition they determined the heat of formation of GeO_2 by oxidation of germanium powder by hypochlorite solution, getting a value of $\Delta H_{298} = 128{\cdot}5$ k.cal./mol. in excellent agreement with two earlier measurements. The value of the latent heat of sublimation of Germanium is taken from Searcy[40] although his results have a slight drift with temperature and Baughan[33] prefers a value of 89 k.cal./mol. Thus we have:-

$GeO(g) = \frac{1}{2}GeO_2(s) + \frac{1}{2}Ge(s)$	$-53{\cdot}7 \pm 1{\cdot}0$
$\frac{1}{2}GeO_2(s) = \frac{1}{2}Ge(s) + \frac{1}{2}O_2(g)$	$+64{\cdot}2$
$\frac{1}{2}O_2(g) = O(g)$	$+59{\cdot}2$
$Ge(s) = Ge(g)$	$+85{\cdot}2 \pm 4{\cdot}0$
	$154{\cdot}9$

Thus $\Delta H_{298} = 154{\cdot}9$ and $\Delta H_o = 154 \pm 5$ k.cal./mol.

For the spectroscopic value of D''_o we may derive a value from the newly discovered E state. The constants given before are $\nu_o = 49144{\cdot}6$ cm^{-1}, $\omega_e = 504{\cdot}3$ and $x_e\omega_e = 4{\cdot}8$. From these the calculated D'_o is 13000 cm^{-1} of which 45% is 5850 cm^{-1}. Adding this to ν_o we have 55000 cm^{-1} = 157 k.cal./mol. in excellent agreement with the thermochemical value above. Neither value is sufficiently accurate to determine to which multiplet the atomic products belong.

The linear extrapolation of the ground state vibrational levels gives $D''_o = 55900$ cm^{-1} or 160 k.cal./mol. and thus we may conclude that the dissociation energy of GeO is 154 ± 5 k.cal./mol.

Stannous Oxide. There is only one known determination of the vapour pressure of SnO, that of Vesselovsky[41]. This has been treated by both Drummond and Barrow (ref. 16, p.148) and Brewer and Mastick[35] but their arrival at the same

conclusion is obscured by their using different values of the latent heat of sublimation of tin. The former use 62 k.cal./mol. after Baughan[33] and arrive at $D_0(SnO)$ = 122·$_2$ k.cal./mol.; the latter use $\Delta H_s(Sn)$ = 70 k.cal./mol. and give the figure of 131·6 k.cal./mol. for the dissociation energy. This last should read 129·$_2$ as the original figure was wrongly corrected from 298°K to 0°K. Brewer[37] claims unpublished justification for his figure and Baughan claims his to be accurate to ±2 k.cal. and we have no means of choosing between them thermochemically.

However, in this case the spectroscopic evidence is rather more exact. The E state lies in the normally accessible ultra-violet and has been extended to near its limit by Eisler and Barrow[27]. A short extrapolation gives $D_0' + \nu_0$ = 131·9 k.cal./mol., sufficiently good evidence that the E state goes to $Sn\ ^3P + O\ ^3P$. The relevant atomic excitation energies are:-

Sn		(in k.cal./mol.)	O	
$^3P_0$	0		$^3P_2$	0
$^3P_1$	4·8		$^3P_1$	0·45
$^3P_2$	9·8		$^3P_0$	0·63
$^1D_2$	24·6		$^1D_2$	45·4
$^1S_0$	49·0			

Drummond and Barrow (loc. cit.) arrived at their thermochemical value of $D''_0 = 122{\cdot}_2$ k.cal./mol. and assumed that the difference between this figure and $131{\cdot}_9$ showed that the E state dissociated to $Sn\ ^3P_2$. However, Brewer's value casts doubt on this, and we can obtain new evidence from these observations in the Schumann region.

It will be recalled that there was continuous absorption between 1926 - 1937 Å $\equiv$ 51920 - 51626 cm^{-1}. This must be caused by a repulsive state of 148 $\pm$ 0·5 k.cal./mol. above the ground state when their internuclear distances are equal. The only possible atomic products for such a state are $Sn\ ^1D_2 + O\ ^3P$, and this means that D''_0 must be less than 148 minus 24·6, i.e. 123·5 $\pm$ 1 k.cal./mol. This strongly supports the lower thermochemical value of 122 k.cal./mol. and if this is so we must see if there are suitable atomic products for the F state, for which ν_0 is 58754, ω_e = 723 and $x_e\omega_e$ = 21. This value of $x_e\omega_e$ is not very good as it comes from one difference only, but using it we get $D'_0 \simeq 6000\ cm^{-1}$, which added to ν_0 gives a total limit of 186 k.cal./mol. The possible atomic products are:-

Sn	O	E_A	$D''_0 + E_A$ in k.cal./mol.
$^1D_2$	$^1D_2$	70	192
$^1S_0$	$^3P_0$	50	172
$^3P_2$	$^1D_2$	55	177

Of these possibilities the second is removed by the presence of the v' = 2 level at 172 k.cal. Of the other two the first is more likely as $^3P + {}^1D$ can only result in a triplet molecular state (see 12) and this transition and the similar one in GeO seem to be too strong for intercombination systems. Thus it is probable that the F level of SnO dissociates to $Sn\ {}^1D_2 + O\ {}^1D_2$ and the extra E_A can be accounted for by reducing $x_e\omega_e$ to 15 cm^{-1}, an error of only 3 cm^{-1} in each of the first two vibrational differences. Such products for the F states are perfectly possible both in GeO, although here the levels show no signs of convergence, and in SnS where it is believed that the F state has become repulsive.

It is concluded that the spectroscopic evidence favours the lower value of D_oSnO and we write:-

D_o SnO = 122 $\pm$ 2 k.cal./mol.; $\triangle H_L$ Sn = 62 $\pm$ 2 k.cal./mol.

Stannous Sulphide. It is unfortunate that there are no recorded measurements of the vapour pressure of this substance; however, it is possible to obtain a spectroscopic value for its dissociation energy and it will be of interest to check this when thermochemical measurements become available. The spectroscopic evidence is of three sorts, firstly the ground state extrapolation, secondly

the limit of the E state and lastly the continuum that we have observed in the vacuum ultra-violet.

The linear extrapolation of the ground state vibrational intervals using the mean of the constants given by Rochester[42] and Shawhan[43] leads to a value of $D''_o \simeq$ 120 k.cal./mol.

The E state of SnS has been studied in absorption by Drummond[8] who extended the system to give a limit at 40850 cm^{-1} above v" = 0. There is a perturbation of the higher vibrational levels which may make this limit not quite exact, but 45% of the limit obtained from extrapolation of the lower (unperturbed) levels gives 41950 cm^{-1} above v" = 0. It has been concluded above that the E states of molecules of this group dissociate to ground state products (multiplet unspecified) and so D''_o can be derived as $116 - E_A$ k.cal./mol. where E_A is the energy of the atomic products. These are listed below in k.cal./mol.

Sn		S	
$^3P_0$	0	$^3P_2$	0
$^3P_1$	4·8	$^3P_1$	1·1
$^3P_2$	9·8	$^3P_0$	1·6
$^1D_2$	24·6	$^1D_2$	26·4
$^1S_0$	49·0	$^1S_0$	63·4

In the vacuum ultra-violet there were two features of great interest. The strong band at 1758 Å surrounded by a continuum particularly to long wave-lengths must come from a repulsive state showing that $D_o'' \leqslant 162{\cdot}5 - E_A$ k.cal./mol In addition the strong bands at 1819, 1804 and 1788 Å form a v' = 0 progression for which no corresponding v' = 1 bands are seen. This implies a barely stable state which has dissociated below the v' = 1 level. Thus D_o'' must lie between 161 and 160 k.cal./mol. minus the atomic excitation energy E_A. Now it was concluded for SnO that the most likely products for an F state were $^1D_2 + {}^1D_2$, and this is confirmed by the strength of absorption in these systems which were photographed at 1150-1250°C whereas the E←X transition required 1350°C. Thus it seems probable that the dissociation energy of SnS is 110 ± 1 k.cal./mol. If this is so, the E states are shown to dissociate to a higher member of the tin multiplet; in SnO apparently it is the $^3P_2$ component, whereas in SnS the $^3P_1$ plus $S\,{}^3P_0$ is possible. However, a slightly higher value for the limit of the E state (corresponding to 45% of an L.B.X.) would be consistent with this state of SnS dissociating to $Sn\,{}^3P_2 + S\,{}^3P_2$.

It should be noted that a much lower value, $D_o \leqslant 68{\cdot}5$ k.cal./mol. is suggested by the work by Shawhan[43]

on the basis of a supposed predissociation in the A – X system. However, no adequate analysis of all SnS bands in this region of the A – X system has yet been put forward, and it seems probable that transitions to more than one upper state are involved. A similar effect occurs in the long-wavelength bands of SnO and SnSe; in SnTe, what appear to be the corresponding bands are resolved into two overlapping systems.[44] Thus the explanation of Shawhan's observations may well lie in an interaction between neighbouring states, and the predissociation cannot be regarded as established.

Rydberg Series of Tin

Experimental. This line spectrum was observed in absorption during the experiments described above on SnO. It first appeared at 1320°C and was well developed at 1400°C, and a print of the plate taken with the furnace at the higher temperature is given in Plate VI.

Results. There are five Rydberg series on the plate, marked A, B, C, D and E, of which A and B are the strongest. The wave-lengths and frequencies of the series are given below, together with the effective quantum number p defined so that the series obey this equation

$$\nu = I - \frac{R}{p^2}$$

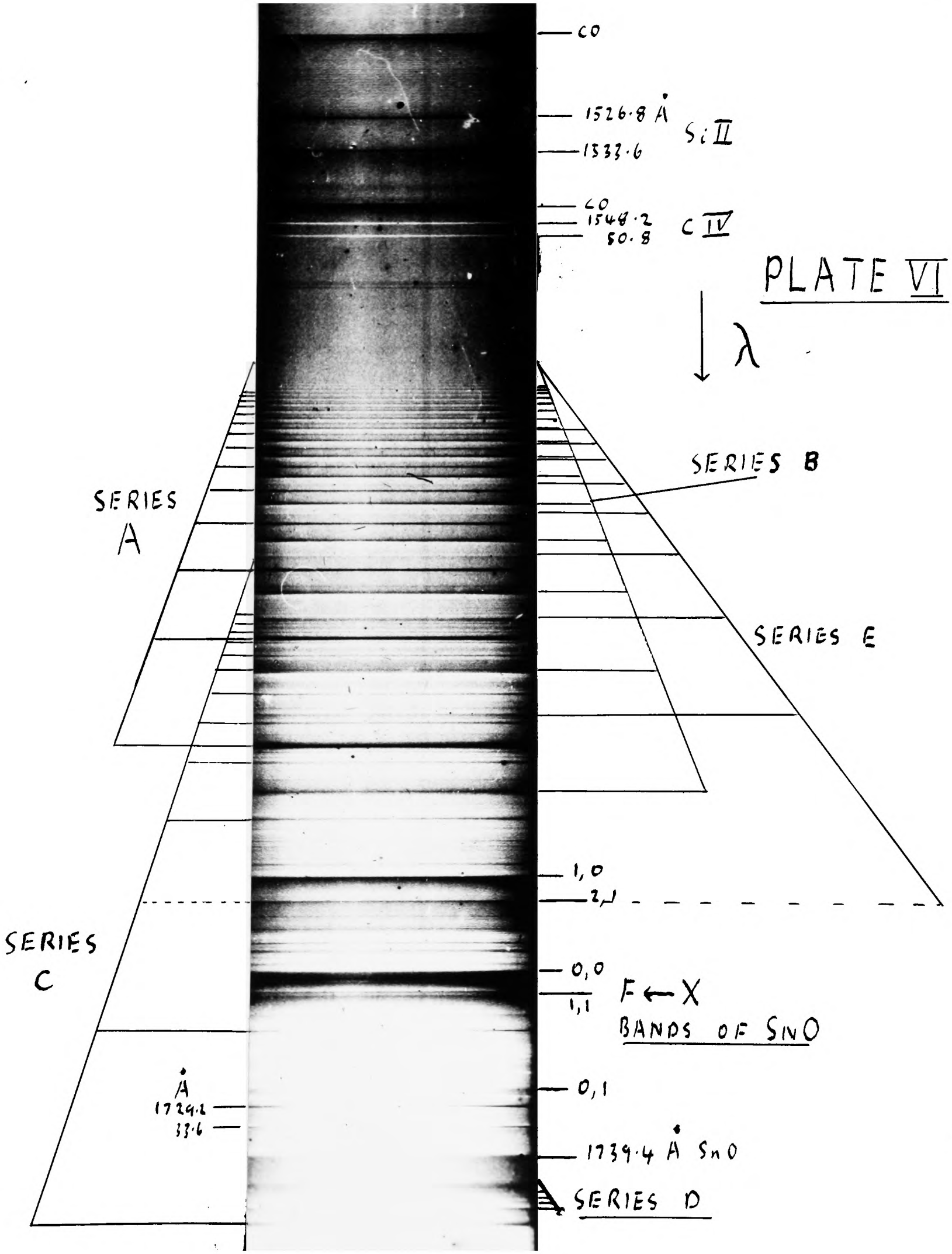
where ν is the frequency of any line,
I is the ionization potential,
and R is the Rydberg constant.

Series A

p	λ_{vac} in Å	ν in cm^{-1}	p	λ_{vac} in Å	ν in cm^{-1}
5·96	1655·71	60397·0	11·94	1594·48	62716·4
6·95	33·66	61212·2	12·94	91·66	827·5
7·94	19·57	61744·8	13·94	89·33	919·6
8·94	10·03	62110·6	14·94	87·49	992·5
9·94	03·25	373·3	15·94	86·01	63051·3
10·94	1598·35	564·5	16·94	84·68	104·2

$$\nu_A = 63484{\cdot}0 - \frac{R}{(n+0{\cdot}94)^2} \quad \text{where } n = 5, 6, 7, \ldots 16$$

PLATE VI


CO
1526·8 Å
Si II
1533·6
CO
1548·2
C IV
50·8
λ
SERIES B
SERIES A
SERIES E
1, 0
2, 1
SERIES C
0, 0
1, 1
F ← X
BANDS OF SnO
Å
1729·2
33·6
0, 1
1739·4 Å SnO
SERIES D

Series B

p	λ	ν	p - 0·48	λ	ν
5·65	1665·24	60051·4	15	1586·65	63025·9
6·58	40·73	60948·4	16	85·28	080·3
7·55	24·53	61556·3	17	84·22	122·5
8·53	13·60	61973·2	18	83·27	160·4
9·50	05·98	62267·3	19	82·49	191·6
10·48	00·41	484·0	20	81·76	220·7
11·48	1596·14	651·1	21	81·17	244·3
12·48	92·96	776·2	22	80·58	267·9
13·48	90·38	878·1	23	80·19	283·5
14·48	88·40	956·4	24	79·84	297·5

$$\nu_B = 63482{\cdot}3 - \frac{R}{(n + 0{\cdot}48)^2} \quad \text{where } n = 5, 6, 7, \ldots 24$$

or better·

$$\nu_B = 63482{\cdot}3 - \frac{R}{\left(n + 2{\cdot}46 + \frac{1{\cdot}80}{n^2}\right)^2} \quad \text{where } n = 3, 4, 5, \ldots 22.$$

Series C, which is considerably weaker than A and B.

p	λ	ν
7·54	1670·80	59852
8·52	59·12	60273
9·52	51·06	567
10·52	45·07	788
11·52	overlapped	
12·52	37·21	61080
13·52	34·52	180
14·52	32·38	260
15·52	30·56	329
16·52	29·12	383

$$\nu_C = 61782{\cdot}7 - \frac{R}{(n + 0{\cdot}52)^2} \quad \text{where } n = 7, 8, \ldots 16$$

Series D

p	λ	ν	$I_{calc.}$
17·5	1748·92	57178	57536
18·5	47·80	215	536
19·5	46·83	246	535
20·5	46·00	274	535

$$\nu_D = 57535 - \frac{R}{(n + 0{\cdot}5)^2} \quad \text{where } n = 17, 18, 19, 20.$$

Series E. This feature is peculiar in appearance, resembling a red-degraded absorption band, or violet-degraded emission one.

p	λ	ν	$I_{calc.}$
8·23	1616·62	61857·5	63477·6
9·23	07·94	62191·4	79·5
10·23	01·71	433·3	81·8
11·23	1597·22	608·8	78·9
12·23	93·68	747·9	81·6
13·23	91·05	851·6	78·6

$$\nu_E = 63479{\cdot}6 - \frac{R}{(n + 0{\cdot}23)^2} \quad \text{where } n = 8, 9, \ldots 13.$$

The most comprehensive examination and analysis of the SnI spectrum is by Meggers[45] from emission plates between 24740 Å to 1697 Å. Tin has atomic number 50 and the outermost electron shell is $5s^2 5p^2$ and the observed lines were almost completely accounted for by the predicted terms for excitation of the two outermost valence electrons.

Electron configuration $5p^2$	Spectral Terms				
	$^3P_0$	$^3P_1$	$^3P_2$	$^1D_2$	$^1S_0$
	Converging to $5p\ ^2P_{\frac{1}{2}}$ (SnII)			Converging to $5p\ ^2P_{1\frac{1}{2}}$ (SnII)	
5pns	$^3P_0$	$^3P_1$		$^3P_2$	$^1P_1$
5pnp	$^3D_1$	$^3D_2$	$^3P_0$ $^3P_1$	$^3D_3$ $^3P_2$	$^3S_1$ $^1D_2$ $^1P_1$ $^1S_0$
5pnd	$^3F_2$	$^3F_3$	$^3D_1$ $^3D_2$ $^3P_0$	$^3F_4$ $^3D_3$ $^3P_2$	$^1F_3$ $^1D_2$ $^1P_1$ $^3P_1$
5pnf	$^3G_3$	$^3G_4$	$^3F_2$ $^3F_3$ $^3D_1$ $^3D_2$	$^3G_5$ $^3F_4$ $^3D_3$	$^1G_4$ $^1F_3$ $^1D_2$

Of these predicted levels, the following were identified by Meggers:-

$5p^2$ (ground state)	all five
5pns	all four
5pnp	Ten levels through 6s-np combinations
5pnd	All except $^3F_4$.

Meggers derives the ionization potential of SnI from four Rydberg series, all 5p-ns.

(1) $5p\ ^3P_0 - ns\ ^3P_1 \rightarrow\ ^2P_{\frac{1}{2}}$ (SnII)
limit at 59160 cm^{-1} ten members

(2) $5p\ ^3P_1 - ns\ ^3P_2 \rightarrow\ ^2P_{1\frac{1}{2}}$ (SnII)
limit at 61703 cm^{-1} five members

(3) $5p\ ^3P_0 - ns\ ^1P_1 \longrightarrow {}^2P_{1\frac{1}{2}}$ (SnII)
limit at 63286 cm^{-1} three members

(4) $5p\ ^3P_1 - ns\ ^3P_0 \longrightarrow {}^2P_{\frac{1}{2}}$ (SnII)
limit at 57640 cm^{-1} three members.

The separation of the $^3P_0$ and $^3P_1$ levels in SnI is 1692 cm^{-1} (Meggers) and the similar separation in the ion $^2P_{\frac{1}{2}} - {}^2P_{1\frac{1}{2}}$ (SnII) is 4252 cm^{-1} from Green and Loring[46]. Substituting these values in Meggers' limits one gets for the ionization potential of tin:-

59160, 59143, 59034, 59332 cm^{-1}

from which Meggers takes a weighted mean of 59155 cm^{-1}.

It is clear from our observed series that a better value is 59228 $\pm$ 5 cm^{-1} derived as follows:-

Series	Ground State	Ionic Limit	
A, B, E	$5p^2\ ^3P_0$	$5p\ ^2P_{1\frac{1}{2}}$	63482 less 4252 gives <u>59230 cm^{-1}</u>
C	$5p^2\ ^3P_1$	$5p\ ^2P_{1\frac{1}{2}}$	61783 plus 1692 less 4252 gives <u>59223 cm^{-1}</u>
D	$5p^2\ ^3P_1$	$5p\ ^2P_{\frac{1}{2}}$	57535 plus 1692 gives <u>59227 cm^{-1}</u>

It remains to be seen to which excited terms of SnI these series correspond.

None of the lines in our series is observed by Meggers in emission, however, from the observed limit it is essential that the strong series A and B of this work should start at $^3P_0$ tin ground state and end at $^2P_{1\frac{1}{2}}$ of the tin ion. Of Meggers 5p - ns series starting from $^3P_0$ we observe four weak lines of ns $^3P_1$ (n = 9, 12, 14, 15) and from 5p $^3P_1$ we observe ns $^3P_2$ where n = 8?, 9, 10, but the latter, which alone leads to $^2P_{1\frac{1}{2}}$ of SnII, starts from the wrong tin multiplet.

However, there are four self-reversed tin lines in Meggers' list which he does not allocate. These appear in absorption with great strength at 1793·4, 1753·3, 1729·2, 1714·1 Å and thus there must be gaps in Meggers' analysis, for these are ground state transitions. In addition the line at 1733·64 Å which Meggers has called 5p $^3P_1$ - 9s $^3P_2$ is anomalously strong in absorption.

5p - np is of course forbidden; there remain the 5p - nd series. Of those starting from $^3P_0$ only two, $^3P_1$ and $^1P_1$ converge on $^2P_{1\frac{1}{2}}$ (SnII). Meggers gives two lines of each of these, n = 5 and n = 6. By substituting our limit in

$$\nu = I - \frac{R}{\left(n - a - \frac{b}{n^2}\right)^2}$$

it is possible to solve for a and b. For $^3P_1$ this gives

a = 0·66 and b = 39·8, but the next members calculated with these constants do not agree with any observed lines; in addition the series A and B must have values of a = 0·06 and a = 0·52 respectively.

However, for $5p\,^3P_0 - nd\,^1P_1$ the constants are a = 1·66 and b = 11·8 and this suggests that series E may be the higher members of this series. In particular the lines at 1650·1 and 1765·0 Å observed in this work, and those at 1765·0 and 1995·0 Å listed by Meggers, can be fitted in. This series is presented for examination.

p	λ in Å	ν in cm^{-1}	n
2·866	1994·98	50125·9	5
4·010	1764·98	56658	6
5·08	1687·56	overlapped	7
6·17	1650·09	60603	8
	overlapped		9
8·23	1616·62	61857·5	10
9·23	1607·94	62191·4	11
↓	↓ as for series E	↓	etc.

The best argument for this scheme is that the values of p fall on a smooth curve, from which this equation for series E is obtained.

$$\nu_E = 63482 - \frac{R}{\left(n - 1{\cdot}76 - \frac{8{\cdot}8}{n^2}\right)^2} \quad \text{where } n = 5, 6 \ldots 15.$$

In a similar manner the series C can be connected with the two strong lines at 1714·1 and 1753·3 Å, both of which are observed but unallocated by Meggers.

p	λ	ν	n
4·81	1753·3	57035	5
5·64	14·12	58339	6
6·57	overlapped		7
7·54	1670·80	59852	8
8·52	59·12	60273	9
9·52	51·06	60567	10
↓	as for series C↓		etc.

In this case also the p values give a smooth curve; however, the correction term (Ritz) that is applied to $(n \pm a)$ at small n values is positive, e.g. at $n = 5$, $p = 4·81$ rather than 4·52. In the $5p\,{}^3P_0 - nd\,{}^1P_1$ series above and in Meggers' 5p - ns series this term is always negative, but it is also positive for our strong series A and B. Now it has been stated (Paschen[47]) that the Ritz correction is negative for transitions to penetrating orbits and positive for non-penetrating. This is consistent with the 5p - ns and 5p - nd series having negative corrections, but it leaves the upper states of the A, B and C series in doubt. The possibility that they are 5p - nf transitions is ruled out by the Laporte rule which states that even

terms combine only with odd and vice versa. Thus the information that can be obtained from these series is a better value for the ionization potential of tin; it is feared that the transitions that are responsible for the series must remain in doubt.

PART II

The Band Spectrum of Aluminium Monofluoride

PART II

The Band Spectrum of Aluminium Monofluoride

The Spectrum of AlF

Introduction

The band spectrum of AlF was investigated by Rochester[48] in 1939 who discovered a system in absorption between 2200 - 2400 Å, designated $A^1\Pi - X^1\Sigma^+$ by analogy with AlCl and AlBr. However, several reasons led us to believe that the vibrational analysis of Rochester was wrong and in an earlier work[2] this system was examined again in emission. A new analysis resulted which was better both in internal consistency and in comparison of the vibrational constants with those of similar molecules. Other emission bands between 3180 - 4180 Å were ascribed to AlF by Yuasa[49] on the grounds that the source (a silica discharge tube) had AlF_3 heated to 700°C in a side-arm. The discharge of 12,000 V. was carried by a low pressure of neon. However, the analysis was most unconvincing for although $\omega' \sim \omega''$, the bands were fitted into a scheme with a very wide Condon parabola. In addition many of the strongest bands on Yuasa's reproduction were not in the analysis at all.

Thus it was thought desirable to photograph our source, which is known to produce AlF emission bands, in this spectral region. Also the work of Sharma[50] on the emission spectrum of AlCl showed a $^3\Sigma \rightarrow {}^3\Pi$ and a $^3\Pi \rightarrow {}^1\Sigma^+$ transition for this molecule in the green and in the violet; it seemed likely that a similar transition to the former could be excited for AlF.

Briefly it may be said that a $^3\Sigma \rightarrow {}^3\Pi$ system was found around 3600 Å and two sets of unidentified bands in the green and in the red. Details of these will be described below. However, while this work was being published,[51] Hugo[52] examined the spectrum under high dispersion and came to the following conclusions:

(i) Our analyses of the $A^1\Pi - X^1\Sigma^+$ were in agreement.

(ii) A rotational analysis of the red system showed it to be $^1\Sigma - A^1\Pi$.

(iii) Hugo observed but has not analysed our $^3\Sigma - {}^3\Pi$ system, and also the green bands.

(iv) There were further weak systems of violet degraded bands at 4450 - 4750 Å, 5490 - 6050 Å, 8200 - 8665 Å.

(v) There was a group of weak complex bands degraded to shorter wave-lengths between 2500-2800 Å.

It seemed likely that the weak systems (iv) had $A^1\Pi$ as their lower state similar to the red bands, in which

case the transition from these states to the ground state would appear in the vacuum ultra-violet. For this reason the absorption spectrum of AlF was examined on our vacuum spectrograph and the results obtained will be described below.

The Emission Spectrum.

The emission bands of the $A^1\Pi - X^1\Sigma^+$ system had been produced from a hollow cathode source running from a 2000 V. D.C. motor generator. The cathode was horizontal and the tube of glass, and a mixture of aluminium and aluminium trifluoride was contained in small foil boats inside the cathode. The trouble with this arrangement was that for some minutes the discharge had to be carried by hydrogen until the cathode became sufficiently hot to vaporize AlF. During this period the powder tended to scatter, and a new pattern of tube was evolved where the cathode was vertical. This tube was of silica and had a furnace wound outside it so that the cathode could be heated externally. A diagram of it is in Fig. XIV. The light was collimated on the spectrograph slit by a quartz prism, and in this case a 1000 V. generator was found more convenient, with a 500 ω resistance in series. The maximum current available was one amp.

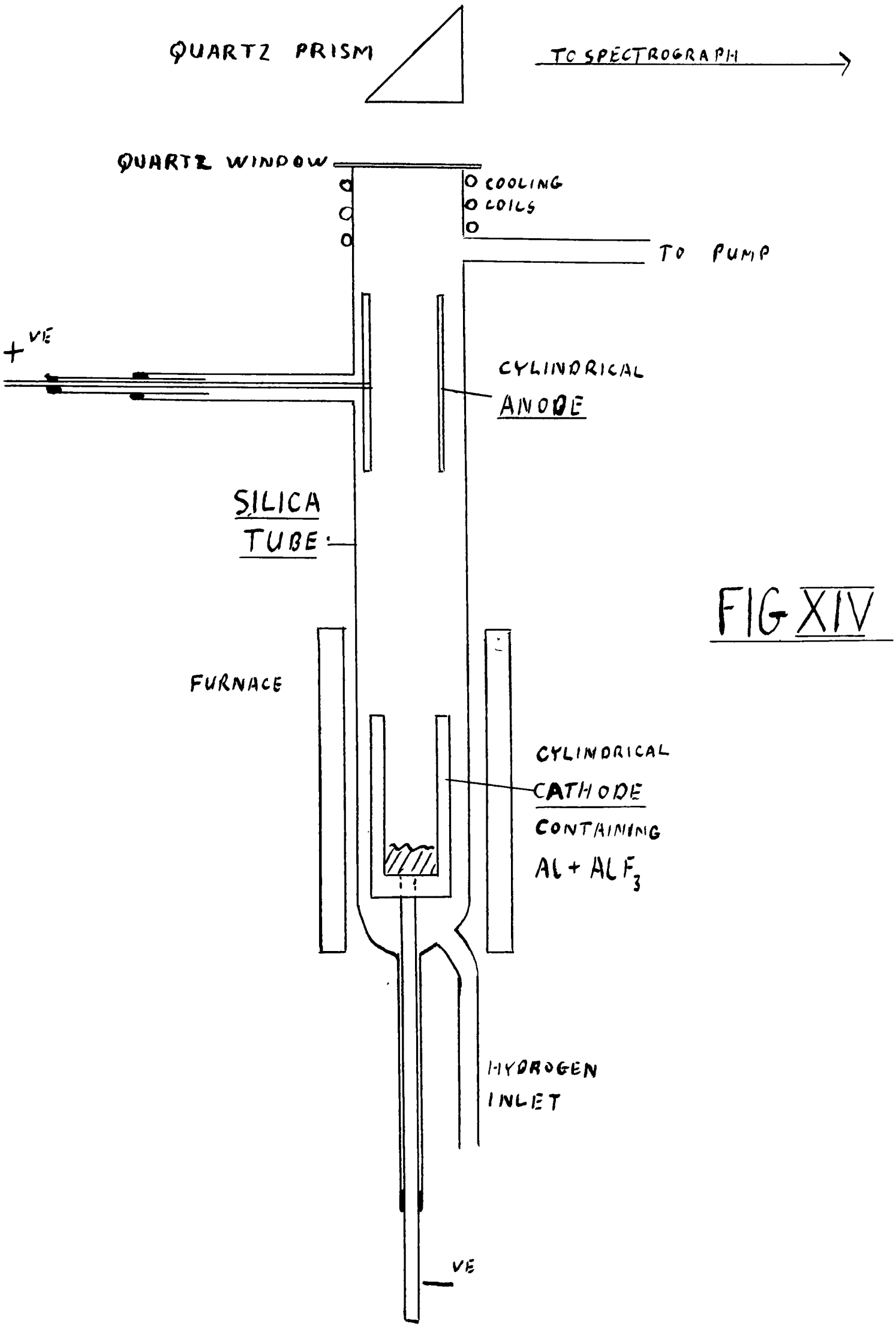

QUARTZ PRISM
TO SPECTROGRAPH
QUARTZ WINDOW
COOLING
COILS
TO PUMP
+VE
CYLINDRICAL
ANODE
SILICA
TUBE
FURNACE
CYLINDRICAL
CATHODE
CONTAINING
Al + AlF3
HYDROGEN
INLET
-VE

FIG XIV

The $^3\Sigma - ^3\Pi$ system. A preliminary exposure was made under low dispersion on the quartz optics of a Hilger E.478 prism spectrograph, and a system observed between 3450-3720 Å. Further Ilford Process plates were taken in the first and second order of 2·4 m. grating [15,000 lines/in. Eagle mounting] having a reciprocal dispersion of about 7·4 Å/mm. in the first order. The system forms three well-defined sequences degraded to the violet in both rotational and vibrational structure, and prints of these sequences from the 2nd order plate are given in Plate VII. The wave-lengths were determined by comparison with internal standards, principally iron and manganese lines from the hot hollow cathode. Although an iron arc was added after exposure by removing the prism from the front of the slit, it was found that the change in collimation caused a slight difference in wave-length between the iron lines from the cathode and those from the arc. The latter were therefore rejected as wave-length standards. The wave-lengths and frequencies of the band-heads are given in table XIV.

The short wave-length sequence is the only one to show any obvious regularity of structure: the heads can be arranged in overlapping groups of five with a moderately constant separation of about 92 cm^{-1}. Assuming that this is the sequence difference and that the values of $x_e\omega_e$ are

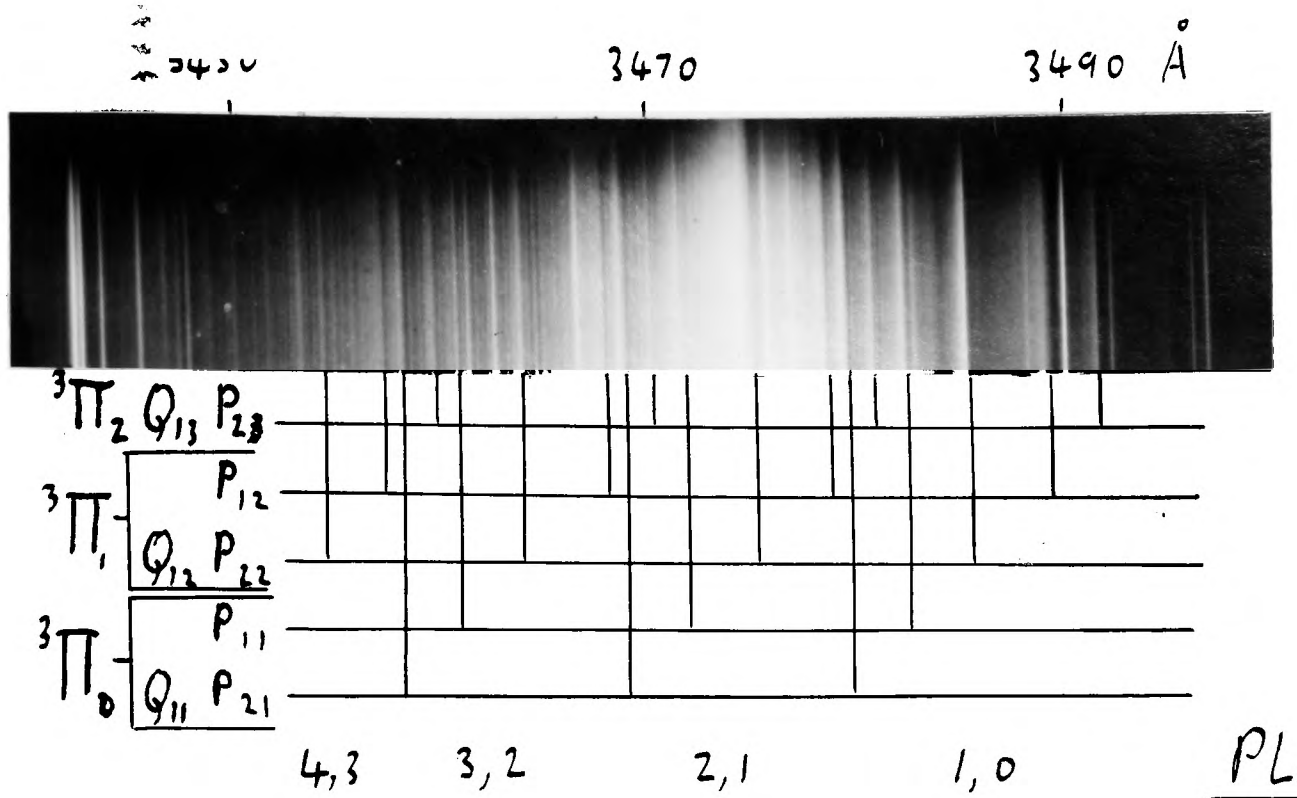
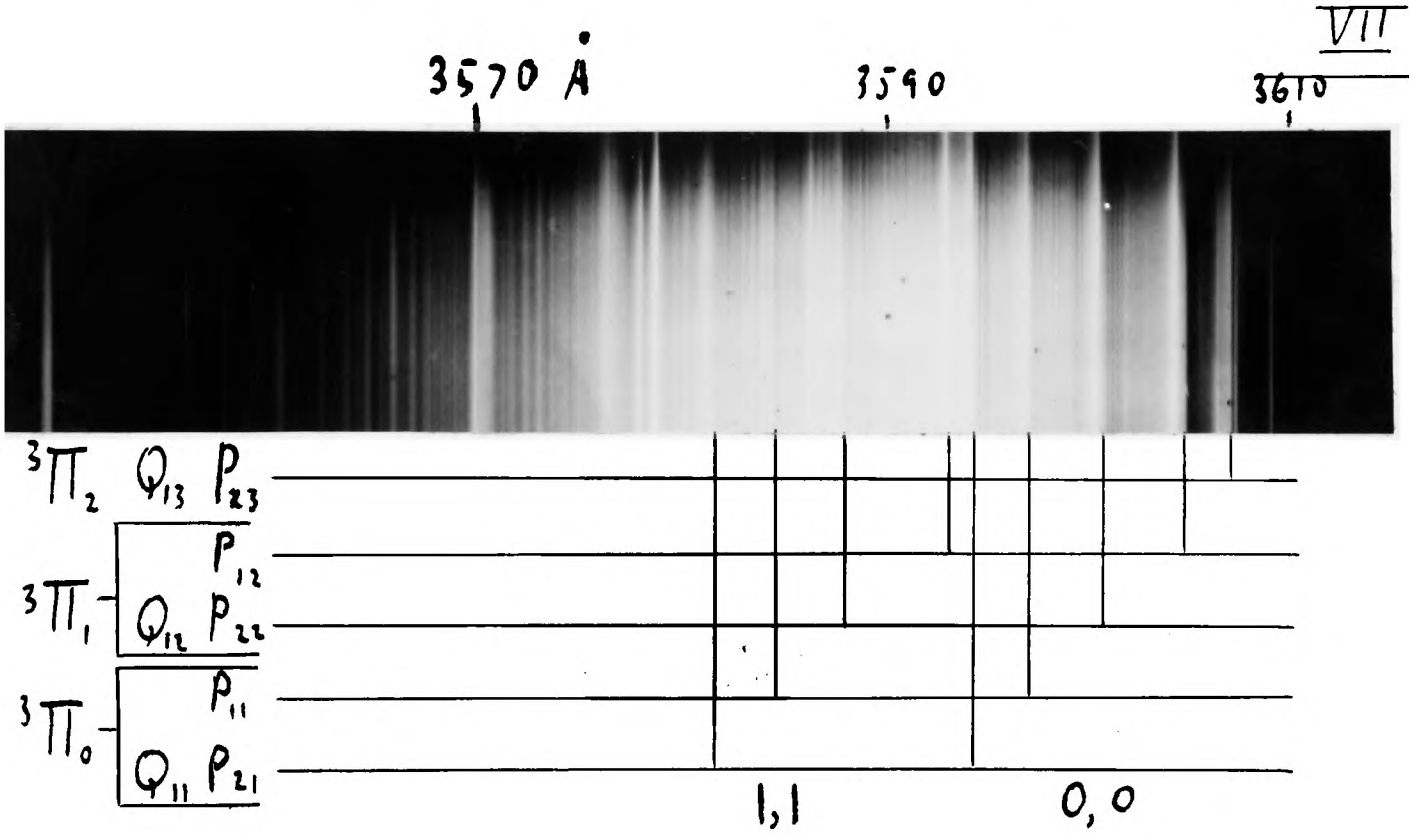
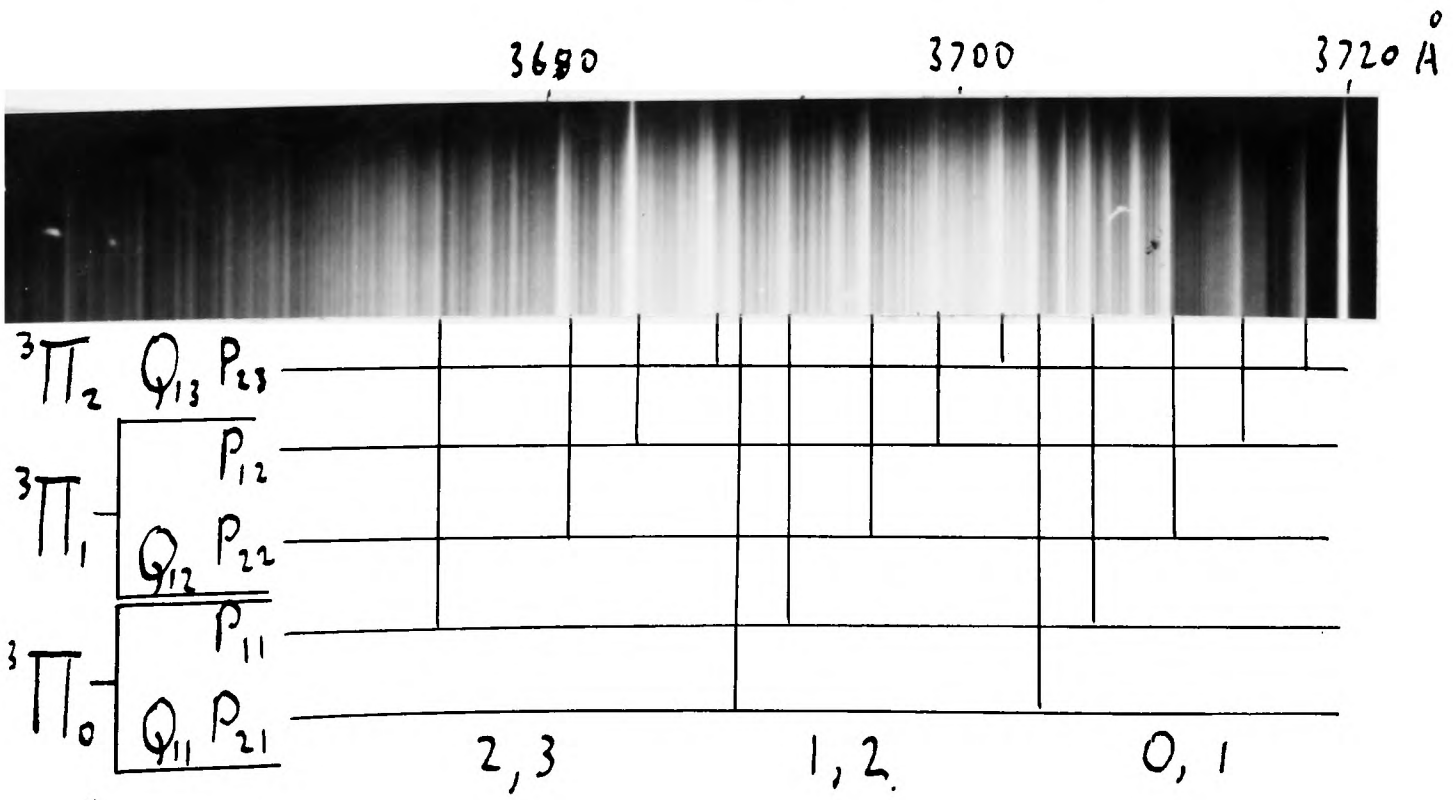

3450
3470
3490 Å
$^3\Pi_2$ Q_{13} P_{23}
$^3\Pi_1$ P_{12} Q_{12} P_{22}
$^3\Pi_0$ P_{11} Q_{11} P_{21}
4,3
3,2
2,1
1,0

PLATE VII


3570 Å
3590
3610
$^3\Pi_2$ Q_{13} P_{23}
$^3\Pi_1$ P_{12} Q_{12} P_{22}
$^3\Pi_0$ P_{11} Q_{11} P_{21}
1,1
0,0


3680
3700
3720 Å
$^3\Pi_2$ Q_{13} P_{23}
$^3\Pi_1$ P_{12} Q_{12} P_{22}
$^3\Pi_0$ P_{11} Q_{11} P_{21}
2,3
1,2
0,1

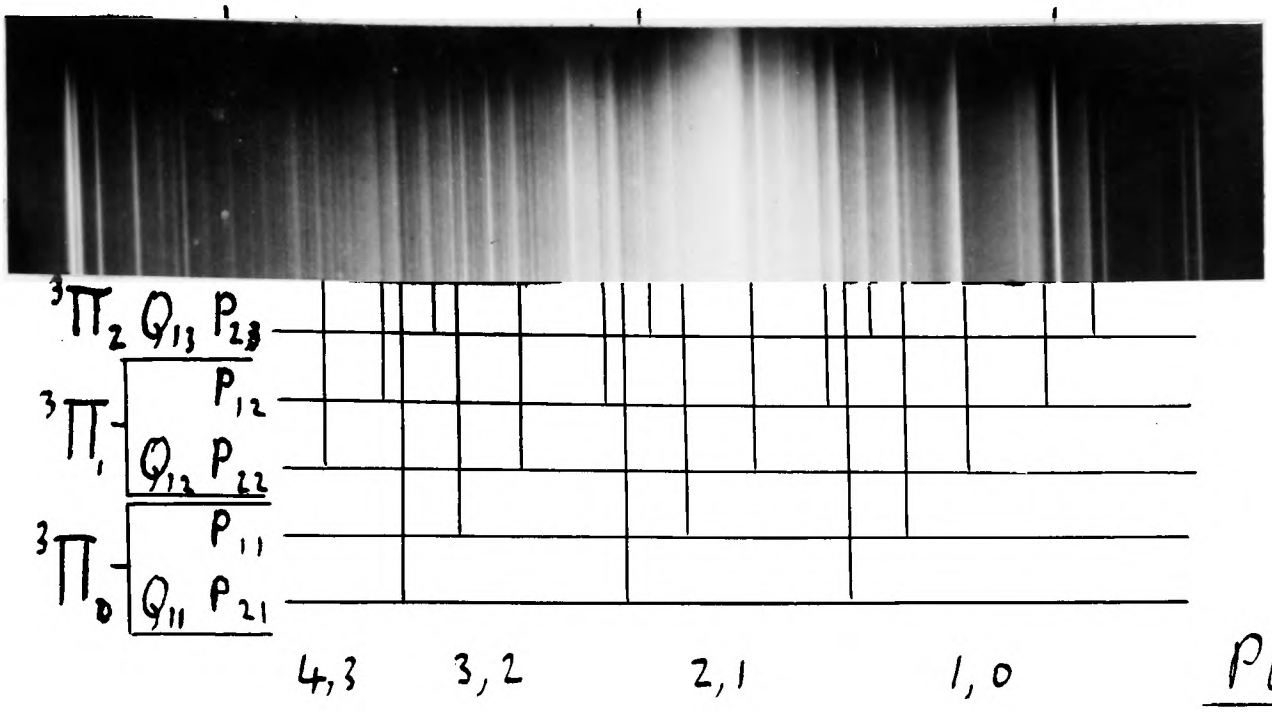
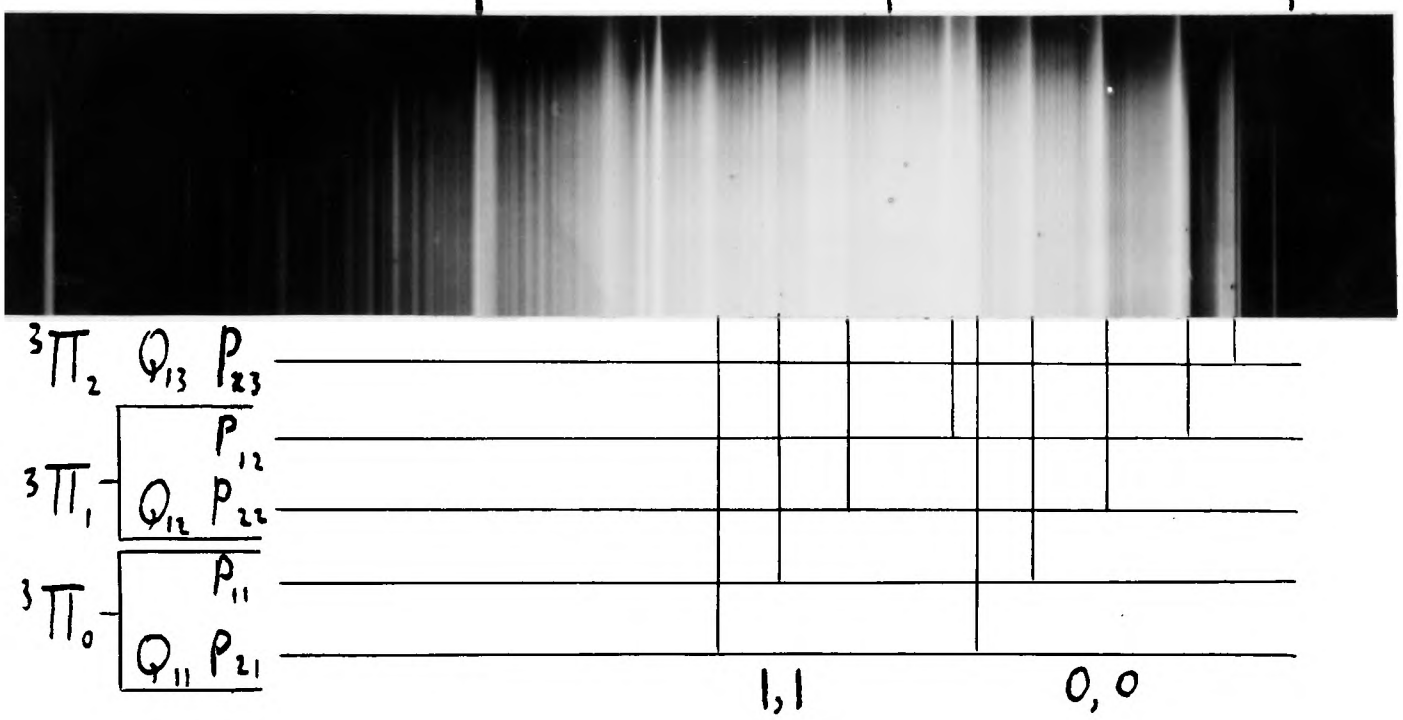
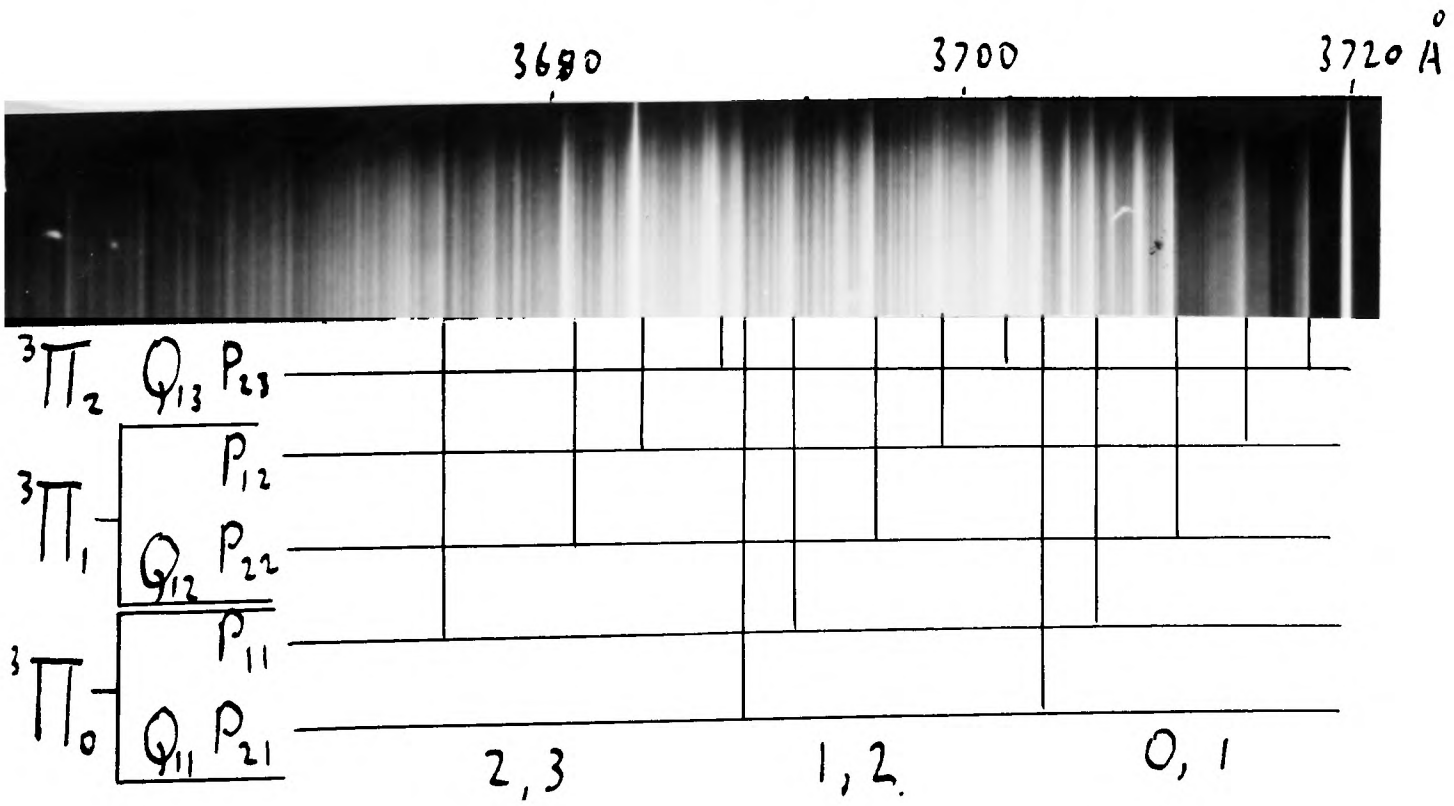
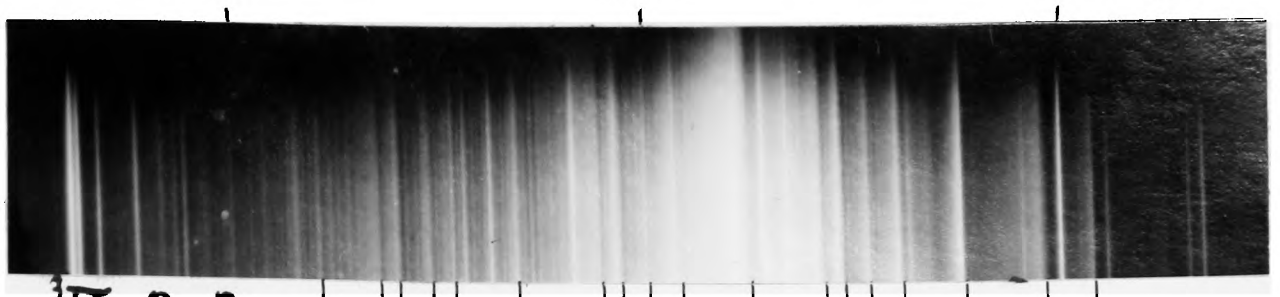

3450
3470
3490 Å
$^3\Pi_2$ Q_{13} P_{23}
$^3\Pi_1$ P_{12} Q_{12} P_{22}
$^3\Pi_0$ P_{11} Q_{11} P_{21}
4,3
3,2
2,1
1,0

PLATE VII


3570 Å
3590
3610
$^3\Pi_2$ Q_{13} P_{23}
$^3\Pi_1$ P_{12} Q_{12} P_{22}
$^3\Pi_0$ P_{11} Q_{11} P_{21}
1,1
0,0


3680
3700
3720 Å
$^3\Pi_2$ Q_{13} P_{23}
$^3\Pi_1$ P_{12} Q_{12} P_{22}
$^3\Pi_0$ P_{11} Q_{11} P_{21}
2,3
1,2
0,1

3450 3470 3490 Å



$^3\Pi_2$ Q_{13} P_{23}

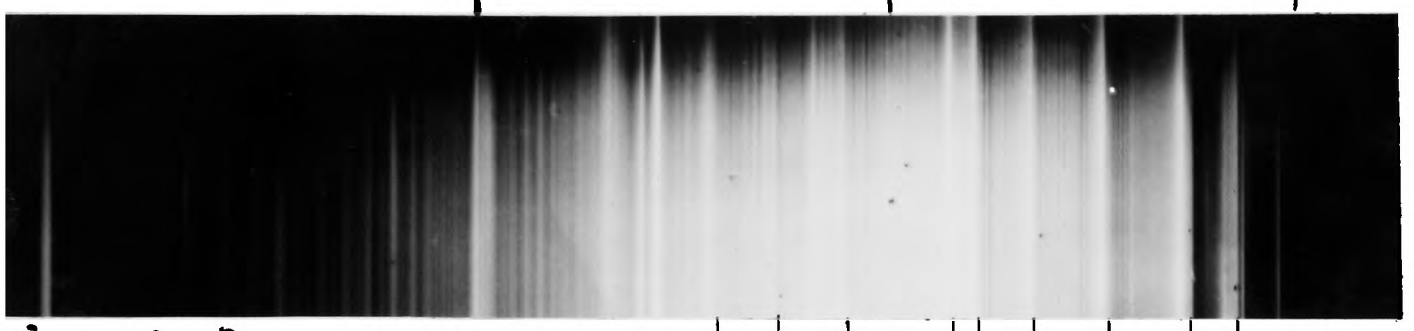
$^3\Pi_1$ P_{12} / Q_{12} P_{22}

$^3\Pi_0$ P_{11} / Q_{11} P_{21}

4,3 3,2 2,1 1,0

PLATE VII

3570 Å 3590 3610



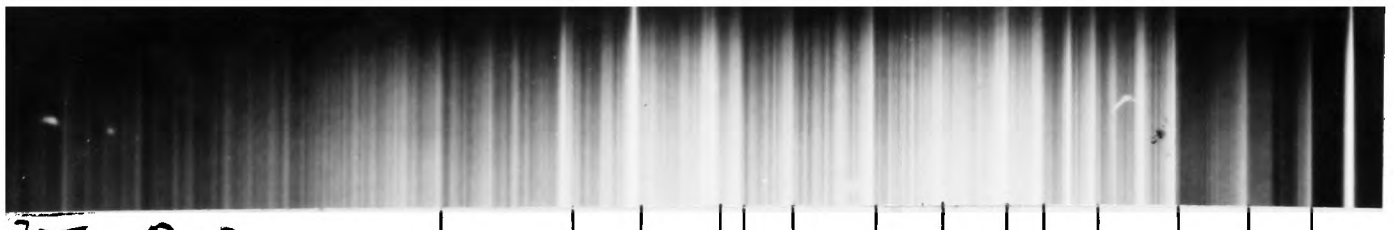
$^3\Pi_2$ Q_{13} P_{23}

$^3\Pi_1$ P_{12} / Q_{12} P_{22}

$^3\Pi_0$ P_{11} / Q_{11} P_{21}

1,1 0,0

3680 3700 3720 Å



$^3\Pi_2$ Q_{13} P_{23}

$^3\Pi_1$ P_{12} / Q_{12} P_{22}

$^3\Pi_0$ P_{11} / Q_{11} P_{21}

2,3 1,2 0,1

Table XIV

Measurements of Band-heads of $^3\Sigma - {}^3\Pi$ System

λ (Å)	ν_{vac} (cm^{-1})	Head	v',v"	Intensity	C-C	$\Delta\nu$, head-origin
3717·91	26889·2	Q_{13},P_{23}		2	1·3	13·5
15·97	903·3	-		1		
14·57	13·4	P_{12}	0 , 1	2	0·5	36·0
10·94	39·7	P_{22},Q_{12}		4	-0·2	9·0
06·76	70·1	P_{11}		4	0·5	26·8
04·11	89·4	Q_{11},P_{21}		3	-0·3	6·7
02·42	27001·7	Q_{13},P_{23}		2	1·9	13·0
00·61	14·9	-		0		
3699·06	26·2	P_{12}	1 , 2	1	-0·1	34·0
95·54	52·0	P_{22},Q_{12}		4	0·2	8·5
91·43	82·1	P_{11}		3	-0·5	25·2
88·78	101·7	Q_{11},P_{21}		4	0·2	6·3
87·11	27113·8*	Q_{13},P_{23}		1	0·7	10·6
84·49	33·1	-		0		
83·50	40·4	P_{12}	2 , 3	0	-0·4	30·4
80·33	63·7	P_{22},Q_{12}		2	0·1	7·6
73·70	212·8*	Q_{11},P_{21}		0	Obs.	5·9
72·16	27224·2*	Q_{13},P_{23}		0	0·3	10·2
69·00	47·7*	P_{12}		0	6·0	27·2
65·28	75·3*	P_{22},Q_{12}	3 , 4	0	0·5	6·8
58·75	324·0*	Q_{11},P_{21}		0	Obs.	5·1

* Indicates a measurement on the 1st order plate only.

[Table continued over]

[Table XIV continued]

λ(Å)	ν_{vac} (cm^{-1})	Head	v',v"	Intensity	O-C	$\Delta\nu$, head-origin
3608·17	27707·0	Q_{13},P_{23}		8	2·0	18·0
05·94	24·1	P_{12}		7	-0·4	46·0
01·41	59·1	P_{22},Q_{12}	0 , 0	10	0·1	11·5
3597·74	87·4	P_{11}		10	3·0	33·6
94·86	809·6	Q_{11},P_{21}		10	0	8·4
92·71	826·2	P_{12}		2	-0·8	45·6
88·21	61·5	P_{22},Q_{12}	1 , 1	5	0·3	11·4
84·68	88·6	P_{11}		4	-0·3	31·2
81·59	912·6	Q_{11},P_{21}		5	0·3	7·8
3492·22	28626·9	Q_{13},P_{23}		3	1·2	21·0
89·71	47·5	P_{12}		4	1·3	48·0
85·55	81·7	P_{22},Q_{12}	1 , 0	5	-0·5	12·0
82·36	708·0	P_{11}		4	-0·1	33·6
79·31	33·2	Q_{11},P_{21}		4	-0·1	8·4
80·82	720·7	Q_{13},P_{23}		3	2·8	21·0
78·40	40·7	P_{12}		4	-0·2	45·6
74·22	75·3	P_{22},Q_{12}		4	0·2	11·4
70·95	802·3	P_{11}	2 , 1	4	-0·5	31·2
68·06	26·4	Q_{11},P_{21}		4	0·2	7·8
69·55	813·9	Q_{13},P_{23}		0	0·1	17·0
67·15	33·8	P_{12}		3	-2·5	42·0
62·96	68·8	P_{22},Q_{12}	3 , 2	2	1·0	10·5
59·72	95·8*	P_{11}		2	0·4	30·4
57·05	918·1	Q_{11},P_{21}		2	-0·1	7·6
58·58	905·5	Q_{13},P_{23}		1	-	-
55·98	27·1	P_{12}	4 3	1	-2·1	40·0
51·99	60·7	P_{22},Q_{12}		0	1·1	10·0

about 5 cm^{-1}, then the sequence differences in the 0,0 and 0,1 sequences should be about 102 and 112 cm^{-1} respectively. The central, most intense, sequence is taken as the 0,0 , and here, as in the 0,1 sequence, groups of five heads can be arranged with differences of the magnitude expected. Thus the outline of the vibrational analysis is fairly clear, but the rough values of $\Delta G_{0,1}$ so derived, namely 920 cm^{-1} for the upper state and 820 cm^{-1} for the lower, show that the transition is not $^3\Pi - X^1\Sigma^+$ as at one time seemed possible, for $\Delta G_{0,1}$ for $X^1\Sigma^+$ is only 794 cm^{-1}. (That this is not the intercombination system is further suggested by its moderate intensity: the system is excited quite strongly in InF, is much less strong in GaF, has not been observed in BF, and might therefore be expected to be very weak in AlF.) By analogy with BF and AlCl, it seems most likely that the system is $^3\Sigma - ^3\Pi$: a definite decision cannot, however, be made without a rotational analysis, which is likely to need very high resolving power.

It is now possible to proceed to examine the conclusions which follow from the suggestion that the system is $^3\Sigma - ^3\Pi$. It is apparent both from Table XIV and from Plate VII that the five heads of each band do not give any constant separations as one might expect in a triplet transition. However, this can be interpreted as arising from the near

equality of B' and B" resulting in head-origin separations of about the same size as the multiplet splitting A in $^3\Pi$. A would be expected to be about 20-40 cm^{-1}, between $A = 64\ cm^{-1}$ for AlCl and $A = -2\ cm^{-1}$ for BF. This would give $Y = A/B \sim 40\text{-}80$, indicating that the $^3\Pi$ state in AlF is probably intermediate in coupling, somewhere between Hund's cases (a) and (b), (see ref.12).

In a $^3\Sigma - ^3\Pi$ transition where $^3\Pi$ is case (a) there are expected 27 branches, for each $^3\Pi$ sub-band has nine branches. This may be shown schematically taking as an example the J = 10 level of $^3\Pi_1$.

$^3\Pi_1$		$^3\Sigma$				
	K	8	9	10	11	12
J = 10	J	7	8	9	10	11
		8	9	10	11	12
		9	10	11	12	13

Thus by applying $\Delta J = 0 \pm 1$ it is apparent that there is one transition to $^3\Sigma$ K = 8, two to K = 9, three to K = 10, two to K = 11 and one to K = 12. When the spin splitting in $^3\Sigma$ is neglected we are left with five branches as the J levels for each K value are now indistinguishable.

As the $^3\Pi$ state approaches case (b) the selection rule $\Delta K = 0 \pm 1$ becomes operative and there are nine strong

branches where $\Delta K = \Delta J$ plus satellite branches where $\Delta K \neq \Delta J$. However, for these bands the equations for the branches may be calculated assuming that $^3\Pi$ is case (a) and that the $^3\Sigma$ spin splitting is negligible. The rotational energies are to a first approximation:-

$$^3\Sigma : \begin{cases} F_1'(J) = B'K'(K' + 1) = B'(J' - 1)J' \\ F_2'(J) = B'K'(K' + 1) = B'J'(J' + 1) \\ F_3'(J) = B'K'(K' + 1) = B'(J' + 1)(J' + 2) \end{cases}$$

$$^3\Pi : F''(J) = B_{eff}''J''(J'' + 1),$$

where $B_{eff}''\left(^3\Pi_0\right) = B^{(1)} = B_v(1 - 2B_v/A)$

$$B_{eff}''\left(^3\Pi_1\right) = B^{(2)} = B_v$$

$$B_{eff}''\left(^3\Pi_2\right) = B^{(3)} = B_v(1 + 2B_v/A).$$

By substituting $\Delta J = 0 \pm 1$ the equations for the 27 branches can be calculated, in accordance with theory there are only five different equations for each sub-band.

For $B' > B''$, the following are head-forming branches:

$^3\Pi_0$, Q-form. Q_{11}, P_{21}. $\nu = \nu_o^{(1)} - (B' + B^{(1)''})J + (B' - B^{(1)''})J^2$

P-form. P_{11}. $\nu = \nu_o^{(1)} + 2B' - (3B' + B^{(1)''})J + (B' - B^{(1)''})J^2$

$^3\Pi_1$, P-form. P_{22}, Q_{12}. $\nu = \nu_o^{(2)} - (B' + B^{(2)''})J + (B' - B^{(2)''})J^2$

O-form. P_{12}. $\nu = \nu_o^{(2)} + 2B' - (3B' + B^{(2)''})J + (B' - B(^{(2)''})J^2$

$^3\Pi_2$, 0-form. Q_{13}, P_{23}. $\nu = \nu_o^{(3)} - (B' + B^{(3)"})J + (B' - B^{(3)"})J^2$

N-form. P_{13}. $\nu = \nu_o^{(3)} + 2B' - (3B' + B^{(3)"})J + (B' - B^{(3)"})J^2$.

The equations for the branches that are not head-forming are given below in general terms, i.e. the necessary superscripts must be added in order that they may apply to any one sub-band.

$$\nu = \nu_o + (B' - B")J + (B' - B")J^2$$

$$\nu = \nu_o + 2B' + (3B' - B")J + (B' - B")J^2$$

$$\nu = \nu_o + 6B' + (5B' - B")J + (B' - B")J^2.$$

As the $^3\Pi$ state approaches case (b) the branches with $\Delta K = \pm 3$ will disappear, and here the $^NP_{13}$ head is not observed; it cannot however, be far from case (a) for heads corresponding to $\Delta J \neq \Delta K$ are observed, although the $^PP_{11}$, $^QQ_{11}$ and $^PP_{22}$ are always the strongest. A plausible allocation of the five observed heads in each band to their correct branches may be made following a consideration of head-origin separations. For example, for $^3\Pi_0$ we may calculate the relative separations from the origin of the Q-form and P-form heads.

Q-form head. $\frac{d\nu}{dJ} = -(B' + B") + 2(B' - B")J$

At the head of the band $\frac{d\nu}{dJ} = 0$, i.e. $J = + \frac{B' + B''}{2(B' - B'')}$

Thus $\nu_{head} - \nu_o = - \frac{(B' + B'')^2}{2(B' - B'')} + \frac{(B' + B'')^2}{4(B' - B'')} = - \frac{(B' + B'')^2}{4(B' - B'')}$.

Similarly $\nu_{head} - \nu_o$ for the P-form heads is given by:-

$$\nu_{head} - \nu_o = - \frac{(B' + B'')^2 - 12\ B'B''}{4(B' - B'')} .$$

Thus the relative head-origin separation in the two heads is

$$\frac{\Delta\nu P}{\Delta\nu Q} = \frac{(B' + B'')^2 + 12\ B'B''}{(B' + B'')^2} = 1 + \frac{12\ B'B''}{(B' + B'')^2} .$$

Now in this case B" and B' must be approximately equal for the head-origin separations are large, thus:-

$$\frac{\Delta\nu P}{\Delta\nu Q} \simeq 4 .$$

Thus by subtracting the frequency of the outer head from that of the inner, and adding one-third of the difference to the frequency of the inner head, the position of the sub-band origin is obtained. Thus the $^3\Pi_0 - {}^3\Pi_1$ origin separation can be found, and if this is constant from band to band, then the allocation of heads should be correct. In fact only the allocation given in table XIV results in constant separations. In this way, the following equation for the band-origins was obtained:

$$\nu = \begin{matrix} 27766{\cdot}8 \\ 719{\cdot}3 \\ 671{\cdot}8 \end{matrix} \Bigg\{ + [933{\cdot}5u' - 4{\cdot}9_0 u'^2] - [830{\cdot}9u'' - 4{\cdot}5_5 u''^2],$$

where $u = v + \frac{1}{2}$. The observed-calculated values given in table XIV have been obtained from these band-origins by subtracting the frequencies of the heads and comparing these differences with those adjusted so that $\Delta\nu(P_{11})/\Delta\nu(Q_{11}) = 4$ and the two O - C values are at a minimum.

The O - C values for the $^3\Pi_2$ heads cannot be obtained in this way as only the $Q_{13} + P_{23}$ head is observed. However, the head-origin separations in $^3\Pi_2$ can be obtained as follows: let x, y, z, be the head-origin separations of the $(Q_{11} + P_{21})$, $(P_{22} + Q_{12})$ and $(P_{23} + Q_{13})$ heads respectively. Then

$$x = -(B' + B^{(1)}{}'')^2/4(B' - B'' + B''^2/24); \quad y = -(B' + B^{(2)}{}'')^2/4(B' - B'');$$
$$z = -(B' + B^{(3)}{}'')^2/4(B' - B'' - B''^{(2)}/24).$$

We may take the numerators as constant, since $2B/A\Lambda \simeq B/24$ affects the terms in $B' - B_{eff}''$ much more than those in $(B' + B_{eff}'')^2$. It is then easy to show that $z = xy/(2x - y)$, and so from the head-origin separations in the $^3\Pi_0$ and $^3\Pi_1$ sub-bands, those for $^3\Pi_2$ can be calculated: O - C values may then be determined for the

$^3\Pi_2$ heads from their calculated origins. For this reason the head-origin separations have been included in table XIV, and it can be seen that the O - C values that result are small and an excellent confirmation that the analysis is correct. This agreement and the values of A, ω_e' and ω_e'' combine strongly to suggest that this is indeed the $^3\Sigma - ^3\Pi$ transition corresponding to those known for BF[66] and AlCl[50]. Further confirmation of this analysis has been obtained recently from the formulae derived by Budó[53] for the relative intensities of the lines of each branch of a $^3\Sigma - ^3\Pi$ transition. Using the value of A = 47·5 derived above and an assumed value of B" = 0·52, Dr. Barrow has calculated the strengths of these branches at J = 10, 30, 50, 70 and 90, omitting the Boltzmann factor. The results are as follows for the head-forming branches only.

J" =	10	30	50	70	90	
Branch						
$Q_{11} + P_{21}$	22·9	93·0	174·9	259·3	343·3	$^3\Sigma - ^3\Pi_0$
P_{11}	7·1	36·4	76·6	119·8	163·2	
$P_{22} + Q_{12}$	20·0	60·5	101·1	141·4	181·6	$^3\Sigma - ^3\Pi_1$
P_{12}	10·3	21·8	23·2	21·2	18·6	
$Q_{13} + P_{23}$	18·7	28·0	26·2	22·6	19·3	$^3\Sigma \quad ^3\Pi_2$
P_{13}	4·2	3·2	1·6	0·8	0·4	

This agrees admirably with the conclusion reached above that

$^{N}P_{13}$ should not appear and that the strongest branches are $^{P}P_{11}$, $^{Q}Q_{11}$, and $^{P}P_{22}$.

The Green System. This band system consists of a very strong central sequence containing bands degraded in both directions, together with flanking sequences degraded to the violet. It was photographed in the first order of the 2·4 m. grating on Ilford H.P.3 plates using exposures from ½ to one hour, with a glass filter before the slit to remove overlapping orders. The outer sequences are very much weaker than the central one and their structure is partly concealed by many strong manganese lines emitted in this region by the hot hollow cathode, made of alloy steel. Reproductions of these sequences are shown in Plate VIII and a list of their wave-lengths, frequencies, intensities (visual) and direction of degradation are given in table XV(a). Some of the weaker bands may be arranged in a Deslandres scheme of double-headed violet-degraded bands, and Hugo (private communication) says he has analysed the rotational structure of such a weak band and found it to be $^{1}\Delta - A^{1}\Pi$. There is no reason to doubt that we have observed the same systems.

$D^1\Delta \longrightarrow A^1\Pi$ 2,1 1,0

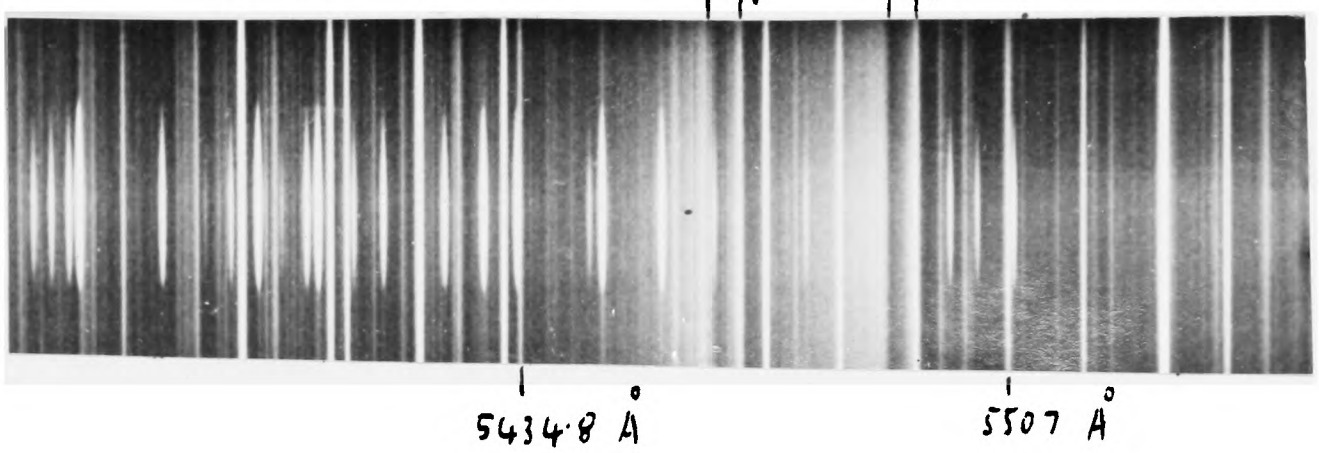
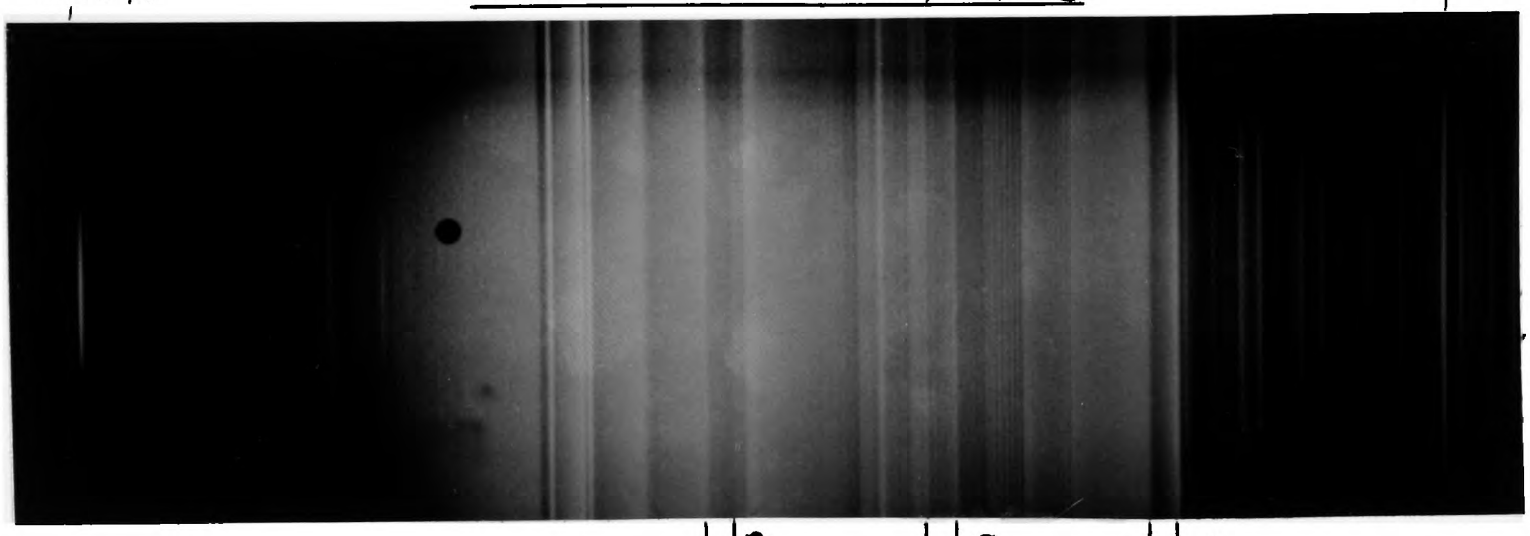


PLATE VIII

5616 Å INTENSE CENTRAL SEQUENCE 5912·6 Å



$D^1\Delta \longrightarrow A^1\Pi$

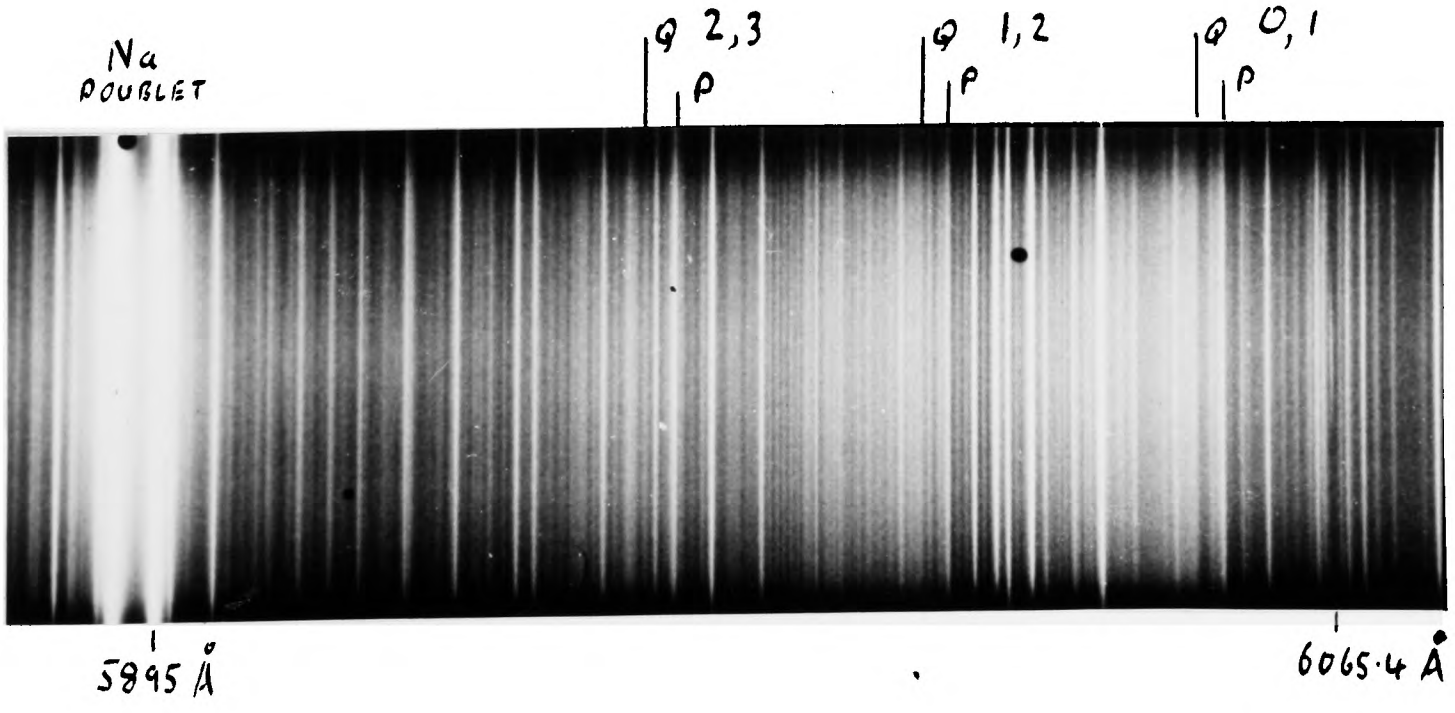


Table XV

Band-heads of AlF

(a) Yellow-Green System

λ(Å)	ν_{vac} (cm^{-1})	Intensity	Degradation	λ(Å)	ν_{vac} (cm^{-1})	Intensity	Degradation
6052·43	16517·7	0	?	5758·48	17360·9	4	line
49·83	524·8	2	V	51·10	383·2	5	R
47·90	530·1	1	line ?	41·57	412·0	4	V
45·91	535·5	2	V	37·35	424·8	4	V
42·77	544·1	2	line	30·68	445·1	6	line
41·16	548·4	0	line	27·33	455·3	4	R
37·12	559·5	0	V	10·99	505·3	10	R
35·37	564·4	0	V	09·18	510·8	3	R
28·84	582·4	0	V ?	05·30	522·7	10	V
09·83	634·9	1	V	5696·23	550·6	10	V
05·94	645·6	1	V ?	87·53	577·4	10	V
5988·58	693·8	1	R ?	80·18	600·2	7	V
70·39	744·7	0	V	5492·75	18190·5	2	V
5774·04	17314·1	10	V	88·16	216·0	2	V
70·04	326·1	8	V	67·15	286·0	2	V
				62·83	300·5	1	V

(b) Red System

λ(Å)	ν_{vac} (cm^{-1})	Intensity	Degradation
7245·94	13797·2	3	V
40·81	806·8	2	V
6790·07	14723·3	10	V
84·98	734·4	8	V
32·44	849·4	10	V
27·53	860·2	8	V
6678·03	970·3	8	V
74·66	977·9	6	V

Deslandres scheme of the $^1\Delta - A\,^1\Pi$ system of AlF

v' \ v"	0		1		2		3
2			18300·5	777·8	17522·7	769·6	16753·1
			18286·0		17510·8?		16744·7
			875·7		877·1		
1	18216·0	791·2	17424·8	779·2	16645·6		
	18200·8		17412·0		16634·9		
	889·9		889·3				
0	17326·1	790·6	16535·5				
	17314·1		16524·8				

The equation found[51] for the $^1\Pi$ state in the $A\,^1\Pi \quad X\,^1\Sigma^+$ transition was $803{\cdot}95\ (v+\tfrac{1}{2}) - 6{\cdot}14_1\ (v+\tfrac{1}{2})^2 - 3{\cdot}9_1 \times 10^{-3}\ (v+\tfrac{1}{2})^4$ and it is apparent that these observed differences are consistent with those expected for the $^1\Pi$ state. Thus the vibrational constants of the $^1\Delta$ state are:-

$$\omega_e = 902{\cdot}6 \quad \text{and} \quad x_e\omega_e = 7{\cdot}5.$$

The remaining strong bands of the 0,0 sequence and the weak ones of the 0,1 appear to have no regular structure. Bands are degraded in both directions implying that the B values of the two states involved are nearly equal or that there are two overlapping systems. It seems likely that the determination of the states involved must wait until a rotational analysis of some of the bands has been completed.

The Red bands. These were photographed between 6500 - 7300 Å on the first order of the 2·4 m. grating. Exposures of about one hour with a wide slit were required to record an image on Ilford Long-range Spectrum plates. These were sensitized by immersion in ·880 ammonia and dried before use, but were still singularly slow above 7000 Å. Four double-headed violet-degraded bands were recorded; prints of them are shown in Plate IX and the measurements given in table XV(b) were obtained by comparison with an iron arc. Lower orders were removed by use of a red filter.

Hugo[52] has recorded the same system with larger dispersion; the wave-lengths of his bands are not available but it is said to stretch from 6790 - 8200 Å showing that his plates are faster than Long-range Spectrum at long wave-lengths and perhaps not so fast at short ones. A rotational analysis showed the system to be $^1\Sigma - A\,^1\Pi$ and Hugo's equation agrees admirably with the Q-heads of table XV except for the 3,2 Q-head. In addition the head-origin separations can be calculated from Hugo's B and α values; the results are listed below.

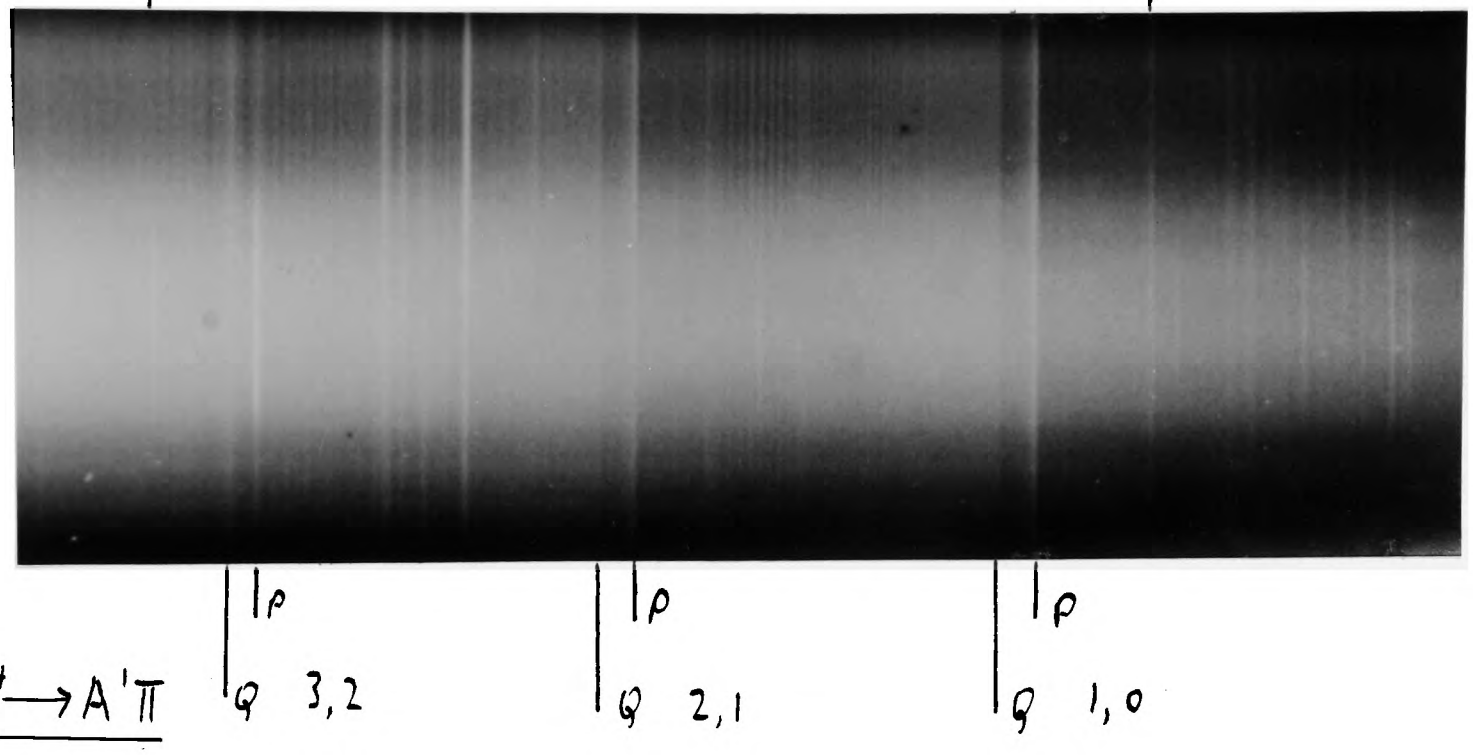
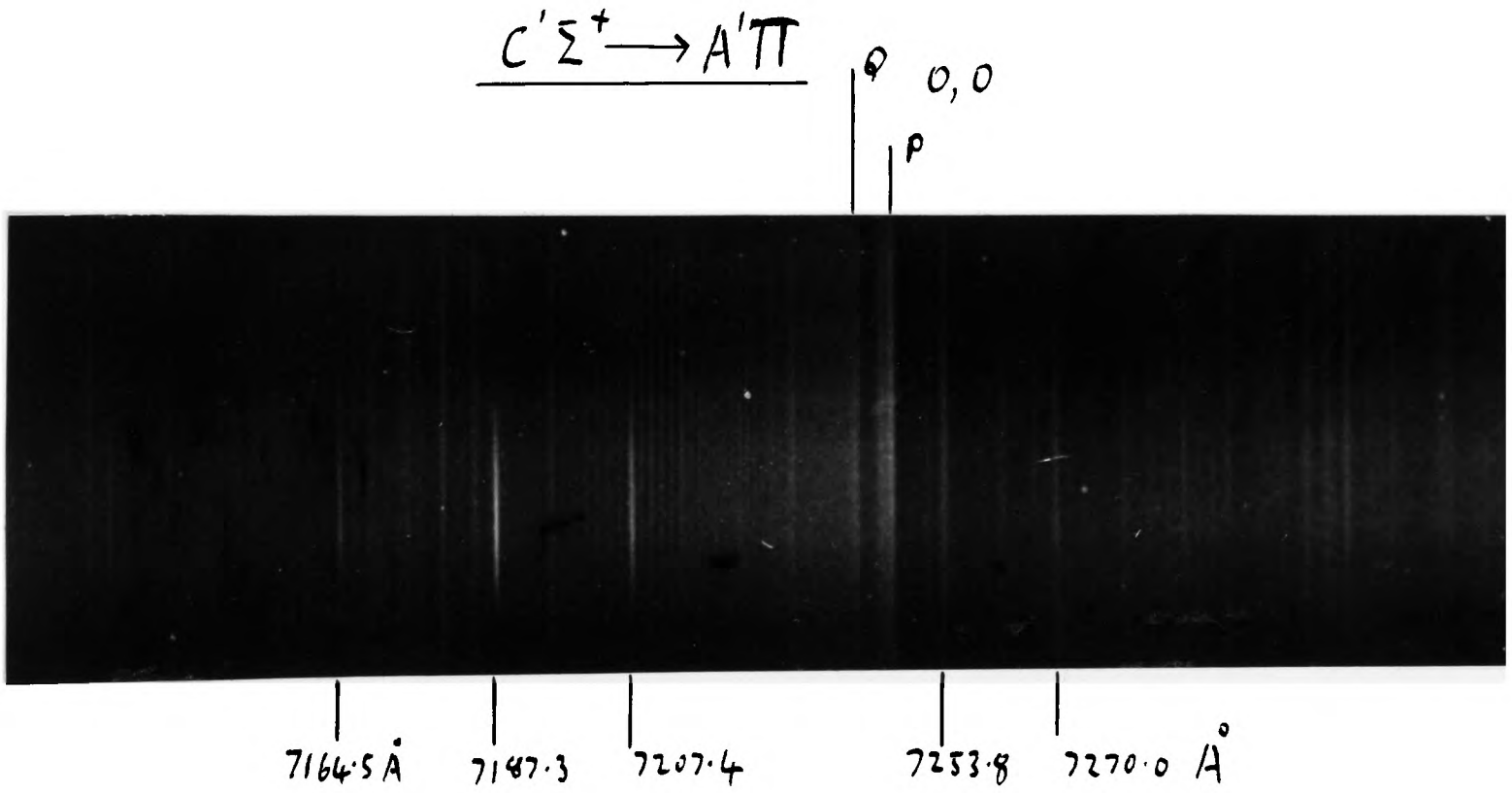

6663.4 Å
6806.5 Å
P
P
P
C ¹Σ⁺ ⟶ A ¹Π
Q 3,2
Q 2,1
Q 1,0

PLATE IX


C ¹Σ⁺ ⟶ A ¹Π
Q 0,0
P
7164.5 Å
7187.3
7207.4
7253.8
7270.0 Å

$^1\Sigma - A\,^1\Pi$ system of AlF

ν observed	ν calc. from Hugo	v'v"	$\Delta\nu$ head-origin
13797·2	13796·5	0,0 P	- 10·2
806·8	806·7	0,0 Q	
14723·3	14723·9	1,0 P	- 10·8
734·4	734·7	1,0 Q	
849·4	851·5	2,1 P	- 8·8
860·2	860·3	2,1 Q	
970·3	981·1	3,2 P	- 7·4
977·9	988·5	3,2 Q	

It is odd that the head-origin separation of our 3,2 band is correct while its position does not agree with the calculated one. Probably Hugo only observed bands with v' = 0, 1, or 2 and his equation does not apply to higher levels without a $y_e'\omega_e'$ term.

The Yuasa Bands. As mentioned in the Introduction Yuasa[49] reported bands due to AlF between 3180 - 4180 Å, but the analysis is doubtful as the bands fall on a very wide Condon intensity parabola for a system with $\omega_e' \sim \omega_e''$. In addition no trace of any of these bands has been found on the plates taken with the hollow cathode source, also Yuasa had exposures of 4-5 hours on a Hilger E.1. spectrograph and could hardly have failed to observe the $A\,^1\Pi - X\,^1\Sigma^+$ system had he in fact had any AlF present. By comparison

with published band-heads it is possible to suggest an emitter for Yuasa's bands, namely the $^3\Sigma^- - ^3\Sigma^-$ system of S_2. Of the twenty-eight heads listed by Fowler and Vaidya[55] in the appropriate region, all but four (one of intensity 2, the others of intensity 1) appear on Yuasa's reproduction, while of the fifty-nine bands given by Yuasa, all those of intensity 3 or more (17 in number), and eight of those of intensity 2 or 1, coincide in wave-length as well as can be expected with the S_2 bands. Thus it is suggested that Yuasa's bands are due to S_2.

This concludes the discussion of the obvious systems in the emission spectrum of AlF; further weak bands were observed but were apparently fragmentary systems and it was not until the absorption spectrum had been examined in the vacuum ultra-violet that the transitions responsible for these bands could be determined. They will be mentioned in the discussion at the end of this section.

The Absorption Spectrum.

It was mentioned in the Introduction that a reason for examining the spectrum of AlF in the vacuum ultra-violet was a desire to find out more about highly excited singlet states, some of which had weak transitions to $A^1\Pi$ in the visible and near u-v. The conditions for the observation

of the $A^1\Pi - X^1\Sigma^+$ transition in absorption were checked by Harris[54] using a mixture of aluminium metal and aluminium trifluoride. The system was reasonably well developed by 900°C, some 600°C lower than Rochester[48] found necessary using AlF_3 alone. It is of interest that none of the other systems seen in emission were found by Harris, confirming the conclusions reached above about their origins.

The first exposure on the vacuum spectrograph was spoiled by the scattering of AlF_3 powder from the furnace. The arrangement for the exposure was identical with that described in Part I of this thesis, and the scattered powder covered the mirror, blocked the slit and even found its way into the spectrograph itself. Blank experiments indicated that this was partly due to the fineness of the powder causing it to scatter on evacuation but more largely due to combined and absorbed water which were pumped off when the furnace was at 1000°C and 120°C respectively. This was overcome by roasting the AlF_3 at 1200°C in an atmosphere of argon and keeping it in a desiccator until use. Aluminium powder was then added and two exposures taken on Kodak plates of half an hour at 820°C and 40 minutes at 920°C.

The strongest feature of the spectrum, which was well developed at the lower temperature, is an intense system

of five sequences between 1780 and 1900 Å. It is degraded to shorter wave-lengths in both rotational and vibrational structure, and an enlargement is given in Plate X. The analysis of this system is obvious from inspection and confirmed by measurement. An interesting head of heads is formed in the 1,0 and 2,0 sequences. The wave-lengths, frequencies, visual intensities, vibrational analysis and O-C values are listed in Table XVI. The calculated values of the frequencies of the heads are given by:-

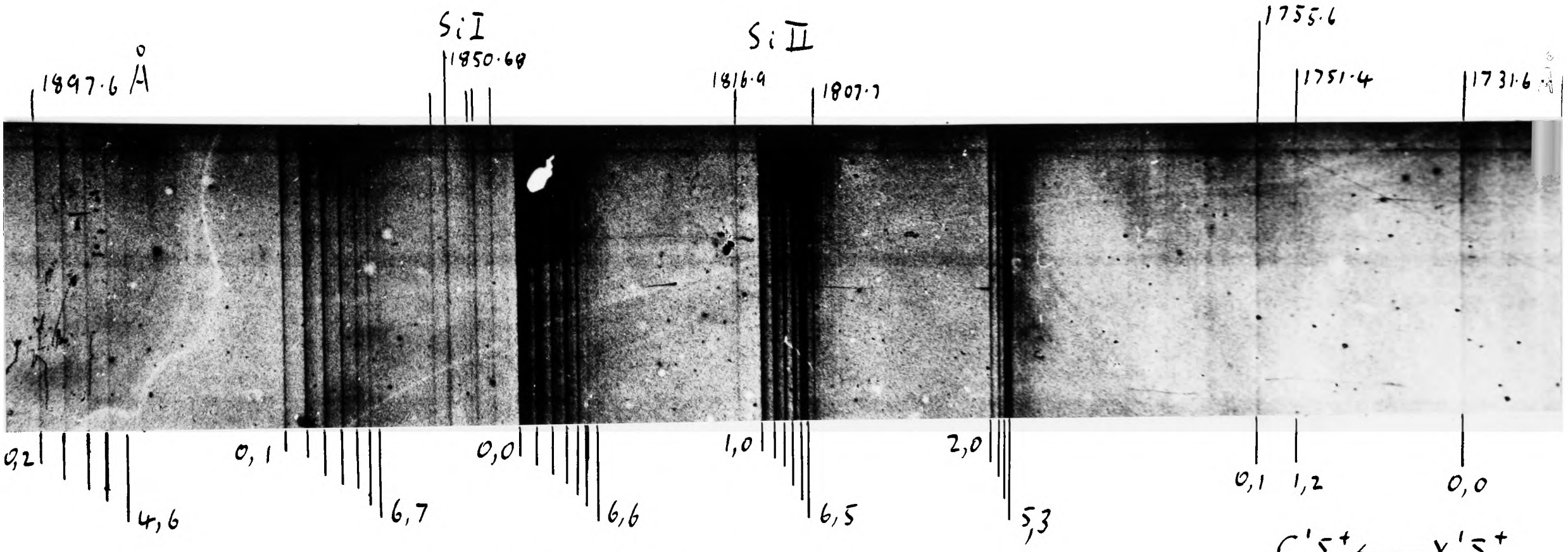
$$\nu = 54241{\cdot}5 + 862\,(v' + \tfrac{1}{2}) - 7{\cdot}0\,(v' + \tfrac{1}{2})^2 - 0{\cdot}012\,(v' + \tfrac{1}{2})^4 - 800{\cdot}5\,(v'' + \tfrac{1}{2}) + 4{\cdot}9\,(v'' + \tfrac{1}{2})^2.$$

Naming the systems in the conventional manner, this may be called the $B - X\,{}^1\Sigma^+$ transition.

Of considerably less intensity are three further bands on Plate X. These are at 1755·62, 1751·37 and 1731·60 Å and form the 0,1, 1,2, and 0,0 bands of a C↔X system thus:-

v' \ v"	0		1		2
1					57098·2
					919·4
0	57750·1	790·1	56960·0	780·2	calc.

Now the upper state C of this transition must be the upper state of the $^1\Sigma - {}^1\Pi$ red bands observed in emission. The 0,0 band of C—A is at 13806·8 cm^{-1}, that of A—X is at 43948·8 cm^{-1} and we may expect that of C—X to be at



$B^1\Sigma^+ \longleftarrow X^1\Sigma^+$

$C^1\Sigma^+ \longleftarrow X^1\Sigma^+$

PLATE X

Table XVI

Band-heads of the B→X system of AlF

λ_{vac} in Å	ν_{vac} in cm^{-1}	Intensity	v' v"	O−C in cm^{-1}
1897·57	52699·0	2	0 , 2	−0·9
94·86	774·3	1	1 , 3	−2·7
92·22	848·0	1	2 , 4	−1·3
89·80	915·7	0	3 , 5	−0·8
87·55	978·7	0	4 , 6	+1·1
69·82	53481·1	4	0 , 1	+0·1
67·45	549·0	5	1 , 2	+0·9
65·32	610·1	5	2 , 3	−0·5
63·24	670·0	4	3 , 4	+2·0
61·47	721·0	2	4 , 5	+1·7
59·95	764·9	1	5 , 6	+1·3
58·75	799·6	0	6 , 7	+0·4
42·55	54272·6	10	0 , 0	+0·9
40·64	328·9	9	1 , 1	+0·1
38·83	382·4	8	2 , 2	+0·7
37·21	430·4	7	3 , 3	+1·1
35·69	475·4	5	4 , 4	+4·6
34·59	508·1	2	5 , 5	+2·8
33·63	536·6	0	6 , 6	+5·5
14·22	55120·1	9	1 , 0	+0·4
12·87	161·2	9	2 , 1	−1·4
11·59	200·1	8	3 , 2	−0·3
10·55	231·8	8	4 , 3	−0·3
09·63	259·9	6	5 , 4	+3·1
09·19	273·4	6	6 , 5	+0·6
1787·25	55951·9	3	2 , 0	−1·4
86·34	980·4	3	3 , 1	−0·9
85·61	56003·3	3	4 , 2	−0·1
85·19	016·4	3	5 , 3	−1·7

57755·6 cm^{-1}. However, for $^1\Sigma - ^1\Sigma$ bands no Q branch appears, and the value of 57750·1 is that of the P branch; the agreement is excellent, and the error in $\Delta G'_{0,1}$ in the C→X system must be partly due to the head-origin correction and partly to the diffuse, weak nature of the heads.

At shorter wave-lengths there appear four more systems due to AlF, one weak and three strong overlapping systems.

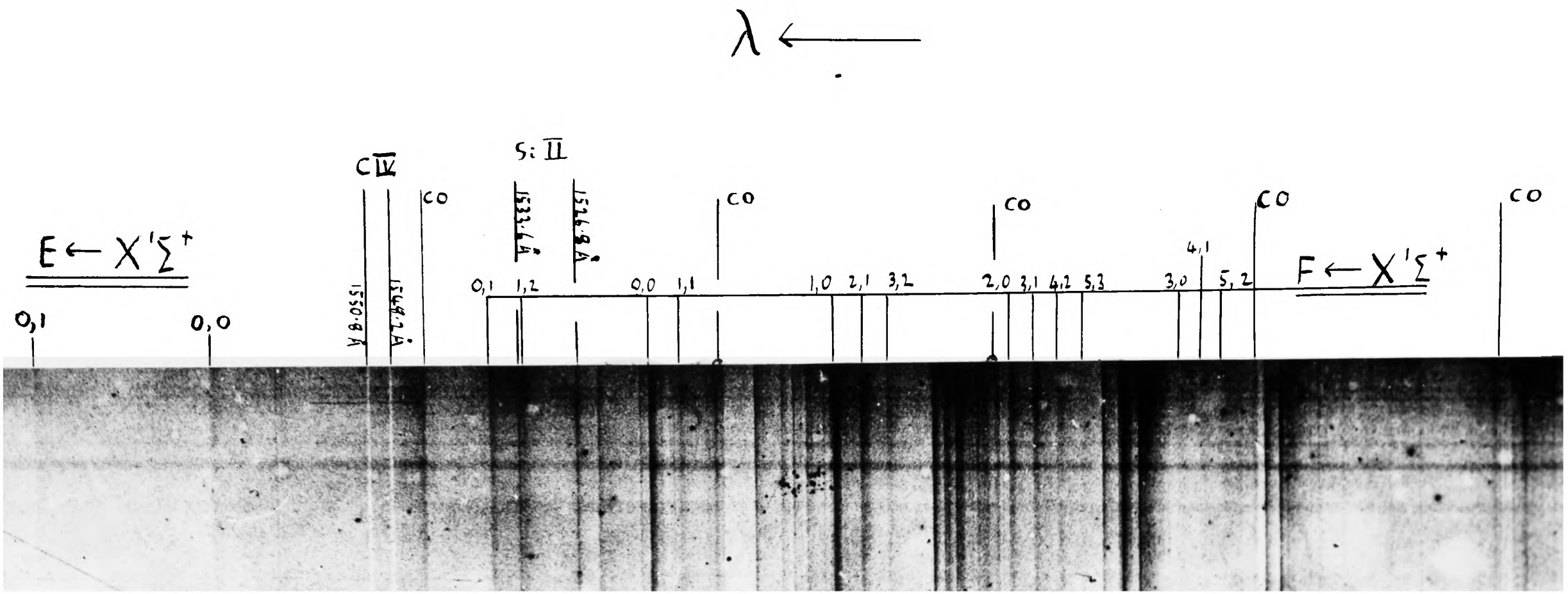
Prints of these are given in Plate XI. The weak system which we may call E→X has two bands degraded to shorter wave-lengths, the 0,0 and 0,1; it may be identified as due to AlF by the ground state difference.

E—X system.

0, 0		0, 1	
λ in Å	ν in cm^{-1}	λ	ν
1568·9	63739	1588·5	62952

A complete list of the wave-lengths, frequencies, intensities, vibrational analysis and O-C values for the three overlapping systems are given in table XVII. The systems are called F, G, and H in increasing frequency of their origins, and system G is the strongest and H the weakest. Their Deslandres schemes are given in table XVIII, and the equations for the vibrational levels of their upper states are of the form:-

$$G_{v'} = \nu_e + \omega_e(v' + \tfrac{1}{2}) - x_e\omega_e(v' + \tfrac{1}{2})^2 - z_e\omega_e(v' + \tfrac{1}{2})^4.$$


λ ←
E ← X ¹Σ⁺
0,1
0,0
CIII
1550.8 Å
1548.2 Å
CO
SiII
1533.4 Å
1526.8 Å
CO
0,1 1,2 0,0 1,1 1,0 2,1 3,2
CO
2,0 3,1 4,2 5,3
CO
4,1 3,0 5,2
F ← X ¹Σ⁺
CO

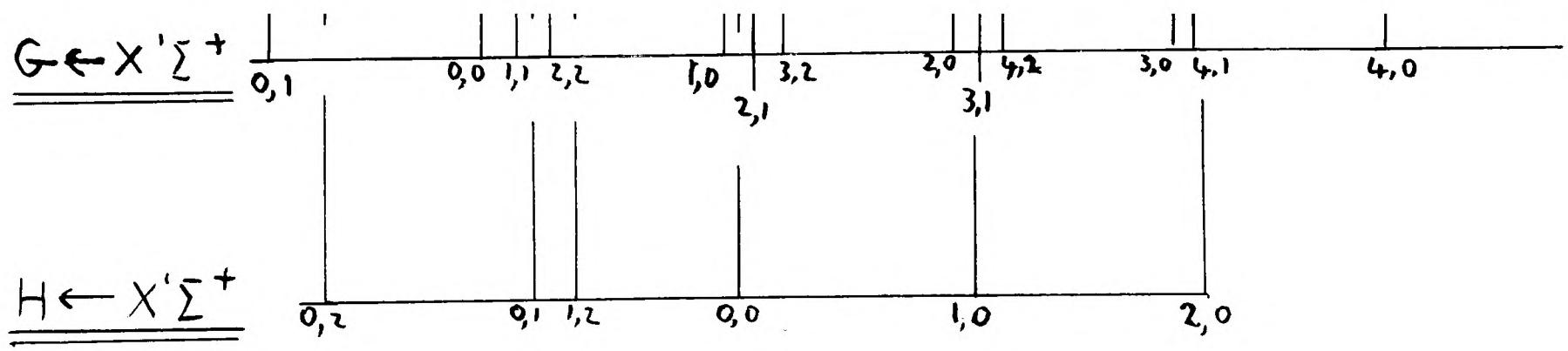

G ← X ¹Σ⁺
0,1
0,0 1,1 2,2
1,0 2,1 3,2
2,0 3,1 4,2
3,0 4,1
4,0
H ← X ¹Σ⁺
0,2
0,1 1,2
0,0
1,0
2,0

PLATE XI

Table XVII

AlF bands of the F, G, and H→X transitions

λ_{vac} in Å	ν_{vac} in cm^{-1}	Intensity	v' v"	O − C
1536·8	65069	1	0 , 1 F	−2
33·3	220	overlapped	1 , 2 F?	−14
24·2	607	2	0 , 1 G	0
19·4	814	1	0 , 2 H	−4
18·3	864	8	0 , 0 F	+2
14·9	66012	0	1 , 1 F	−3
06·1	398	4	0 , 0 G	0
02·9	537	2	1 , 1 G	−2
01·5	600	1	0 , 1 H	+1
1499·9	669	2	2 , 2 G	−4
97·9	762	0	1 , 2 H	0
96·8	807	10	1 , 0 F	+1
93·6	951	3	2 , 1 F	0
90·5	67092	0	3 , 2 F	−2
85·1	335	6	1 , 0 G	+5
83·9	392	4	0 , 0 H	+2
82·5	455	4	2 , 1 G	+1
79·9	571	0	3 , 2 G	0
76·2	741	2	2 , 0 F	−1
73·3	877	1	3 , 1 F	+2
70·4	68007	0	4 , 2 F	+1
67·7	134	0	5 , 3 F	−1
65·3	245	3	2 , 0 G	0
63·4	334	2	1 , 0 H	0
63·0	354	10	3 , 1 G	+2
61·1	442	8	4 , 2 G	−8
53·8	787	0	4 , 1 F	+1
51·3	904	0	5 , 2 F	−2
46·2	69145	4	3 , 0 G	+2
44·6	226	5	4 , 1 G	−5
43·8	264	0	2 , 0 H	0
28·1	70025	0	4 , 0 G	+3

Table XVIII

Deslandres Schemes of the F, G, and H→X transitions

F→X	5					68904	770	68134
						797		
	4			68788	781	68007		
				911		915		
	3			67877	785	67092		
				926				
	2	67741	790	66951				
		934		939				
	1	66807	795	66012	792	65200 ?		
		943		943				
	0	65864	795	65069				
	v'/ v"	0		1		2		3
G→X	4	70025	799	69226	784	68442		
		880		872		871		
	3	69145	791	68354	783	67571		
		900		899		902		
	2	68245	790	67455	786	66669		
		910		918				
	1	67335	798	66537				
		937		931				
	0	66398	791	65607				
	v'/ v"	0		1		2		
H→X	2	69264						
		930						
	1	68334				66762		
		942				948		
	0	67392	792	66600	786	65814		
	v'/ v"	0		1		2		

These constants have the following values:-

State	ν_e	ω_e	$x_e\omega_e$	$z_e\omega_e$
$X^1\Sigma^+$	-	800·5	4·9	
F	65785	955	5·0	0·01
G	66325	948	8·0	0·02
H	67312	958	7·0	

The electronic configuration of these states is not clear; as far as can be seen the bands are all single-headed with the exception of the 0,0 H and 2,1 G bands. This implies that they are all $^1\Sigma$ states or that the difference in B values between the upper and lower states is such that the heads are not resolved. Due to the increase in wave numbers per Angstrom as λ decreases, the minimum separation between resolvable heads is about 10-15 cm^{-1} at this point in the spectrum. This matter will be further mentioned in the discussion at the end of this section.

At still shorter wave-lengths there is a confused mass of band-heads which do not fall into obvious systems. It is possible that amongst them a Rydberg series may be found, however this has not yet proved possible. A reproduction of that portion of the spectrum is given in Plate XII, and a list of wave-lengths, frequencies and estimated intensities given in table XIX.

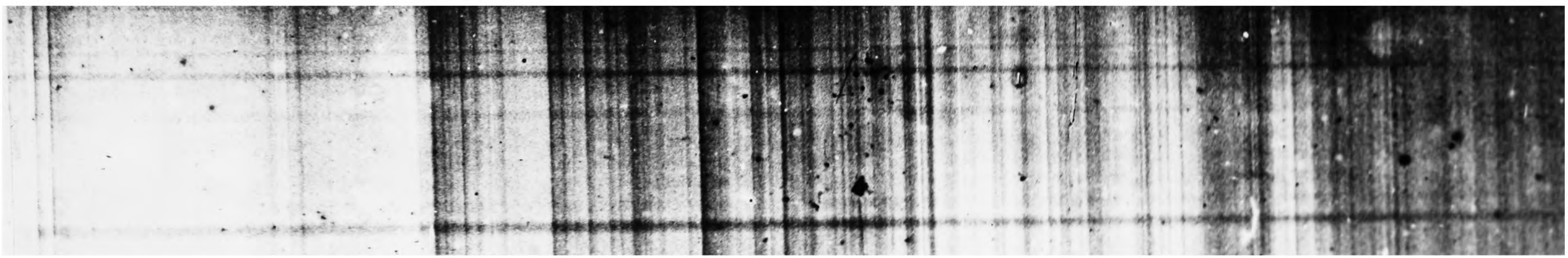


PLATE XII

9421

Table XIX

Violet-degraded band-heads, believed to be due to AlF

λ_{vac} in Å	ν_{vac} in cm^{-1}	Intensity	λ_{vac} in Å	ν_{vac} in cm^{-1}	Intensity
1402·4	71307	1	1369·3	73028	6
00·7	71391	4	63·1	361	4
1399·5	455	1	59·6	549	6
98·8	491	1	57·3	674	1
97·2	570	2	48·9	74135	1d
95·7	650	1	45·1	347	2
94·2	727	0	41·6	538	3
86·9	72103	5	34·7	921	1
85·5	177	2	33·7	977	0
84·2	241	0	31·2	75122	1
82·7	323	3	28·2	292	1
80·2	453	2	26·9	365	1
77·5	597	3	23·4	564	1
74·5	752	1	16·5	960	1
70·8	949	1	10·2	76321	1

Discussion.

The results given above for aluminium monofluoride form an admirable example of the two complementary methods for obtaining information about the highly excited states of a molecule. The examination of the spectrum in the Schumann region is preferably first carried out in absorption in order that the results may be interpreted simply, for emission sources, except for stable gaseous species, tend to emit the spectra of impurities. The observation of absorption spectra alone has the disadvantage that only states with the same multiplicity as the ground state are observed, at least for light molecules and short path lengths. In addition $\Delta\Lambda$ must equal 0 ± 1, for example in this case there is no observed transition to $^1\Delta$ at 61275 cm^{-1}. Thus the additional observations in the normal photographic region are required, for here transitions between the excited states may be recorded in emission and the use of large gratings gives the dispersion necessary for rotational analyses. These analyses enable the electron configurations of the states to be decided, but such transitions are often so weak that only one or two bands will be seen, and the vibrational constants of the states must come from the vacuum region observations. In addition many less stable diatomic molecules are dissociated

by the normal energetic discharges and the highly excited levels are never sufficiently populated for their transitions to be recorded. Work on more mild discharges for this purpose remains to be done. It is of interest to speculate on the reasons for the stability of the upper states of AlF and BF; many of these excited upper states are above the dissociation limit of AlF (see below) yet their transitions to $A^1\Pi$ are quite intense. Similar experiments with a hollow-cathode discharge for SiO failed to reveal the corresponding emission systems; it may be that the paramount factor is the physical one and that heated AlF_3 plus molten aluminium produces a steady stream of gaseous AlF, while Si + SiO_2 (both solid) do not produce similar amounts of SiO. However, a further examination of the emission plates of AlF taken on the first order of the 2·4 m. grating revealed bands which must be due to transitions from the F, E and G levels to $A^1\Pi$. The F—A is the best developed of these, and a Deslandres scheme of the bands is below.

<u>F→A system, observed</u>.

v' \ v"	0	1	2
1			21286·2
0	21911·7	21122·1	

The frequencies of these bands can be calculated from those of the $A^1\Pi - X^1\Sigma^+$ observed before[2] and from the F→X bands listed above.

<u>F→A system, calculated.</u>

v' \ v"	0	1	2
1			21286
0	21915	21123	

The agreement is extremely good and confirms all three analyses. The wave-lengths, frequencies and O−C values of these weak bands are below; all are violet-degraded.

λ_{air} in A	ν_{vac} in cm^{-1}	v' v"	O−C in cm^{-1}
4450·14	22464·9	0 , 0 G→A	?
4453·17	22449·6	0 , 0 G→A	0
4562·50	21911·7	0 , 0 F→A	-3
4696·56	21286·2	1 , 2 F→A	0
4733·06	21122·1	0 , 1 F→A	-1
4744·48	21071·3	?	
4746·88	21060·6	?	
5051·64	19790·1	0 , 0 E→A	0

It is unfortunate that the expected position of the H→A 0,0 band lies under the Q branch of an AlH band at 4259·5 Å, but the agreement for the other systems is very good. With the exception of G→A these bands appear to be single-headed, and so do those in the vacuum region; for $^1\Pi - ^1\Pi$

transitions only one head is expected as the intensity of the Q branch falls rapidly with increasing J, but for $^1\Sigma - {}^1\Pi$ or $^1\Pi - {}^1\Sigma$ there will be two heads, whose separation will depend on the relative B values. Thus the assumption that the E and F states are either $^1\Pi$ or $^1\Sigma$ involves the conclusion that two heads are unresolved in either the vacuum region or in the 4500 Å region. The former is intrinsically more likely as the wave-number dispersion at 1500 Å is about eight times less than that of 4500 Å. Thus the states E and F may tentatively be called $^1\Pi$ although the determination of their configuration really waits on the rotational analysis of the emission bands. However, the G→A band appears double-headed, and so it is likely that the G state is $^1\Sigma^+$. In the light of this conclusion it is interesting that it is the P head of the 0,0 band of G→A that agrees with the measured head of G←X in the vacuum region. This is reasonable as the B values of the 0 levels of both $A^1\Pi$ and $X^1\Sigma$ have been shown[51] to be nearly equal. It is also possible that the double-headed band at 4744·5 and 4746·9 Å may be part of another $^1\Delta - A^1\Pi$ transition, for no corresponding bands are seen in the Schumann region.

With the information now available it is possible to draw up a scheme of singlet energy levels for AlF and this

is shown in Fig. XV with the observed transitions. However, further examination of the emission plates showed other weak groups of complex bands whose wave-lengths and frequencies are given in table XX , together with the relative intensity of the sequences. The two short-wave sequences were measured on a plate taken on the Hilger quartz spectrograph, the others on the first order of the grating. There is an unfortunate gap between the two plates at 2616 – 2680 Å. No attempt has been made to analyse these systems; it would probably be impossible on the basis of the present spectrograms and it is likely that Hugo[52] will have observed the stronger bands under higher dispersion. In any case they are almost certainly triplet-triplet transitions and little information of value can be gained from them until the height of the $^3\Pi$ state above the ground state is known. This intercombination system $a^3\Pi - X^1\Sigma^+$ has been observed in absorption for GaF and InF by Welti and Barrow[56] and for AlCl by Sharma[50] (in emission) and the similar system for CO is the Cameron bands. For BF, however, no such transition has been observed, and it will be weak in AlF for the selection rule $\Delta S = 0$ applies to both case a and case b but holds less and less rigorously as the multiplet splitting increases. This splitting is 47·5 cm^{-1} in AlF $^3\Pi$, while

Table XX

Weak violet-degraded band-heads, believed to be due to AlF

λ_{air} in A	ν_{vac} in cm^{-1}	Intensity	λ_{air} in A	ν_{vac} in cm^{-1}	Intensity
2531·50	39490·7		2823·18	35410·6	
31·00	498·4		24·87	35389·6	
29·76	517·4		27·36	358·3	
28·64	534·7		28·73	341·1	
27·76	549·1	1	30·17	323·1	
26·93	561·8		31·76	303·4	
25·95	577·2		34·36	35271·0	
24·40	601·4		35·75	253·7	
23·13	621·3		37·00	238·2	3
2593·67	38543·9		38·63	217·9	
92·33	563·7		39·37	208·7	
91·30	579·1		41·00	35188·6	
90·77	586·9		41·74	179·4	
89·03	613·0	3	42·78	166·5	
88·28	624·1		43·93	152·2	
87·00	642·9		44·91	140·2	
85·07	672·1		46·66	118·6	
84·42	681·9		48·25	35098·0	
2703·34	36980·5				
04·95	958·3				
06·80	933·1	2	2868·60 ?	33676·1	
09·32	898·7		70·87	650·3	
10·75	879·2		71·23	646·3	
2764·33	36164·5		72·91	627·3	4
65·97	142·9	1	74·55	608·7	
68·29	112·7		76·60	585·6	
72·64	056·1		77·45	576·0	
74·24	035·3				
76·38	007·5	5			
78·56	35979·2				
80·31	956·6				

it is -2 cm^{-1} for BF, 41·5 cm^{-1} for CO, 64 cm^{-1} for AlCl and 334 cm^{-1} for GaF. Thus we should expect the AlF intercombination system to be about as strong as the CO Cameron bands; in order to observe it in absorption some long-path technique using concave mirrors will be necessary, but it may well occur weakly in emission. For this reason it is interesting that the weak bands at 2968 – 2978 Å seem to have much less complex structure than the others, in particular the long-wave end of the system starts with two double heads whose intensities are 5, 3, 8 and 10, starting at the outermost. These could well be the heads of $^3\Pi_0$ and $^3\Pi_1$ to $^1\Sigma^+$, for the Q head of $^3\Pi_0 - {}^1\Sigma$, although forbidden in case a, does actually appear for the Cameron bands (as a branch, see Rao[57]). The separation between the "Q heads" in these AlF bands is 41·7 cm^{-1}, the difference between this and the origin separation of 47·5 cm^{-1} is rather large to be accounted for by head-origin separation for Q branches. Against this view that the 33627 cm^{-1} group is the 0,0 bands of an AlF $^3\Pi - {}^1\Sigma^+$ transition are the following figures. These are values of $\frac{\nu_o\ ^3\Pi_1}{\nu_o\ ^1\Pi_1}$ for related molecules.

AlF	?	AlF	?	GaF	0·708	InF	0·734
CO	0·749	AlCl	0·644	GaCl	0·744		
N_2	0·846	AlBr	0·664	GaBr	0·803		
		AlI	0·723	GaI	0·796		

From these it would be expected that this ratio should be about 0·62, i.e. $\nu_0\ ^3\Pi_1 = 27250\ cm^{-1}$ rather than 33627 cm^{-1}. However it is impossible to put much weight on extrapolations of this sort and in the absence of better evidence the 33627 cm^{-1} may tentatively be assumed to be the intercombination system.

Of the other complex sequences the ones at 2531 – 2523 and 2594 – 2584 Å are apparently either 1,0 and 0,0 or 2,0 and 1,0; the corresponding 0,1 or 0,0 is probably missing between 2616 and 2680 Å. These heads have differences of about 930 – 940 cm^{-1} giving vibrational constants similar to those of $^3\Sigma$. Of the other sequences that at 2774 – 2780 Å is probably the 0,0, with a corresponding 1,0 sequence at 2703 – 2710 Å separated by perhaps 940 cm^{-1}. The lengthy series of heads between 2823 and 2848 Å contains the 0,1 sequence, and differences of about 820 cm^{-1} perhaps indicate that the lower state is $^3\Pi$. These states have been added to fig. XV at the right-hand side with the relevant atomic products in the middle.

For the moment, let the dissociation energy of AlF be taken at 145·7 k.cal./mol. This figure will be justified later. It was shown[2,51] that the $^1\Pi$ state dissociated into ground state products (multiplet unspecified) and thus had a small potential maximum. The

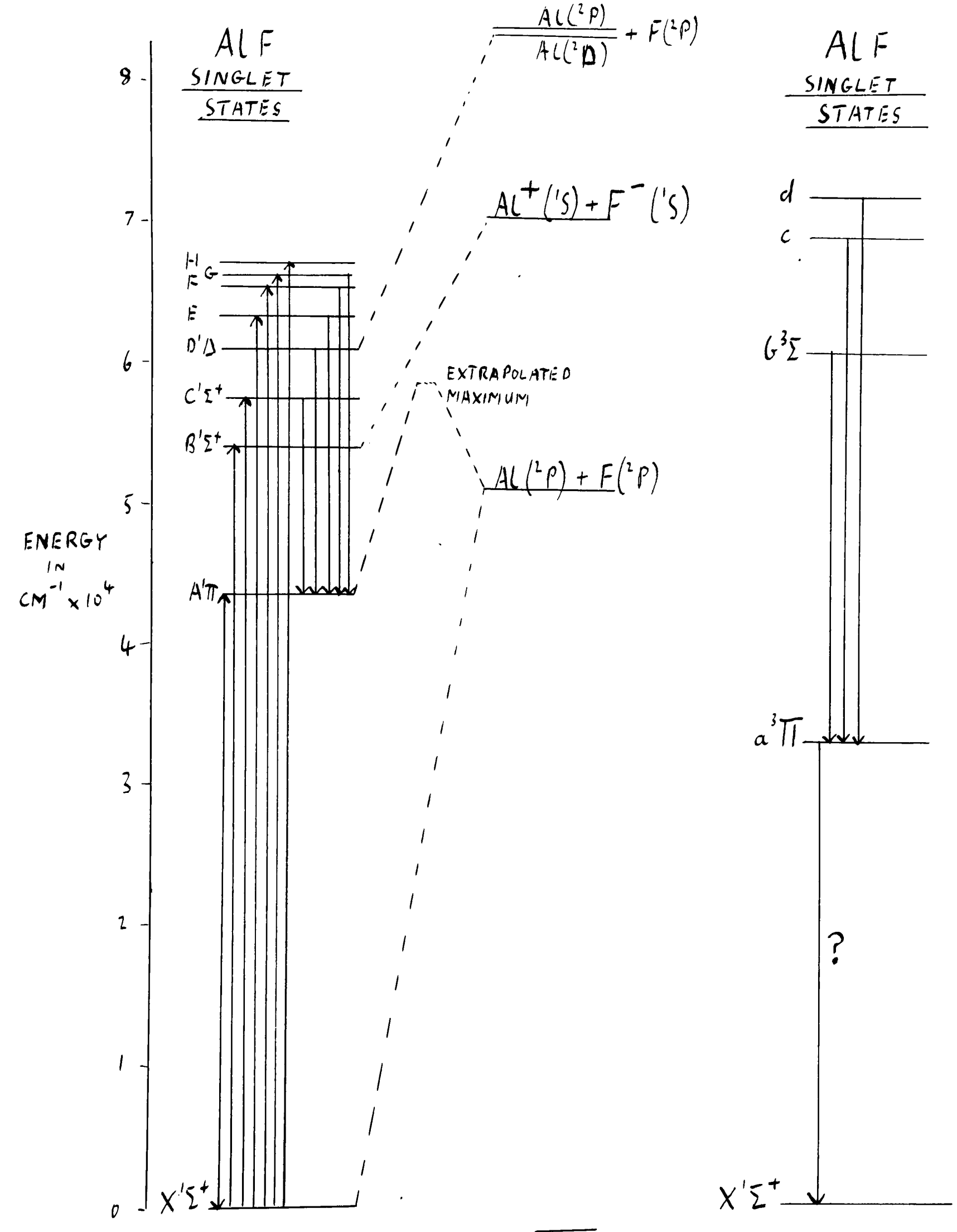

AlF
SINGLET
STATES
ENERGY
IN
CM⁻¹ x 10⁴
8
7
6
5
4
3
2
1
0
H
G
F
E
D'Δ
C'Σ⁺
B'Σ⁺
A'Π
X'Σ⁺
Al(²P) + F(²P)
Al(²D)
Al⁺('S) + F⁻('S)
EXTRAPOLATED
MAXIMUM
Al(²P) + F(²P)
AlF
SINGLET
STATES
d
c
G³Σ
a³Π
?
X'Σ⁺

FIG XV

next state whose products can be fixed with certainty is the $D^1\Delta$, for this can only arise from Al ^2P + F ^2P or Al ^2D + F ^2P. The first Al ^2D_g is at 32435 cm^{-1} above Al ^2P_u ground state, while the first excited ^2P_u state is at 32950 cm^{-1}. Thus the dissociation energy required for $D^1\Delta$ of AlF is 22300 $\pm$ 250 cm^{-1}, while that obtained from a linear extrapolation of vibrational frequencies obtained from the green bands is 26700 cm^{-1}. This is eminently reasonable.

The next state whose products can be decided is the B singlet state. The transition from this state to $X^1\Sigma^+$ is extremely strong; it is not possible to give absolute intensities but the system was well developed to v' = v" = 6 at 800°C when the $A^1\Pi$ and H, G and F transitions were still quite weak. Now it seems likely that the B – X system is of the strongest type of sub-Rydberg transition, the so-called charge-transfer spectra. The strength of these has been shown by Mulliken[58] to be due, on a molecular orbital picture, to an electron being transferred from a bonding to an antibonding orbit. The equivalent atomic orbital idea is a transition from a state arising from M + X to one arising from $M^+ + X^-$ or $M^- + X^+$. The example quoted is the Schumann-Runge system of O_2, a $^3\Sigma_u^- - {}^3\Sigma_u^-$ transition. Here either one may say an electron is changed

from $\pi_u 2p$ to $\pi_g 2p$, or that the upper state is derived from $O^+ + O^-$. Unfortunately in this case the $^3\Sigma_u$ upper state has been shown to dissociate to $O\,^3P + O\,^1D$, however this is explained[58] by interaction between $^3\Sigma_u^-$ from $O^+(^4S) + O^-(^2P)$ and a repulsive $^3\Sigma_u^-$ from $O\,^3P + O\,^1D$.

In AlF no such explanation is needed; the ionization potential of aluminium is 48280 cm^{-1} and the electron affinity of fluorine is 82 k.cal. (after Evans, Warhurst and Whittle[59]) which equals 28650 cm^{-1}. Thus the $Al^+ + F^-$ limit lies at 70530 cm^{-1}, or 16260 cm^{-1} above v' = 0 of the B state of AlF. The limit derived from a linear extrapolation of the B state vibrational differences is 26500 cm^{-1}, whereas that obtained using the rather large quartic $z_e\omega_e'$ term is 12500 cm^{-1}, and it might be expected that the real limit would lie between the two. In addition it was shown by Mulliken (loc. cit.) that for these transitions $\Delta\Lambda = 0$, and so the B state of AlF must be $B\,^1\Sigma^+$, a state which may correctly arise from $Al^+(^1S_g) + F^-(^1S_g)$, and is the only state to do so.

In a similar manner the $C\,^1\Sigma^+$ state may be supposed to dissociate to $Al\ ^2S_g + F\ ^2P$ and the other four singlet states E, F, G and H also to go to $Al\ ^2D_g$ or ^2P_u. These two sets of products may give four $^1\Sigma^+$ states and five $^1\Pi$ ones so there is no possibility of deciding the electronic configuration of these levels from their products.

Dissociation Energy. It now remains to justify the value of 145·7 k.cal./mol. used above for the dissociation energy of AlF. This has been considered before[2,51], and the thermochemical values used were:

$$Al(c) + \tfrac{1}{2}F_2(g) \rightarrow AlF(g) \quad - 49{\cdot}7 \text{ k.cal./mol.}$$
$$Al(g) \rightarrow Al\ (c) \quad - 77$$
$$\tfrac{1}{2}(F + F) \rightarrow \tfrac{1}{2}F_2(g) \quad - 19$$

The heat of formation of AlF is from Gross et alia,[50] the heat of dissociation from Evans et alia[59] (confirmed by Doescher[61]), and that of $\triangle H_L$ Al taken originally from Eucken[62]. The first two values were considered to be good, and the latter has been recalculated from the vapour pressure data of Farkas[63] and Bauer and Brunner[64]. The method is this:- from the Sackur-Tetrode equation, the published vapour pressure data, and the known electronic energy levels, the entropy of the vapour is calculated at the various measured temperatures. The entropy of the liquid is found by extrapolating the data given in Kelley.[30] At equilibrium the change in free energy during evaporation is zero, thus the heat change equals the entropy change times the temperature. To this heat change is added the latent heat of fusion which gives the latent heat of sublimation at the various temperatures. These latent heats are corrected to 298°K by Kirchoff's equation. The

data and results are given below; the first measurement is from Farkas, the rest from Bauer and Brunner.

Temp. ^{o}K	p in mm. Hg	S^{T}_{gas}	S^{T}_{liquid}	$\Delta H^{T}_{Sublimation}$	$\Delta H^{298}_{Sublimation}$
1476	0·1	69·619	20·22	75480	77480
1734	0·67	62·072	21·25	73350	76350
1974	10·0	57·348	21·92	72510	76590
2093	29·8	55·483	22·40	71810	76510
2237	100·6	53·608	22·77	71560	77030

Thus the value of ΔH_{L} of aluminium may be taken as 76·8 k.cal./mol. This value is confirmed by more recent values of the vapour pressure determined by Brewer and Searcy[65]; their value for the latent heat is 77·4 $\pm$ 1·4 k.cal./mol.

References

1. Downie, A. R. D.Phil. Thesis, Oxford, 1950.

2. Rowlinson, H. C. Part II Thesis, Oxford, 1951.

3. Collins, G. and Price, W. C. Rev. Sci. Instruments, 5, 423, 1934.

4. Worley, R. E. Rev. Sci. Instruments, 13, 67, 1942.

5. Garton, W. R. S. J. Sci. Instruments, 30, 119, 1953.

6. Discussion on Band-Spectra. Proc. Phys. Soc., 56, 204, 1944.

7. Barrow, R. F. and Vago, E. E. Proc. Phys. Soc., 58, 538, 1946.

8. Drummond, G. D.Phil. Thesis, Oxford, 1952.

9. Tombs, N. C. and Welch, A. J. E. J. Iron and Steel Inst., 172, 69, 1952.

10. Kiess, C. C. J. Research Nat. Bur. Standards, 21, 185, 1938.

11. Moore, C. E. Nat. Bur. Standards. Circular 467, Vol.I, 1949.

12. Herzberg, G. Spectra of Diatomic Mols., 2nd Ed. Van Nostrand, 1950.

13. Cameron, W. H. B. Phil. Mag., 3, 110, 1927.

14. Pankhurst, R. C. Proc. Phys. Soc., 52, 707, 1940.

15. Woods, L. H. Phys. Rev., 63, 426, 1943.

16. Drummond, G. and Barrow, R. F. Proc. Phys. Soc., A 65, 277, 1952.

17. Moffitt, W. Proc. Roy. Soc., A 196, 524, 1949.

18. Mulliken, R. S. Rev. Mod. Phys., 4, 1, 1932.

19. Takamine, T., Tanaka, Y. and Iwata, M. Sci. Pap. Inst. Phys. Chem. Res. (Tokyo), 40, 371, 1943.

20. Tanaka, Y. Sci. Pap. Inst. Phys. Chem. Res. (Tokyo), 39, 447, 1942.

21. Worley, R. E. Phys. Rev., 64, 207, 1943.

22. Hopfield, J. J. and Birge, R. T. Phys. Rev., 29, 922, 1927.

23. Lagerqvist, A. and Uhler, U. Ark. Fys., 6, 95, 1953.

24. Dennis, L. M. and Hulse, R. E. J. Amer. Chem. Soc., 52, 3553, 1930.

25. Sen Gupta, A. K. Proc. Phys. Soc., 49, 543, 1939.

26. Loomis, F. W. and Watson, T. F. Phys. Rev., 45, 805, 1934.

27. Eisler, B. and Barrow, R. F. Proc. Phys. Soc., 62 A, 740, 1949.

28. Rochester, G. D. Proc. Roy. Soc., A150, 668, 1935.

29. Maeder, R. Helv. Phys. Acta, 21, 411, 1948.

30. Kelley, K. K. U.S. Bureau of Mines. Bull.476, 477, 1949.

31. National Bureau of Standards. Washington. "Selected Values of Chemical Thermodynamic Properties". Circular 500. 1947 and 1950.

32. Grube, G. and Spiedel, H. Zeit. Elektrochem., 53, 339, 1949.

33. Baughan, C. Quat. Rev. of Chem. Soc., 1953.

34. Schäfer, H. and Hörnle, R. Zeit. Anorg. und Allgem. Chem., 263, 261, 1950.

35. Brewer, L. and Mastick, D. F. J. Chem. Phys., 19, 834, 1951.

36. Gel'd, P. V. and Kochnev, M. I. Doklady Acad. Nauk. U.S.S.R., 61, 649, 1948.

37. Brewer, L. Chemical Reviews, 52, 1, 1953.

38. Bues, W. and von Wartenberg, H. Z. Anorg. u. Allgem. Chem., 266, 281, 1951.

39. Jolly, W. L. and Latimer, W. M. J. Amer. Chem. Soc., 74, 5757, 1952.

40. Searcy, A. W. J. Amer. Chem. Soc., 74, 4789, 1952.

41. Vesselovsky, B. K. J. Appl. Chem. U.S.S.R., 16, 397, 1943.

42. Rochester, G. D. Proc. Roy. Soc., A 150, 668, 1935.

43. Shawhan, E. N. Phys. Rev., 48, 521, 1935.

44. Barrow, R. F. and Vago, E. E. Proc. Phys. Soc., 56, 78, 1944.

45. Meggers, W. F. J. Res. Nat. Bur. Standards, 24, 153, 1940.

46. Green, J. B. and Loring, R. A. Phys. Rev., 30, 574, 1927.

47. Paschen, F. J. Opt. Soc. of America, 16, 231, 1928.

48. Rochester, G. D. Phys. Rev., 56, 305, 1939.

49. Yuasa, T. Sci. Rep. Tokyo, Bun. Dai, 3, 239, 1938.

50. Sharma, D. Astrophys. J., 113, 210, 1951.

51. Rowlinson, H. C. and Barrow, R. F. Proc. Phys. Soc., A 66, 437, 1953.

52. Hugo, T. J. and Naudé, S. M. Phys. Rev., 90, 318, 1953.

53. Budó, A. Zeit. fur. Phys., 105, 579, 1937.

54. Harris, N. C. Part II Thesis, Oxford, 1953.

55. Fowler, A. and Vaidya, W. M. Proc. Roy. Soc., A 132, 310, 1931.

56. Welti, D. and Barrow, R. F. Proc. Phys. Soc., A 65, 629, 1952.

57. Rao, K. N. Astrophys. J., 110, 304, 1949.

58. Mulliken, R. S. J. Chem. Phys., 7, 20, 1939.

59. Evans, M. G., Warhurst, E. and Whittle, E. J. Chem. Soc., 317, 1524, 1950.

60. Gross, P., Campbell, C. S., Kent, D. J. C., Levi, D. L. Discussions of Faraday Soc., 4, 206, 1948.

61. Doescher, R. N. J. Chem. Phys., 19, 1070, 1951.

62. Eucken, A. Metallwirt, 15, 63, 1936.

63. Farkas, A. Z. Phys., 70, 737, 1931.

64. Bauer, E. and Brunner, R. Helv. Chim. Acta, 17, 958, 1934.

65. Brewer, L. and Searcy, A. W. J. Amer. Chem. Soc., 73, 5308, 1951.

66. Paul, F. W. and Knaus, H. P. Phys. Rev., 54, 1072, 1938.

ACKNOWLEDGEMENTS

It is with great pleasure that I record my gratitude to Dr. R. F. Barrow for his helpful advice and encouragement during the past two years.

I also wish to thank the Department of Scientific and Industrial Research for the award of a maintenance grant.